Tesis Doctoral

Ingenería de Telecomunicación

Técnicas de diversidad para sistemas de DVB de última generación

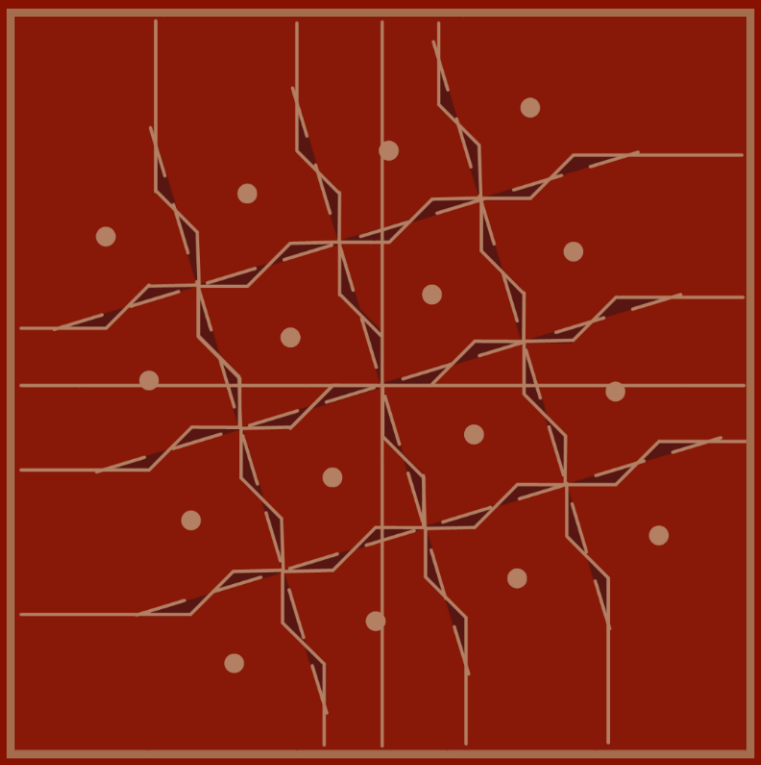

Autor: Darío Pérez-Calderón Rodríguez

Director: Vicente Baena Lecuyer

Dep. Ingeniería Electrónica

Escuela Técnica Superior de Ingeniería

Universidad de Sevilla

2017

Tesis Doctoral
Ingeniería de Telecomunicación

Técnicas de diversidad para sistemas de DVB de última generación

Autor:

Darío Alfonso Pérez-Calderón Rodríguez

Director:

Vicente Baena Lecuyer

Profesor titular

Dep. de Ingeniería Electrónica

Escuela Técnica Superior de Ingeniería

Universidad de Sevilla

Sevilla, 2017

PhD Dissertation

Diversity Techniques for DVB cutting-edge systems

Darío Alfonso Pérez-Calderón Rodríguez

Departamento de Ingeniería
Electrónica
Universidad de Sevilla

Tutor: Vicente Baena Lecuyer

PhD Dissertation

24-05-2016

Abstract

After the Analog black out (in Spain this happened in April 2010), the digital TV era started officially. In Europe the Digital Video Broadcasting (DVB) Project leaded the standardization process that would end with a series of worldwide accepted standards as DVB Terrestrial (DVB-T). The standardization process of the different standards allowed to develop cutting edge technologies to be applied in them making this family of standards state of the art ones in the date they were released.

The technical content in this PhD. dissertation was developed while participating in the standardization process of Digital Video Broadcasting Second generation Terrestrial (DVB-T2) and Digital Video Broadcasting Next Generation Hand-held (DVB-NGH). The dissertation is focused in the diversity techniques applied in the aforementioned standards, Rotated Constellations in DVB-T2 and Multiple Input - Multiple Output (MIMO) schemes in DVB-NGH. The gain that can be obtained by applying these techniques in their corresponding standards and also the drawbacks that can be found. As main contribution, several techniques to reduce the complexity introduced in the system by the usage of Rotated Constellations and MIMO are presented. All the techniques presented are focused on the detection process of the transmitted data and look for a trade off between performance loss and hardware complexity reduction, that is a critical aspect when regarding to mobile systems as DVB-NGH.

To my parents, Darío and Margarita, and sister, Margarita, who made me to get to be who I am. To my wife Lena, whose love enlightened even the darkest of my days. To my son Daniel,the first, and who I hope one day can read and probably understand this. To my daughter Aurora, the second and last by now, who also I hope can read and understand what I am writing here and if necessary explain to Daniel ...

Acknowledgements

There are many people who I would like to acknowledge, so just in case I forget someone in particular I would like to thank everyone that shared a moment with me these years, because from everyone I could learn a bit and step by step I could reach this moment when I am finishing my PhD. dissertation. So let's start from the beginning, although I already dedicated this dissertation to my parents also I must thank them for my education, the values they gave to me, all that somehow made me be the stubborn being that can reach the "end of the way". They have always been there when I needed them and also when I didn't, I will never be able to repay all they have given to me.

Thanks to my sister, yes I know I'm being repetitive but it is a must. She has been very competitive from the very beginning and I wasn't, she made me be much more ambitious and always wanting to improve myself.

Thanks to Dani, not my son, he has been my friend since I was 6, and still he is! (Some raindrops have fallen since then, also my hair!). Thanks to him I started loving sports and started playing handball, he also was there in difficult moments and of course in many more good ones.

Thanks to Juanma, we also know each other since we were six, but our friendship really bloomed when we went to the university, we studied together and lived in the same room for 5 years, he was my example to follow in many aspects, I really admire him. I wouldn't say he is just my friend he is apart from some ADN incompatibilities like my older brother (although he is younger than me).

Thanks to Núñez, we have lived a lot of magical moments together (we have crafted together our own armors and weapons!, not everyone has performed together as Saint Seiya characters), spent hours and hours playing countless games and also he has been there always I have needed him, and it feels also like he were my younger brother.

Thanks to Fran, one of the most innocent (in the good sense of the word) people I have ever met and probably one of the most brilliant one. He could stand a year living with me, and that is a difficult task.

Thanks to Vicente, that trusted in me and let me work with a wonderful team. I have learned a lot from him, and in many aspects is an example to follow if I want to get where I really want to be in my life.

Thanks to José, a really kind heart person with whom I have spent who knows how many hours in these years, countless parties, fairs, and funny moments that I will barely ever forget. And also I have learned a lot from him not only about engineering. The same I could say about Patricio, but with the advantage that foreigners can understand him when speaking Spanish.

Thanks to my friends Carou, Copito, Nai, Lija, Luki, and Ana they have been always there since I knew them and without them many things wouldn't had had any sense. They are my non blood related family the ones with whom I have shared travels, dinners, games, celebrations, countless hours ... they are just great and they made me a better person.

Thanks to Cinta and Jorge, that have helped me in my academic way (as teachers and after as team mates).

Thanks thanks to Luismi, Antonio, Sebas, Vito, Elo, José Luis for the moments we shared in the Cave. Also to the new Cave generation, Ignazio, Inma, Lidia, Abril, ... they make much more enjoying the workday.

And at last but not least, indeed not even close, thanks to my wife,

Lena who has supported me, who loves me as I am, who has given me the most beautiful present that a man can have in his life, my son and daughter, and who makes me wake up every morning with a smile even if it is 6:30 in the morning.

Contents

Acronym list

3GPP	*Third Generation Partnership Project*
ACE	*Active Constellation Extension*
AWGN	*Additive White Gaussian Noise*
BCH	*Bose-Chaudhuri-Hocquengham*
BER	*Bit Error Rate*
BICM	*Bit Interleaving Coding and Modulation*
CBC	*Complement Block Coding*
CDMA	*Code Division Multiple Access*
CNR	*Carrier to Noise Ratio*
COFDM	*Coded Orthogonal Frequency Division Multiplexion*
CP	*Cyclic Prefix*
CPE	*Continual Pilots Estimation*
CR	*Coding Rate*
CSP	*Common Simulation Platform*
DBPSK	*Differential Binary Phase Shift Keying*

ACRONYM LIST

DFT	*Discrete Fourier Transform*
DVB	*Digital Video Broadcasting*
DVB − C	*Digital Video Broadcasting Cable*
DVB − H	*Digital Video Broadcasting for Handheld*
DVB − NGH	*Digital Video Broadcasting Next Generation for Handhelds*
DVB − S	*Digital Video Broadcasting by Satellite*
DVB − S2	*Second Generation Digital Video Broadcasting Satellite*
DVB − SH	*Digital Video Broadcasting Satellite Handheld*
DVB − T	*Digital Video Broadcasting Terrestrial*
DVB − T2	*Second Generation Digital Video Broadcasting Terrestrial*
ELG	*European Launch Group*
eSFN	*enhanced Single Frequency Network*
eSM	*enhanced Spatial Multiplexing*
ETSI	*European Telecommunications Standards Institute*
FEC	*Forward Error Correction*
FFT	*Fast Fourier Transform*
FURIA	*Futura Red Integrada Audiovisual*
GI	*Guard Interval*
GIE	*Grupo de Ingeniería Electrónica*
HD	*High Definition*
HDL	*Hardware Description Language*
HDTV	*Hihgh Definition Televsion*

HLSI	*Hierarchical Local Service Insertion*
ICI	*Inter Carrier Interference*
IFFT	*Inverse Fast Fourier Transform*
ISI	*Inter Symbol Interference*
JRC	*Journal Citation Report*
LDPC	*Low Density Parity Check*
LLR	*Log Likelihood Ratio*
LTE	*Long Term Evolution*
MC − CDMA	*Multi Carrier Code Division Multiple Access*
CBC	*Modified Complement Block Coding*
MFN	*Multiple Frequency Network*
MIMO	*Multiple Input - Multiple Output*
MISO	*Multiple Input Single Output*
ML	*Maximum Likelihood*
MoU	*Memorandum of Understanding*
MPE	*Multi Protocol Encapsulation*
OFDM	*Orthogonal Frequency Division Multiplexing*
OLSI	*Orthogonal Local Service Insertion*
PAM	*Pulse Amplitude Modulation*
PAPR	*Peak to Average Power Ratio*
PDF	*Probability Density Function*
PH	*Phase Hopping*

ACRONYM LIST

PhD	*Philosophae Doctor*
PLP	*Physical Layer Pipes*
PSK	*Phase Shift Keying*
Q	*Quadrature component*
QAM	*Quadrature Amplitude Modulation*
QPSK	*Quadrature Pulse Shift Keying*
RF	*Radio Frequency*
RME	*Rayleigh Memoryless with Erasures*
RMSE	*Root Mean Square Error*
RQD	*Rotated Constellation and cyclic Q Delay*
rSM	*rotated Spatial Multiplexing*
SBC	*Simple Block Coding*
SC	*Single Carrier*
SCOFDM	*Single Carrier Orthogonal Frequency Division Multiplexion*
SDTV	*Standard Definition Television*
SFN	*Single Frequency Network*
SIMO	*Single Input - Multiple Output*
MISO	*Single Input Single Output*
SM	*Spatial Multiplexing*
SMS	*Short Message Service*
SNR	*Signal to Noise Ratio*
SSD	*Signal Space Diversity*

ACRONYM LIST

TDM	*Time Division Multiplexion*
TDT	*Terrestrial Digital Television*
TFS	*Time Frequency Slicing*
TM	*Technical Module*
TR	*Tone Reservation*
TV	*Television*
UHF	*Ultra High Frequency*
UMTS	*Universal Mobile Telecommunications System*
XPD	*Cross Polar Discrimination*

Figure list

Table list

Chapter 1

Introduction

Nowadays, wireless communication systems have a performance close to the theoretical limits exposed by Shannon [2]. This is mainly due to the mature state of the technologies applied in them. Clear examples of this are the 802.11 family standards (a, b, g, n), 802.16 (WiMax) or the mobile telephone standards as Universal Mobile Telephone System (UMTS). Increasing the data rate in this kind of systems (power, bandwidth and complexity limited) represents a very challenging task. But this increase is an actual necessity due to the each time more demanding consumer's habits, not restricted to the traditional SMS and phone call services any more. The arrival of smartphones and other devices such as tablets generated a new scenario that demands each time more capacity to cope the users necessities. This also is applied to traditional broadcasting systems: high definition (HD) TV, interactive services require a much higher capacity than the offered by the first generation of digital TV.

The development of the second generation terrestrial digital video broadcasting (DVB-T2) standard [3] and the availability of free frequencies in the UHF band after the analog television switch-off in Europe enabled the television operators to offer new services with the current network planning, such as HDTV transmissions or new datacasting services. For this purpose, the DVB-T2 specification was developed with state of the art technology providing a high capacity increase (about 70%) over the existing digital video broadcasting terrestrial (DVB-T) standard [4]. Also the DVB Proyect has developed the new mobile stan-

dard Digital Video Broadcasting Next generation for Handhelds (DVB-NGH) [5]. This standard takes as basis DVB-T2, and provides a huge increase when compared with its predecessor DVB-H [6].

In Both of the cited standards one of the keys for this capacity increase is the diversity; frequency, time and space provide the degrees of liberty necessary to exploit the resources that the wireless channel gives us. In this PhD. dissertation this will be the keystone under study, how diversity improves the system performance, its main drawbacks and it will be also studied how to minimize them finding a good trade-off between performance and implementation simplicity.

1.1 Motivation and research line

The beginnings of the investigations presented in this PhD. dissertation are enclosed in the frame of the FURIA (Futura Red Integrada Audiovisual) project, in which the Electronic Engineering Group (GIE) of the University of Seville took part. This project studied, among others, the DVB-T2 standard; the PhD. candidate started studying the diversity techniques present in this standard focusing in one of the most promising ones, the rotated constellations and cyclic Q (quadrature component) delay (RQD) (this technique will be widely studied in chapter 3). RQD provides a huge performance gain in severe propagation conditions, but it has an important drawback increasing the detection process complexity at the receiver side.

Later, the research group started participating in the DVB-NGH standardization process, taking active part in the MIMO (Multiple Input-Multiple Output) working group, presenting the results obtained in different teleconferences and international meetings, attending personally to the ones held in Helsinki (hosted by Nokia, June 22nd – 24th, 2010), Valencia (iTEAM Research Institute,Universidad Politécnica de Valencia, December 14th to 16th, 2010), Paris (Espace Hamelin, Telecom Bretagne, February 22nd to 24th, 2011), and Munich (hosted by LG, April 12th to 14th, 2011). During this process the MIMO diversity techniques presented in chapter 4 were studied. These techniques provide a considerable capacity gain to the system becoming a key feature to be able to satisfy future consumer's necessities. However, the diversity provided by MIMO techniques as

rotated constellations implies a complexity increase in the detection process and in the case of MIMO a much more important one.

1.2 Main targets

The studies carried out during the PhD. can be summarized in the following main points:

- Study of the diversity precedents in DVB standards: Rotated Constellations. Main benefits and drawbacks, its implementation in DVB-T2 and contributions to its complexity reduction.
- Study of the MIMO techniques proposed for the DVB-NGH standard. Main benefits and drawbacks. Contributions for the complexity increase inherent to MIMO schemes reduction.

1.3 Dissertation's outline

In the following paragraphs how the rest of the dissertation is organized will be briefly summarized.

As a state of the art study, chapter 2 will give a brief overview of the most relevant DVB standards for this dissertation. In chapter 3 the diversity precedents in DVB-T2 standard will be deeply studied. Rotated constellation principles will be exposed as well as its implementation in DVB-T2. After that the performance achievable will be studied by means of MATLAB® based simulations, ending the chapters with the main contributions proposed to reduce the complexity increase consequence of the use of RQD.

In chapter 4 the basic principles of MIMO systems are explained in order justify the addition to DVB-NGH standard.

In chapter 5, a study of the capacity improvement that MIMO offers to DVB-NGH MIMO is shown together with a complexity reduction method that will simplify the receiver hardware implementation. Moreover, a novel SISO codification technique based on the ones studied in this chapter is presented.

Finally, chapter 6 presents the most important conclusions that can be obtained from all the work carried out. Also the main future research lines will be stated.

1.4 Methodology

For the study of the performance of the different techniques applied to DVB-T2 the GIE developed a MATLAB® based simulation platform that was taken by the DVB Project as validation tool for DVB-T2 standard compliant systems. This DVB-T2 baseband floating point transmission chain model is known as Common Simulation Platform (CSP)[7], and it was used for all the DVB-T2 simulation results obtained during the PhD. development. Moreover the CSP was used as basis for the simulation chain used to evaluate the MIMO performance in DVB-NGH, cross-checking its results with top level companies as Samsung, LG, Panasonic, Sony, etc.

1.5 Contributions

During the investigation period of this PhD. dissertation the work performed has derived in the following publications in high prestige magazines indexed in the Journal Citation Report (JRC):

- Perez-Calderon, Dario; Baena Lecuyer, Vicente; Oria, Ana Cinta; Garcia Doblado, Jose; "Diversity Technique for OFDM Systems: Enhanced Time-Frequency Multiplexing (eTFM)," *IEEE Transactions on Broadcasting*, vol. 62, issue 3, pp. 505-511, 2016.

- García-Doblado, José; Oria-Oria, Ana Cinta; Baena, V.; López-González, Patricio; Pérez-Calderón-Rodríguez, Darío Alfonso; "Cubic Metric Reduction for DCO-OFDM Visible Light Communication Systems," *Journal of Lightwave Technology*, vol. PP, issue 33, pp. 1971-1978, 2015.

- Pérez-Calderón-Rodríguez, Darío Alfonso; Baena, V.; Chavez-Orzaez, Jorge; Oria-Oria, Ana Cinta; García-Doblado, José; "Simplified Detection for

DVB-NGH MIMO Decoders, *IEEE Transactions on Broadcasting*, vol. 61, issue 1, pp. 84-90, 2015.

- Pérez-Calderón-Rodríguez, Darío Alfonso; Baena, V.; García-Doblado, José; Oria-Oria, Ana Cinta; López-González, Patricio; "Simplified Metrics Calculation for Soft Bit Detection in DVB-T2," *Radioengineering*, vol. 23, issue 1, pp. 399-404, 2014.

- Oria-Oria, Ana Cinta; López-González, Patricio; García-Doblado, José; Pérez-Calderón-Rodríguez, Darío Alfonso; Baena, V.; "L1 Signaling Mobility Performance in DVB-T2 Receivers," *Microelectronics Journal*, 2013.

- García-Doblado, José; Oria-Oria, Ana Cinta; Pérez-Calderón-Rodríguez, Darío Alfonso; López-González, Patricio; Baena-Lecuyer, Vicente; "Improved power efficiency for DVB-SH transmitters," *Microelectronics Journal*, vol. 44, issue 10, pp. 897-903, 2013.

- Pérez Calderón Rodríguez, Darío Alfonso; Baena Lecuyer, Vicente; Oria Oria, Ana Cinta; López González, Patricio; García Doblado, José; "Simplified Rotated Constellation Demapper for Second Generation Terrestrial Digital Video Broadcasting," *IEEE Transactions on Broadcasting*, vol.59, Issue 1, pp. 160-167, 2013.

- García Doblado, José; Oria Oria, Ana Cinta; Pérez Calderón Rodríguez,Darío Alfonso; López González, Patricio; Baena Lecuyer, Vicente "Improved power efficiency for DVB-SH transmitters,"; *Microelectronics Journal, Elsevier,* ISSN 0026-2692, 2013.

- Oria Oria, Ana Cinta; Baena Lecuyer, Vicente; Granado Romero, Joaquin; Chavez Orzaez, Jorge; López González, Patricio; García Doblado, José; Pérez Calderón Rodríguez, Darío Alfonso; "Reduced complexity ICI cancellation scheme for OFDM DVB-SH receivers," *Microprocessors and Microsystems. Elsevier,* vol.36, Issue 5, pp. 393-401, 2012.

- D. Pérez Calderón Rodríguez, Darío Alfonso; Baena Lecuyer, Vicente; Oria Oria, Ana Cinta; López González, Patricio; García Doblado, José; "Rotated

constellation demapper for DVB-T2," *IEE Electronic Letters*, vol.47, Issue 1, pp. 31-32, 2011.

- Oria Oria, Ana Cinta; Baena Lecuyer, Vicente; Granado Romero, Joaquin; García Doblado, José; Pérez Calderón Rodríguez, Darío Alfonso; López González, Patricio; Ortiz,David; "Performance Evaluation of Complementary Code Combining Diversity in DVB-SH," *Digital Signal Processing, Elsevier,* Issue 6, pp. 718-724, 2011.

- García Doblado, José; Baena Lecuyer, Vicente; Oria Oria, Ana Cinta; Pérez Calderón Rodríguez, Darío Alfonso; López González, Patricio;"Coarse time synchronisation for DVB-T2," *IEE Electronic Letters*, vol.46, Issue 11, pp. 797-799, 2010.

Moreover the performed work has lead also to contributions to national and international congress:

- Pérez-Calderón-Rodríguez, Darío Alfonso; Baena, V.; García-Doblado, José; López-González, Patricio; Oria-Oria, Ana Cinta; Chavez-Orzaez, Jorge; "CDMA PLC communications system" in *XXIX Conference on Design of Circuits and Integrated Systems*, 2014, Madrid (Spain).

- López-González, Patricio; Baena, V.; Oria-Oria, Ana Cinta; García-Doblado, José; Chavez-Orzaez, Jorge; Granado-Romero, Joaquin; Pérez-Calderón-Rodríguez, Darío Alfonso; Dominguez-Amarillo, Eugenio; "A Power Line Sensor Network for monitoring MPPTs" in *28th Edition of Conference on Design of Circuits and Integrated Systems (DCIS)*, 2013, San Sebastaián (Spain).

- Pérez-Calderón-Rodríguez, Darío Alfonso; García-Doblado, José; López-González, Patricio; Baena, V.; Chavez-Orzaez, Jorge; Oria-Oria, Ana Cinta; Dominguez-Amarillo, Eugenio; "CDMA based PLC system for SMGs" in *28th Edition of Conference on Design of Circuits and Integrated Systems (DCIS)*, 2013, San Sebastaián (Spain).

- Pérez-Calderón-Rodríguez, Darío Alfonso; García-Doblado, José; López-González, Patricio; Baena, V.; Oria-Oria, Ana Cinta; "Técnica de diversidad temporal-frecuencial para sistemas OFDM" in *XXVIII SIMPOSIUM NACIONAL DE LA UNIÓN CIENTÍFICA INTERNACIONAL DE RADIO*, 2013, Santiago de Compostela (Spain).

- López González, Patricio; Oria Oria, Ana Cinta; Baena Lecuyer, Vicente;García Doblado, José; Pérez Calderón Rodríguez, Darío Alfonso;"L1 Signaling Mobility Performance in DVB-T2 Receivers,"in *Proc. 2012 Int. Conf on Digital Circuit and IntegratedSystems (DCIS 2012)*, 2012, Avignon (France).

- Pérez Calderón Rodríguez, Darío Alfonso; García Doblado, José; López González, Patricio; Oria Oria, Ana Cinta; Baena Lecuyer, Vicente;"Simplified metrics for DVB-NGH MIMO," in *Proc. 2012 Int. Conf on Digital Circuit and Integrated Systems (DCIS 2012)*, 2012, Avignon (France).

- Pérez Calderón Rodríguez, Darío Alfonso; García Doblado, José; López González, Patricio; Oria Oria, Ana Cinta; Baena Lecuyer, Vicente; "Tecnologías clave en DVB-NGH," in *XXVII Simposium Nacional de Unión Científica Internacional de Radio*, 2012, Elche (España).

- García Doblado, José; Pérez Calderón Rodríguez, Darío Alfonso; López González, Patricio; Baena Lecuyer, Vicente; "Improved power efficiency for DVB-SH transmitters," in *Proc. 2011 Int. Conf on Digital Circuit and Integrated Systems (DCIS 2011)*, 2011, Albufeira (Portugal).

- López-González, Patricio; Baena-Lecuyer, Vicente; Oria-Oria, Ana Cinta; Pérez-Calderón-Rodríguez, Darío Alfonso; "M-binary Turbo Decoder Acceleration using CUDA," in *Proc. 2011 Int. Conf on Digital Circuit and Integrated Systems (DCIS 2011)*, 2011, Albufeira (Portugal).

- Pérez Calderón Rodríguez, Darío Alfonso; García Doblado, José; López González, Patricio; Oria Oria, Ana Cinta; Baena Lecuyer, Vicente; "Codificación MIMO para NGH," in *XXVI Simposium Nacional de Unión Científica Internacional de Radio*, 2011, Leganés (España).

- Oria Oria, Ana Cinta; López González, Patricio; García Doblado, José; Pérez Calderón Rodríguez,Darío Alfonso; Baena Lecuyer, Vicente; Ortiz, David; "Reduced complexity ICI cancellation scheme for OFDM DVB-SH receivers," in *Proc. 2010 Int. Conf on Digital Circuit and Integrated Systems (DCIS 2010)*, 2010, Lanzarote (España).

- Pérez Calderón Rodríguez, Darío Alfonso; García Doblado, José; López González, Patricio; Oria Oria, Ana Cinta; Baena Lecuyer, Vicente; "Análisis del ángulo de rotación en DVB-T2," in *XXV Simposium Nacional de Unión Científica Internacional de Radio*, 2010, Bilbao (España).

- Pérez Calderón Rodríguez, Darío Alfonso; Oria Oria, Ana Cinta; García Doblado, José; López González, Patricio; Baena Lecuyer, Vicente; Lacadena, Ignacio; "Rotated constellation for DVB-T2," in *Proc. 2009 Int. Conf on Digital Circuit and Integrated Systems (DCIS 2009)*, 2009, Zaragoza (España).

- Oria Oria, Ana Cinta; García Doblado, José; López González, Patricio; Pérez Calderón Rodríguez, Darío Alfonso; Granado Romero, Joaquin;Ortiz, David; "Complementary code combining in DVB-SH,"in *Proc. 2009 Int. Conf on Digital Circuit and Integrated Systems(DCIS 2009)*, 2009, Zaragoza (España).

Part of the work in this PhD. study has also presented in DVB-NGH standardization meetings and teleconferences:

- Darío Pérez-Calderón Rodríguez, Vicente Baena Lecuyer, Carlos Pardo, "SFNs", DVB Document TM-NGH373, August 2010.

- Darío Pérez-Calderón Rodriguez, "AICIA SFNs Power Imbalance" DVB Document TM-NGH419, September 2010.

- Darío Pérez-Calderón Rodríguez, Vicente Baena Lecuyer, "AICIA NGH 15 channel model results" DVB Document TM-NGH656, February 2011.

- Darío Pérez-Calderón Rodríguez, "AICIA results high correlation" DVB Document TM-NGH731, February 2011.

1.6 Projects and contracts

During the PhD. studies the candidate has participated in the following projects and contracts:

- Name: TECNOPORT 2025

  Code: 0452/2284

  Ámbito: Nacional

  Manager: Torralba-Silgado, Antonio Jesus

  Beginning date: 15/07/2014

  End date: 15/09/2015

  Quantity: €6.374.310,10

- Name: CENIT SINTONÍA/INTEGRASYS

  Code: PI-0583/2009

  Project manager: Baena-Lecuyer, Vicente

  Beginning date: 23/11/2009

  End date: 30/11/2011

  Quantity: €16.000,00

- Name: FURIA 3: FUTURA RED INTEGRADA

  Code: SN-0745/2009

  Project manager: Baena-Lecuyer, Vicente

  Beginning date: 01/01/2009

  End date: 31/12/2010

  Quantity: €113.953,00

- Name: INTEGRASYS/CENIT INTEGRA

  Code: PI-0692/2009

  Project manager: Baena-Lecuyer, Vicente

Beginning date: 01/12/2008

End date: 31/12/2011

Quantity: €44.400,00

- Name: TID-DVB SIDSA

  Code: PI-0693/2009

  Project manager: Baena-Lecuyer, Vicente

  Beginning date: 01/01/2008

  End date: 31/12/2010

  Quantity: €450.000,00

- Project: EVECOM-COMUNICACIONES PLC PARA RECARGA DE VEHÍCULOS ELÉCTRICOS

  code: PI12/1225

  Project range: Autonómica

  Founding program: Junta de Andalucía. Proyectos de aplicación de conocimiento 2012

  Project manager: Baena, V.

  Beginning date: 30/06/2014

  End date: 30/06/2015

  Quantity: €32.640,68

- Project: HELIOS

  Code: PI-57086

  Project range: Autonómica

  Founding program: Incentivos de la Junta de Andalucía. Proyectos de Aplicación de Conocimiento

  Founding entity: Junta de Andalucía

  Project manager: Baena, V.

Beginning date: 03/01/2014

End date: 30/04/2015

Quantity: €80.446,40

- Project: EDELWEISS: DISEÑO DE UN SISTEMA DE COMUNICACIONES INALÁMBRICAS INTRA-SATÉLITE DE ALTA EFICIENCIA

  Code: TIC-7095

  Project range: Autonómica

  Founding program: Proyectos de Excelencia de la Junta de Andalucía

  Project manager: Aguirre Echanove, Miguel Ángel

  Beginning date: 01/08/2012

  End date: 31/07/2015

  Quantity: €180.000,00

- Project: AYUDA SUPLEMENTARIA PLAN PROPIO. PROYECTO: ARQUITECTURAS PARA LA FUTURAGENERACIÓN DE ESTÁNDARES DE TELEVISIÓN DIGITAL

  Code: CICE

  Project range: Autonómica

  Founding program: Plan Propio, Universidad de Sevilla

  Project manager: Baena-Lecuyer, Vicente

  Beginning date: 30/03/2011

  End date: 31/12/2011

  Quantity: €2.176,90

- Project: NUEVAS ARQUITECTURAS PARA LA FUTURA GENERACIÓN DE ESTÁNDARES DE TELEVISIÓN DIGITAL Code: TEC2010-17029

  Project range: Nacional

  Founding program: Otros programas del plan nacional I+D, Ministerio de Ciencia y Tecnología

Project manager: Baena-Lecuyer, Vicente

Beginning date: 01/01/2011

End date: 31/12/2013

Quantity: €41.190,00

- Project: AYUDA A LA CONSOLIDACIÓN DE GRUPOS DE INVESTIGACIÓN

  Code: 2009/TIC-192

  Project range: Autonomic

  Founding program: Otros programas, Junta de Andalucía

  Project manager: Torralba-Silgado, Antonio Jesus

  Beginning date: 01/01/2010

  End date: 31/12/2011

  Quantity: €24.925,64

- Project: FURIA2: FUTURA RED INTEGRADA AUDIOVISUAL

  Code: TSI-020100-2008-630

  Project range: National

  Founding program: Programa de Fomento de la Investigación Técnica (PROFIT), Ministerio de Industria, Turismo y Comercio

  Project manager: Baena-Lecuyer, Vicente; Torralba-Silgado, Antonio Jesus

  Beginning date: 01/01/2008

  End date: 31/12/2008

  Quantity: €54.000,53

1.7 Intelectual property

The following patent has been developed during the PhD. studies, being one of the proposed simplifications in this dissertation.

- **Decodificador de constelaciones rotadas y método de decodificación**

  Type: Patente de invención, Propiedad industrial

  Concession date: 24/11/11

  Type of protection: European

  Authors: Baena-Lecuyer, Vicente; Pérez-Calderón-Rodríguez, Darío Alfonso; Oria-Oria, Ana Cinta; García-Doblado, José; López-González,Patricio

Chapter 2

DVB Standards

2.1 Introduction

By the end of 1991 the broadcasting institutions, equipment manufacturers, and European regulator institutions gathered to discuss about the foundation of a group which target were to supervise the introduction of the Digital Television. This group, that was known as European Launch Group (ELG), set a frame based on the agreement, and through it the most suitable technologies to be used in this deployment were proposed. A Memorandum of Understanding (MoU) was elaborated establishing the basis for all the competitors in order to have a market based on the confidence and mutual respect. This memorandum was signed in 1993 by all the components of the ELG. Since that date, the group changed its name and adopted the one that holds nowadays: DVB Project.

Today the DVB Project is the organization in charge of creating and proposing the standardization processes for the digital television. It is constituted by more than 270 institutions and enterprises from all over the world. The standards proposed by the DVB Project have had a wide international acceptance in Europe and almost every continent, just in the USA and Japan the DVB Project standards coexist with other systems. All over the world more than 500 million receivers meet DVB standards [8].

In this chapter some of the DVB standards will be briefly described, focusing on the ones in which contributions this dissertation presents are based on: DVB-

T2[3] and DVB-NGH[5]. By doing so the main characteristics of OFDM systems will be exposed, and will help to understand the rest of the chapters in this PhD dissertation together with its contributions.

2.2 DVB-T

When the DVB Project started its work in 1993, the development of standards for cable and satellite markets were the priority. The existence of less technical problems and a simpler climatic regulation, made the services based in these standards to be deployed in a short period of time. In fact, the industry gave priority to the satellite and cable broadcasting solutions in detriment of the Terrestrial Digital Television (TDT). This came from the technical difficulties inherent to a wireless broadcast system; a higher noise power, limited bandwidth, interferences and multipath propagation scenarios. However, after the development of DVB-S and DVB-C, the DVB Project set the commercial requirements to define how to implement a terrestrial broadcasting system. DVB-T[4] was designed to satisfy the aforementioned requirements.

DVB-T is a technical standard that specifies the frame structure, channel coding and modulation for the transmission of the TDT. The first version of the standard was published in March 1997 and it became the most used standard of this kind of systems in the world. DVB-T is a flexible system that allows the networks to be designed for a wide bunch of services, from the High Definition Television (HDTV) defined by the time (MPEG2 input) to Standard Definition Television (SDTV), for fixed, portable, mobile and even handheld reception.

2.2.1 DVB-T basics

DVB-T was one of the first standards using Orthogonal Frequency Division Multiplexion (OFDM) modulation. In this case DVB-T is a Coded OFDM (COFDM) system, due to the fact that the modulated data bits are previously coded by a Forwar Error Correction (FEC) stage. In the following subsections the main principles of DVB-T will be briefly summarized, although this dissertation is partly based on its successor DVB-T2[3] a quick overview will help to understand the

importance of the improvements in DVB-T2.

2.2.1.1 FFT size

The Fast Fourier Transform (FFT) size defines the number of subcarriers in the OFDM system and together with the symbol duration it defines the transmission bandwidth.

In DVB-T there are two FFT sizes available, 2K and 8K. A higher FFT size allows to have a higher capacity when compared to lower ones having the same Cyclic Prefix (CP) length (this feature will be explained in the following subsection). However, increasing the FFT size also carries some drawbacks; the coherence time of the channel must be longer than the symbol time, so long FFT sizes are not suited for mobile reception; the distance between carriers decreases so the Inter Carrier Interference (ICI) probability increases due to the Doppler effect or synchronization errors.

In most of the countries that adopted DVB-T the chosen transmission mode was 8K. Although, in the United Kingdom the adopted one was the 2K mode to ease the development of low cost receivers.

2.2.1.2 Cyclic prefix

The CP is a copy of part of the original data that is inserted at the beginning of the symbol (see Figure 2.1), this redundancy protects the symbol from Inter Symbol Interference (ISI) and defines the maximum delay between multipaths that the system can stand. Usually the delay in propagation scenarios is not that long, the problem comes with Single Frequency Network (SFN) configurations, the interference from different transmitters allocated in different geographical points produces extremely long delays. Having a long GI simplifies the network planning at the cost of reducing the available capacity.

2.2.1.3 Constellation and codification

For DVB-T three possible constellations were set: QPSK, 16-QAM, and 64-QAM with Gray mapping. In the FEC 5 code rates were adopted: 1/2, 2/3, 3/4, 5/6, and 7/8. The FEC process was divided in two steps, the first one applying a

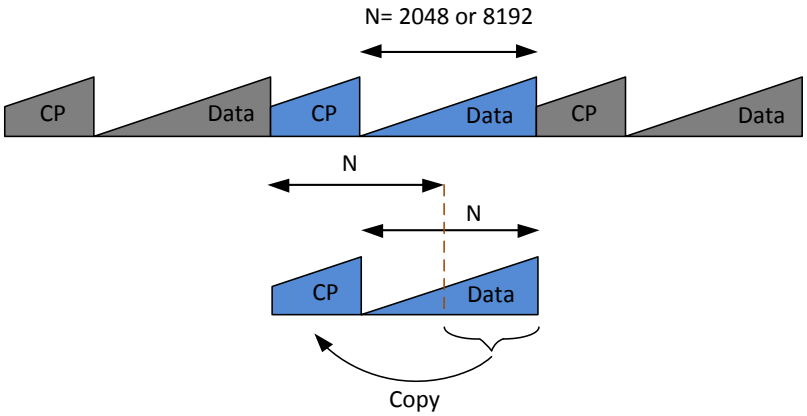

Figure 2.1: Cyclic Prefix insertion

Reed-Solomon[9] code acting as a block code corrector. The second stage applies a convolutional corrector code that always gives a 1/2 code rate, to obtain the other available code rates a puncturing process is applied.

DVB-T also offers the possibility of using hierarchical modulations [10]. This modulation technique allows to have a better quality of service where the signal power is high enough to demodulate the whole information, in locations where the signal power is low only basic information is detected.

2.2.1.4 Interleavers

In DVB-T two interleavers are defined. The first one, known as outer interleaver, is a convolutional interleaver and shuffles the data bits after the Reed-Solomon coding. The main objective of this interleaver is to protect the data stream against long burst errors. The second interleaving process takes place after the convolutional encoding and consists of a combination of a bitwise interleaving and a blockwise one. In the first one, the bits inside of 126 bits blocks are interleaved and after the blocks themselves are also shuffled. This interleaver protects the data stream against frequency selective propagation scenarios.

2.3 DVB-T2

The DVB-T2 standard [3] was released in 2009. This standard was developed by the DVB Project to substitute its already obsolete predecessor, DVB-T. One of the main commercial requirements set for the DVB-T2 development was a capacity increase over 30% when compared with DVB-T. This target was widely cleared, having DVB-T2 up to a 70% capacity gain over DVB-T. This is possible thanks to the state of the art techniques applied to the physical layer of the standard. The main commercial requirements set for DVB-T2 were:

- DVB-T2 transmissions must be able to be received by the already existing domestic antennas, also they must be able to reuse the already existing transmission structures in order to reduce the deployment barriers.
- DVB-T2 is oriented to fixed and portable reception, being mobile one a secondary objective.
- DVB-T2 must provide a capacity gain greater than 30% over DVB-T.
- DVB-T2 must provide service oriented robustness.

The full list of commercial requirements that were set for DVB-T2 can be found in [11].

2.3.1 Physical layer

DVB-T2 presents a physical layer which takes some features from its predecessors, DVB-T and DVB-S2. From DVB-T it takes its modulation scheme (COFDM) and from DVB-S2 the FEC (Low Density Parity Check + Bose Chaudhuri Hocquenghem, LDPC+BCH). Moreover, DVB-T2 used cutting edge technologies by the time it was developed (the final version was released in 2009 as stated before), adding interleavers and new configuration parameters that made it a much more flexible standard than its predecessors.

For the frame building, the DVB-T2 standard compliant systems take as input one or more digital data streams that are carried into PLPs (Physical Layer Pipes). A PLP has direct correspondence with a data channel in the modulator.

Due to the fact that every data channel can offer different services and then require different quality parameters, each PLP can have a different configuration of the physical layer depending on the necessities of the transported service. Figure 2.2 shows how the physical layer can be divided into 4 functional parts, input processing, Bit Interleaving Coding and Modulation (BICM), frame builder, and OFDM generation.

The first block performs the adaptation to the upper layer (as stated before the input data consists of one or more PLPs), then the BICM is performed. From Figure 2.2 it can be seen that the first process to be carried out in the BICM is the FEC encoding, using LDPC block codes with different code lengths available (16K and 32K). The resulting bits are interleaved and mapped into the different available constellations. As a novelty, after mapping bits into constellations, a diversity technique known as Rotated Constellations is applied, which target is to improve the performance into severe propagation scenarios. This technique will be widely studied during the dissertation in chapter 3. Finally the cells (a sub-carrier of the OFDM symbol) inside a same FEC block will be interleaved and also a time interleaver will be applied. After the BICM block the frame builder generates a single OFDM symbol stream from the input PLPs and the signalling information. This stream is not complete yet, in the last stage the OFDM generator applies the MISO (Multiple Input Single Output) processig if enabled, it inserts pilots and reserves carriers for PAPR (Peak to Average Power Ratio) reduction purposes, then applies the corresponding IFFT (Inverse Fourier Fast Transform) and adds a cyclic delay and the special signalling symbols (P1 and P2).

As it can be seen DVB-T2 presents many novelties compared to its predecessor DVB-T, in the following subsections the more relevant ones will be briefly explained.

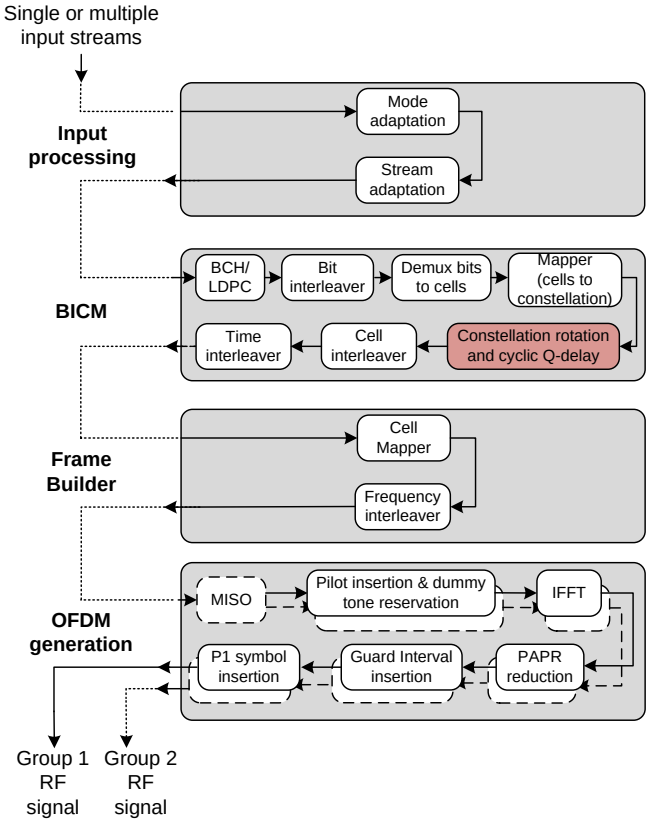

Figure 2.2: DVB-T2 block diagram

2.3.1.1 Additional bandwidths

For professional use DVB-T2 includes 10 MHz bandwidth (communication between cameras and mobile studios), this mode is not expected to be available for traditional consumers.

In order to make DVB-T2 able to operate in narrower RF channels assignations (as III and L bands) a 1.712 MHz mode (suitable for mobile applications) is also included.

2.3.1.2 Extended carrier mode (for 8K, 16K, and 32K)

The higher the number of carriers of the mode the more abrupt its spectrum is attenuated outside the interest band. Also increasing the number of carriers allows to increase the amount of data in a OFDM symbol. The gain that can be obtained is between 1.4% in 8k mode and 2.1% in 32k mode. This feature is optional due to the fact that it is not compatible with the critical spectrum mask defined in [3] so it can only be applied when the normal one is accepted as shown in Figure 2.3.

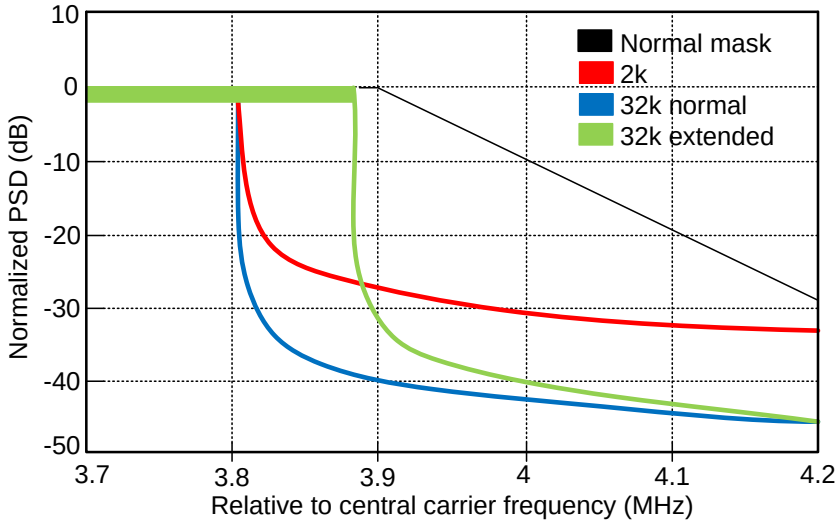

Figure 2.3: DVB-T2 block diagram

2.3.1.3 Alamouti MISO

DVB-T already supported SFNs, this kind of configurations can lead to a performance degradation due to the presence of similar power signals generating deep fadings. In order to overcome this problem DVB-T2 introduces Alamouti coding (as depicted in Figure 2.4). This MISO system is characterized by transmitting by one antenna an unmodified version of the original stream and by the other one a modified version, in this case the symbols are swapped in pairs (in the frequency domain) and conjugated, additionally one of them suffers a sign inversion. By performing this process at the receiver the signals can be combined in a way that the resulting SNR is higher. The extra complexity introduced by the use of this technique is negligible at the receiver side.

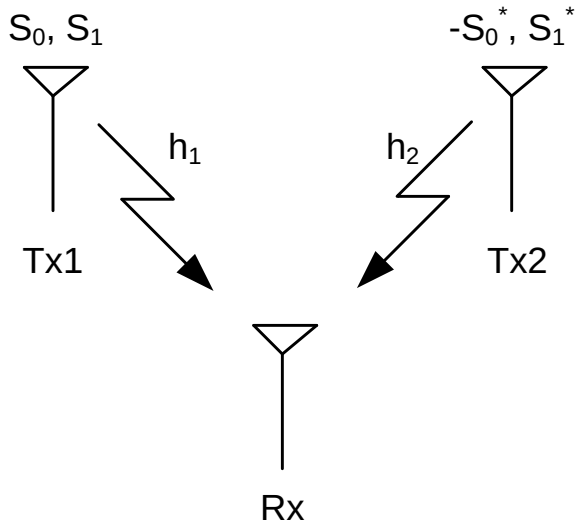

Figure 2.4: Alamouti MISO transmission scheme

2.3.1.4 Preamble

The OFDM symbols of a DVB-T2 signal are grouped in frames that start with a preamble composed by several special symbols, P1 and P2.

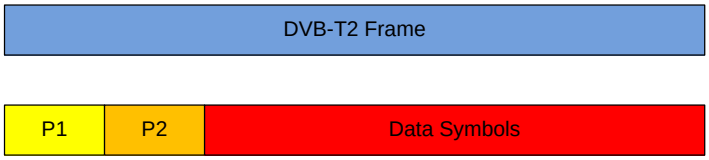

Figure 2.5: Preamble structure in the DVB-T2 frame

The P1 symbol is used for temporal and frequency synchronization tasks. It is modulated with a BPSK constellation and guard intervals are included at the beginning and the end of the symbol.

After the P1 symbol there are one or more P2 symbols (depending on the FFT size). These symbols carry the static, dynamic and configurable signalling information for the physical layer. The first group of bits have a predefined codification and modulation, the rest of the bits can be modulated using QPSK, 16-QAM or 64-QAM but have a fixed code rate of 1/2. P2 symbols can also contain data from the common PLP or the data PLPs.

2.3.1.5 Pilot patterns

As in DVB-T, pilot carriers are defined in DVB-T2 for different purposes (channel estimation, synchronization, ...). Among them three different types can be distinguished: scattered and continual.

Scattered pilots have defined phase and magnitude and are mainly used for channel estimation. These pilots are inserted into the DVB-T2 signal in regular time and frequency intervals, as explained in [3]. DVB-T used a fixed scattered pilot pattern, DVB-T2 offers a higher flexibility having 8 available scattered pilot patterns. The usage of the different pilot patterns depends on the FFT size and the guard interval selected, having as main target to reduce the pilot overhead maintaining a good channel estimation quality. In the example shown in Fig-

ure 2.6 and Figure 2.7 it can be seen how the pilot overhead is reduced from 8% to a 4% by using the pattern named PP3 [3] instead of PP7 with a guard interval of 1/8. One of the pilot patterns, PP8, is conceived to be used by receivers with data based channel estimation.

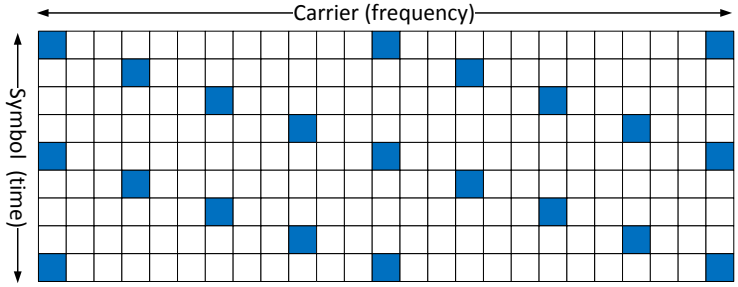

Figure 2.6: PP7. Pilot pattern used in DVB-T

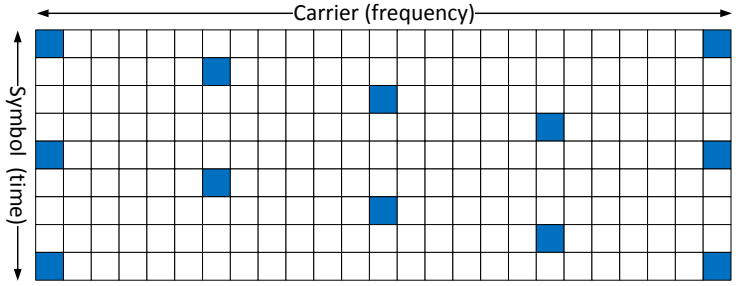

Figure 2.7: PP3

For continual pilots the overhead percentage reduction depends also on the FFT size, leading to a reduction that varies from 2.7% for the 8K mode to 0.7% for the 32K mode, without affecting the performance of the fine frequency synchronization neither of the detection algorithms based on Continual Pilots Estimation (CPE).

2.3.1.6 High order constellation

In DVB-T the higher order constellation was 64-QAM, having a rate of 6 bits per symbol and carrier. In DVB-T2, the use of 256-QAM, depicted in Figure 2.8,

increases this rate to 8 bits per symbol and carrier, representing an increase of a 33% in spectral efficiency and capacity for a given code rate. This constellation will require a higher SNR (about 5dB higher depending on the propagation scenario and the code rate used in the FEC).

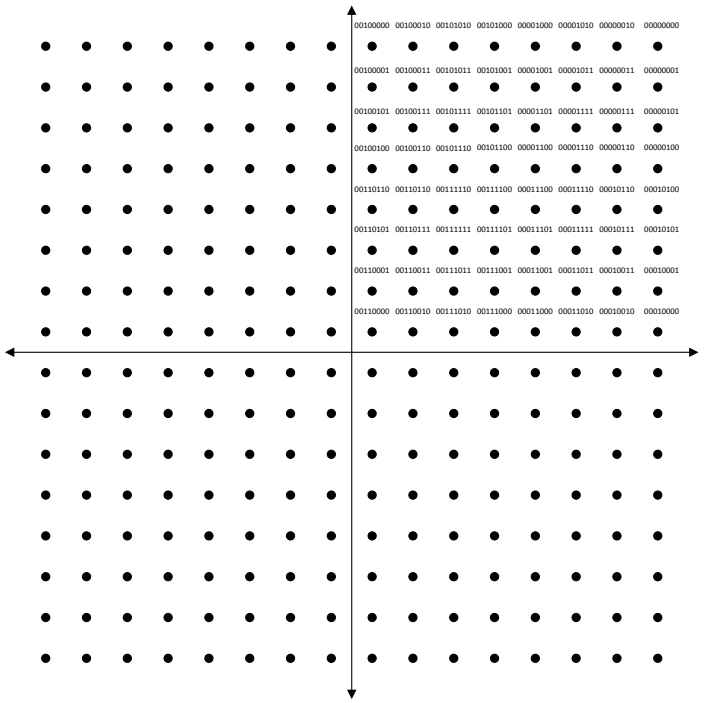

Figure 2.8: 256-QAM constellation

As the rest of constellations the 256-QAM follows a Gray mapping in order to minimize the errors while detecting the signal, this can be observed in Figure 2.8 for the first quadrant, the rest of the quadrants are symmetrically distributed (the two most significant bits determine the quadrant where the point lies).

2.3.1.7 Rotated Constellations

Rotated constellations was one of the promising innovations introduced in DVB-T2. This technique consists in applying a rotation in the complex plane to the original QAM constellation and after to perform a cyclic delay in the quadrature

component (Q), that's why it is known as Rotated Constellation and cyclic Q delay (RQD). The shape of the constellation after the rotation process and the cyclic Q delay can be observed in Figure 2.9.

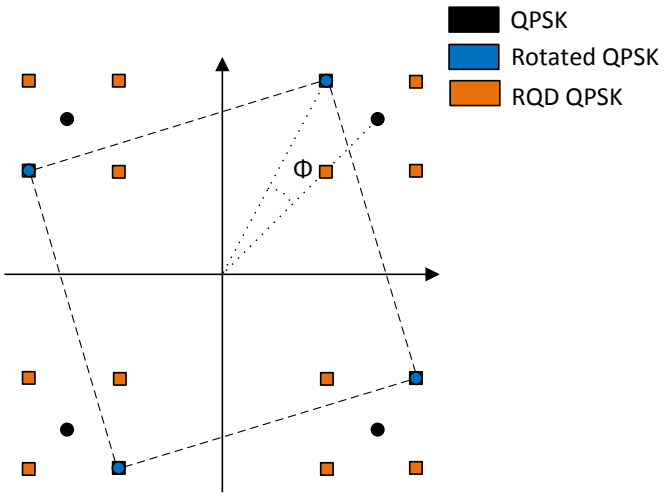

Figure 2.9: QPSK constellation, rotated QPSK, and RQD QPSK

Once the constellation is rotated each component (in phase and quadrature) has enough information to determine what point was transmitted. However if the carrier is attenuated or erased by a fading event the information is lost, that's why a cyclic Q delay is performed, if one of the components is erased the remaining one, that is transported by another subcarrier, will be enough at the receiver side to perform a correct detection. This technique will be widely studied in chapter 3, being one of the main topics in this PhD. dissertation.

2.3.1.8 16K and 32K FFT sizes

Increasing the FFT size leads to a smaller spacing between carriers in the frequency domain and to a longer time duration of the OFDM symbol. The first consequence of a higher FFT size is a higher sensibility to the Doppler dispersion. This makes high FFT sizes less suited for mobile reception. The higher time duration of the OFDM symbol brings an advantage when adding the guard

interval, for a given guard interval duration the guard interval fraction is smaller when the symbol is longer in the time domain. As an example Figure 2.10 shows two different time duration symbols with the same guard interval duration. The overhead reduction in DVB-T2 goes from 2.3% to 17.6%, note that this increases the effective data rate in the same percentage.

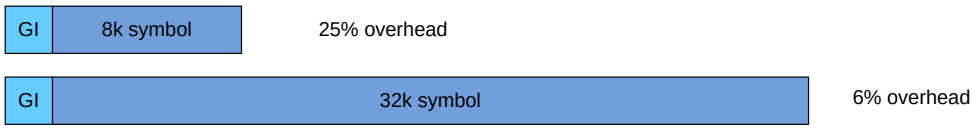

Figure 2.10: Overhead reduction example

2.3.1.9 Forward error correction, LDPC/BCH

FEC codes applied in DVB-T were based in convolutional and Reed-Solomon codes. DVB-T2 applies the codes proposed by Gallager [12], the LDPC. Before the LDPC encoding, a BCH coding is also applied. The LDPC codes have a more complex physical implementation than the convolutional codes but the correcting performance is much higher.

2.3.1.10 Interleaving stages (time, bit, cell, and frequency)

The main target of the interleaving stages is to scatter the information along the frame in the different domains (time, bit, cell, and frequency) so impulsive noise or selective frequency fading don't affect to long consecutive bit sequences of the original data stream.

The most important addition in DVB-T2 is the time interleaver, protecting the data stream from impulsive noise and temporal fading in the propagation channel.

2.3.1.11 PAPR reduction techniques

A high Peak to Average Power Ratio (PAPR) can decrease the efficiency of the RF power amplifier. DVB-T2 introduces two techniques to reduce this undesired

effect in the OFDM signal, ACE (Active Constellation Extension) and tone reservation. These techniques lead to a considerable reduction of the PAPR having as main drawback a slight increase of the average transmitted power (in the case of ACE) or a 1% capacity loss (in the case of tone reservation).

ACE (Active Constellation Extension) reduces PAPR by extending the external points of the constellation in a determinate way, as shown in Figure 2.11. Tone reservation reduces the peaks of the signal in the time domain by using reserved carriers in frequency. Both techniques are complementary, so they can be combined.

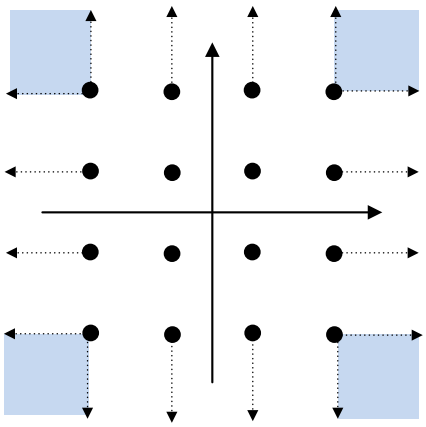

Figure 2.11: ACE technique for 16-QAM

2.4 DVB-NGH

Standards as DVB-H [6] and DVB-SH [13] tried to bring the television to handheld devices in the last two decades, but the lack of a clear business model and the high deployment costs made these standards not to succeed as expected.

The changes in the use habits of the consumers of technological products, tablets and smartphones mainly, have renewed the interest in multimedia broad-

casting for mobile devices. This trend has impulsed the appearance of new technologies that can cope with the consumer's demands.

Digital Video Broadcasting Next generation for Handhelds (DVB-NGH [5]) evolves from DVB-T2 [3] to deal with the demanding mobile environment in the same way that DVB-H did with DVB-T. DVB-T2 is still a reference in terms of robustness, flexibility, and spectral efficiency (offering up to 50% more than any other system existing nowadays), this is the reason why DVB-NGH takes it as a basis. The main target of this standard is to become a reference for mobile broadcasting; in order to achieve this, DVB-NGH is the first mobile broadcasting system using a Multiple Input-Multiple Output (MIMO) scheme in one of its profiles surpassing in this way the Shannon capacity limit for traditional communication systems with only one transmitter/receiver antenna.

The standardization process of DVB-NGH started in 2010 and finished in 2012, but even surpassing nowadays systems performance its commercial success is not clear, there are no plans for a commercial implementation in the moment of writing this dissertation. However, whether it commercially succeeds or not, the usage of state of the art technologies applied in DVB-NGH will make it a reference standard for future generations of broadcasting systems.

DVB-NGH presents 4 profiles, base terrestrial, MIMO terrestrial, hybrid terrestrial/satellite, and hybrid MIMO terrestrial/satellite. The only mandatory profile is the base one, based on the mobile profile of DVB-T2, known as DVB-T2 Lite (and developed during the standardization process of DVB-NGH as a result of it). This profile introduces many technical novelties respecting to DVB-T2:

- Lower code rates for the Forward Error Coding (FEC), down to 1/5.
- Non uniform constellations for 64-QAM and 256-QAM.
- 4 dimension rotated constellations for QPSK.
- Inter frame convolutional interleaver.
- Adaptive cell quantization.
- Improvement of the L1 signalling and overhead.

- Local content insertion techniques (hierarchical and orthogonal).
- New distributed MISO technique known as enhanced SFN (eSFN).

The base profile provides a complete description of the system, the other three only remark the differences with the base one.

The MIMO profile describes a 2x2 system with cross-polarization, allowing spatial multiplexing through the pairs of antennas at the transmitter and the receiver side. The main contributions of this profile are the use of a coding technique called enhanced Spatial Multiplexing (eSM) and a new bit interleaver optimized for iterative decoding.

The hybrid profile allows to complement the terrestrial coverage with a satellite component in the S or L bands. A long time interleaver is added (of about 10 seconds) and Single Carrier OFDM (SC-OFDM) is used.

2.4.1 Base profile

As mentioned previously, DVB-NGH is based in DVB-T2, introducing robustness and spectral efficiency improvements.The block diagram of the base profile BICM of DVB-NGH is shown in Figure 2.12, where the main differences with DVB-T2 are remarked.

As it can be observed, only the short codeword length (16K) for the LDPC is available, new and more robust code rates are adopted. The interleaving memory is halved. The rotated constellations are no longer applied to 256-QAM. 4D rotated constellations are available for QPSK; non-uniform constellations are available for 64-QAM and 256-QAM. The parity interleaver is applied to all the constellations (QPSK included). The I/Q interleaver substitutes the Q-Delay applied in DVB-T2 in order to achieve a better usage of the signal/space diversity separating the I and Q components of the same data the maximum possible in time and frequency. An improvement is introduced in the time interleaver by using a convolutional interleaver for the inter frame interleaving, maintaining the block interleaver only for intra frame interleaving. Adaptive quantization is used to optimize the interleaving memory in low order constellations. As a comparison, with the same memory as in DVB-T2, DVB-NGH can obtain 4 times deeper time interleaving.

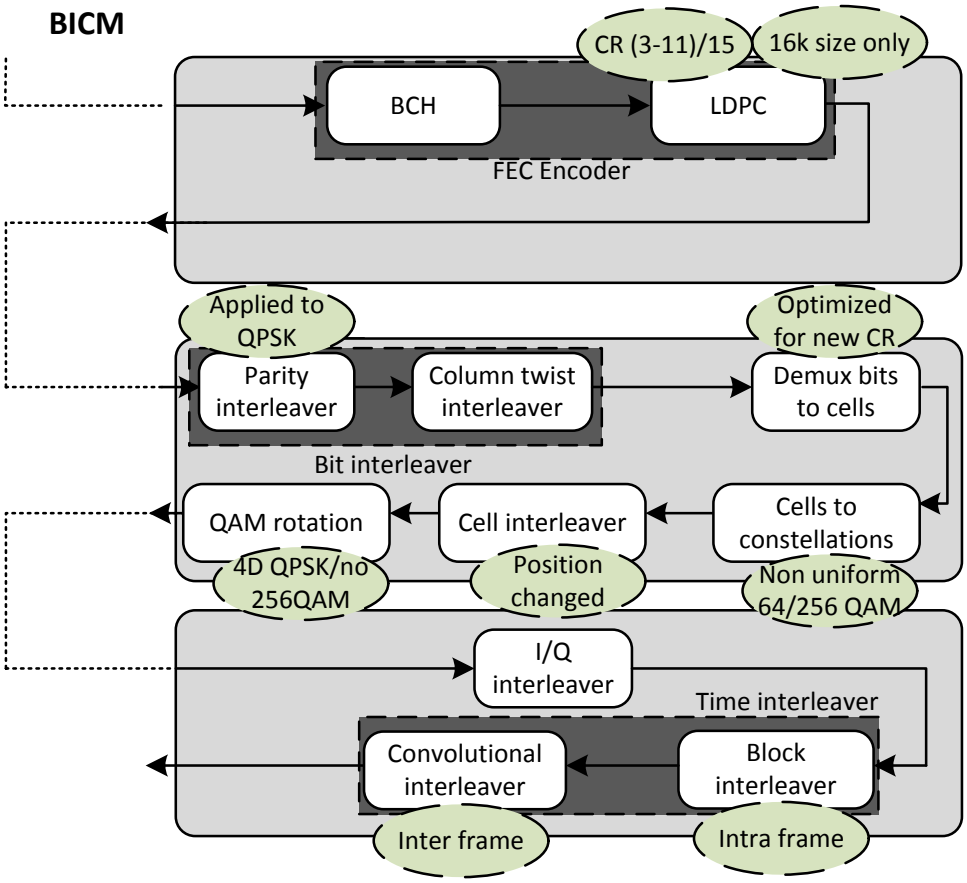

Figure 2.12: DVB-NGH base profile BICM

2.4.1.1 Time Frequency Slicing (TFS)

With this technique the tendency of transmitting services in a single RF channel is changed, TFS consists in transmitting in different RF channels and time instants. It was originally proposed during the DVB-T2 standardization process, but due to the necessity of having two tuners at the receiver side it remained as an informative part of the standard, not normative. TFS can provide very high gain in terms of capacity (due to the improvement in statistical multiplexion) and coverage (due to the improvement of the frequency diversity). It is important to remark that with the current legislation of the spectrum, the licenses are conceded for a determinate channel, this means that the insertion of TFS would need a change in the spectrum management.

2.4.1.2 Local services insertion

Two complementary techniques for local content insertion are adopted in DVB-NGH, hierarchical and orthogonal. Both methods carry a high performance gain when compared to the traditional SFNs, but each one is adequate for different use cases being necessary a study of the scenario to choose the more adequate one.

Hierarchical Local Service Insertion (HLSI) uses hierarchical modulation, that allows to combine two independent data streams in one with different robustness. In hierarchical modulation the local content is transmitted in a stream with low priority over the general content, This is depicted in Figure 2.13, where (a) shows the reception near a global content transmitter, (b) shows the reception of an intermediate point between a global content and local content transmitters, and finally (c) shows the reception near a local content transmitter.

HLSI can be used to transmit local services to areas close to the transmitter, in other areas the reception of local contents can be impossible (as depicted in Figure 2.13 for the **a** terminal). A drawback of this technique is the interference produced between layers, every layer acts as noise to the other, this makes the coverage of the global service decrease.

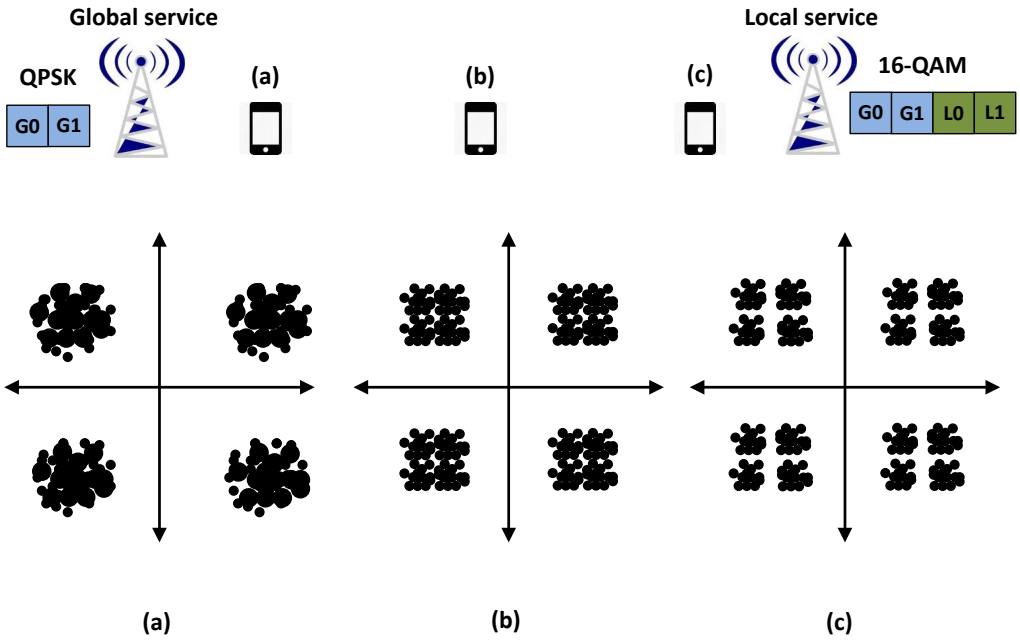

Figure 2.13: Hierarchical modulation scenario example

Orthogonal Local Service Insertion (OLSI) defines a group of subcarriers in OFDM specific symbols that can be used only by concrete transmitters to transmit local services. Each transmitter will have only a subset of this group of subcarriers.

The main benefits of this technique are that the global content is not degraded and that the local content has the same coverage as the global. As a drawback, the gain of SFNs is not fully exploited, unless several transmitters transmit the same local content in the same area.

2.4.1.3 Enhanced Single Carrier Frequency Network (eSFN)

DVB-NGH has adopted the distributed MISO escheme based on Alamouti coding [14] and a novel technique known as eSFN. These techniques are applied through several antennas in a SFN reusing the DTT infrastructure, being compatible with receivers with a single antenna. Alamouti is applied to a couple of transmitter antennas while eSFN can be applied to multiple ones.

eSF is a cyclic delay diversity scheme that consists in applying a linear predistortion function to the signal in a way that the channel estimation at the receiver is not affected. This technique improves the frequency diversity of the channel without needing additional pilots or additional signal processing to demodulate at the receiver. This improves the Alamouti coding, that needs to double the number of pilots in order to estimate each channel's response. eSFN can also be used to identify the different transmitters by using different predistortion functions.

2.4.2 MIMO profile

A MIMO 2x2 with cross-polarization optional profile is defined in DVB-NGH. The aim is to take advantage of all the diversity degrees available in this kind of systems in order to surpass the capacity limits of traditional SISO systems. The standard uses as MIMO coding eSM-PH. This will be explained and widely studied in chapter 5.

2.4.3 Hybrid profile

DVB-NGH contemplates an optional profile in which a satellite component can be used to complement the coverage offered by the terrestrial component. In this profile an extended inter frame time interleaver is defined. SC-OFDM is the selected modulation for the satellite component, in order to reduce the PAPR in hybrid MFNs. The scheduling of the two components must be in a way that the parallel reception of the two signals in receivers with only one tuner is possible. This is achieved thanks to concepts as logic channel and logic channel groups.

In the hybrid profile an external memory is used for the time inter frame interleaver.

2.4.4 Hybrid MIMO profile

A MIMO hybrid profile is contemplated, in this profile MIMO can be used in the terrestrial and/or satellite component. The contemplated cases are one or two terrestrial antennas (linear polarization, cross polarization) and one or two satellite antennas (cross polarization, reverse circular polarization),then enabling the use of up to 4 transmitter antennas. At least one of the components must use 2 antennas, if not the case would be considered in the hybrid profile instead. It is possible to use SFN and MFN configuration. In the case that MFN configuration is chosen, the modulation to use will be SC-OFDM and traditional Spatial Multiplexing (SM) is used instead of enhanced Spatial Multiplexing plus Phase Hopping (eSM-PH). In the SFN configuration the satellite component repeats the terrestrial transmission. The different configurations available are shown in Table 2.1.

Virtual MIMO (VMIMO) is used when there is single polarization in one of the components, this emulates an optimized 2x1 channel, however VMIMO is not practical in the satellite component due to its high requirements in Carrier to Noise Ratio (CNR).

Tx #	Terrestrial	Satellite	Rate 1	Rate 2
2	Single pol.	Single pol.	eSFN, Alamouti	-
3	Dual pol.	Single pol.	eSFN, Alamouti + QAM	VMIMO
3	Single pol.	Dual pol.	eSFN, Alamouti + QAM	VMIMO
4	Dual pol.	Dual pol.	eSFN, Alamouti + Alamouti	eSM-PH eSM-PH + eSFN

Table 2.1: Possible hybrid MIMO profile configurations

Chapter 3

Diversity in DVB-T2

The constantly evolving world of communication systems represents an essential part in the nowadays society, not in vain it is called the information society. The appearance of new devices as smartphones and tablets have taken this social truth to a new stage changing the concept of communication and allowing people to stay permanently connected to a huge resource of information. In this each time more demanding environment the improvement of the communication techniques is a must.

The nowadays state of the art technologies for wireless communications as 802.11(a, b, g, n), 802.16 (WiMax), UMTS (Universal Mobile Telephone System) LTE (Long Term Evolution) are in a very mature state, reaching a capacity close to the Shannon's limit theory [2]. In order to surpass the limitations described by the information theory to this kind of systems it is necessary to use new schemes that provide new propagation paths and hence a capacity increase. The first studies in this field were carried out by Winters [15], Foschini [16] and Telatar [17], and their promising results leaded to a very high interest in this new field.

MIMO techniques represent one of the main investigation lines in the aim of increasing the robustness and capacity in communication systems. Before starting with this kind of schemes it is convenient to carry out an overview of the main precedents of diversity techniques applied in DVB standards, as the one used in DVB-T2 [3] known as Rotated constellations and Q Delay (RQD).

3.1 Introduction

The constellation rotation technique, originally suggested in [18], was introduced in the DVB-T2 standard. This technique was studied in [19]-[20] as a technique to improve the diversity order of BICM scheme over fading channels. Subsequently, in [21] a study about the application of this technique to advanced FEC code solutions such as turbo or LDPC was presented. On the other hand, this technology has been previously applied in different systems as MC-CDMA (Multi-Carrier Code-Division Multiple Access) [22]. This method is also known as Signal Space Diversity (SSD), since its final purpose is to increase the diversity order, that is, to achieve a redundancy in information bits of the coded modulation, to improve the receiver performance, above all in severe propagation scenarios. In this chapter, the principles of this technique are presented. Also, a study in detail of how it is implemented in DVB-T2 is carried out. Finally, some proposals will be presented in order to overcome the main drawback introduced by the use of this technique.

3.2 Rotated Constellation theory

Rotated constellation technique is introduced in the DVB-T2 standard to improve the performance of the system exploiting the frequency diversity that this technique offers. The main principles of this technique consist in rotating the constellation points a certain angle in the complex plane. The aspect of the traditional Quadrature and Amplitude Modulation (QAM) constellation and the one after the rotation can be seen in Figure 3.1(a) and Figure 3.1(b) respectively. As a result of the rotation, if the angle is properly chosen, each of the projections on the imaginary and real axis of the constellation points bear all the information relative to the m mapped bits of the 2^m-QAM constellation. As an example, for a 16-QAM constellation, instead of 4 projections in each axis there will be 16 as it can be followed from Figure 3.1(b).

After the rotation the I and Q components of a same constellation point are separated by an interleaving process. As a result the I and Q components of the same symbol travel in different carriers and time instants. This also makes two

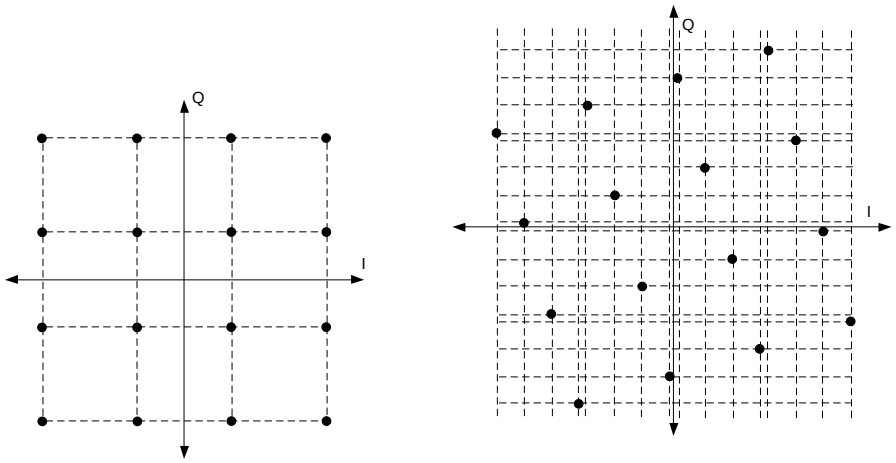

(a) (b)

Figure 3.1: Original 16-QAM constellation(a) and rotated version (b)

different carriers to bear the same information, as if an internal repetition code was used. In the case of a 16-QAM modulation, the resulting "virtual" constellation obtained after the whole process is depicted in Figure 3.2. As it can be easily seen the result is a higher order irregular QAM constellation (256 constellation points), maintaining the spectral efficiency of the 16-QAM. This provides additional diversity that improves the performance when correcting errors derived from the propagation along the transmission channel. When a carrier is attenuated or erased because of a fading, the information in it can still be recovered because it travels also in another carrier.

The optimum rotation angle depends on the order of the chosen modulation, the propagation scenario and the mapping. It is not possible to take into account every possible propagation scenario, hence the rotation angles applied usually are a good trade-off solution; they will not be the optimum for every propagation scenario, but will improve the system performance when compared to the usage of traditional QAM constellations.

Clearly, the main advantage of the rotated constellation technique is that it allows to recover the transmitted information at the receiver's side even in the extreme case when one of the components (I or Q) is completely erased because

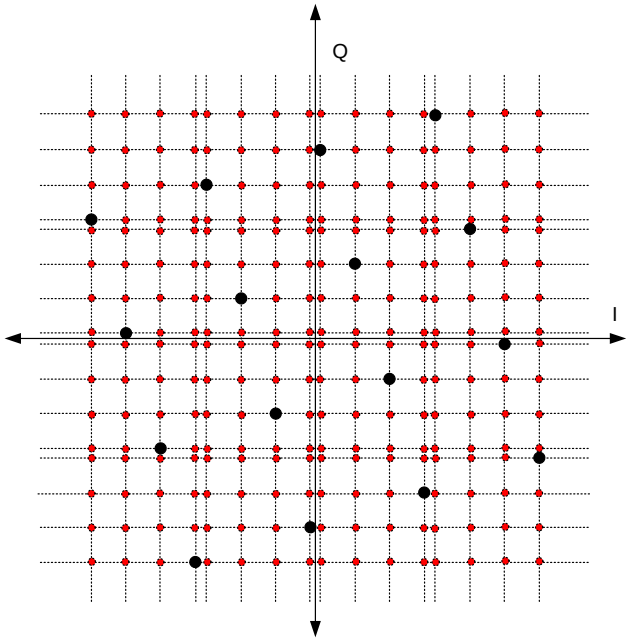

Figure 3.2: Virtual constellation after the RQD process

of the propagation along the transmission channel.

3.2.1 Rotated Constellations in DVB-T2

In a DVB-T2 system, the block that carries out the constellation rotation is included in the BICM scheme, after the bit interleaver and before the cell and time interleavers (that further improve the redundancy obtained by applying the interleaving process to the I and Q components). The position of this block is highlighted in Figure 3.3. After rotating and interleaving the I and Q components, the resulting constellation is similar to sending a higher-order constellation (Figure 3.2), but with optimization of the spectral efficiency as stated in section 3.2. This is observed when the projections of the rotated constellation points on the I and Q axis are carried out. For example, in a M-QAM constellation, if the rotation technique is used, the number of projections on each axis is M. However, if a non-rotated M-QAM constellation is used, the number of projections is on each axis $\sqrt{M}$. In addition, as DVB-T2 specifies the use of Gray symbol map-

ping, I and Q channels of a conventional constellation can be mapped separately as two independent $\sqrt{M}$-PAM. Instead, when a rotated M-QAM constellation is applied, the result is equivalent to map two related M-PAM.

DVB-T2 specification proposes to implement the interleaving process to make I and Q fade independently through a simple cell delay in only one of the two components. This idea was initially suggested in [23]. More precisely, a cyclic delay of an OFDM cell within a FEC block in the quadrature component must be applied. This cyclic Q delay must be removed in the receiver when rotated constellations are used. This is done by delaying the I component another OFDM cell. Thus, both components are aligned.

The LDPC decoding requires the use of soft decisions or metrics, known as Log Likelihood Ratios (LLRs). If rotated constellations are not used, a conventional one-dimensional demapper can be applied. However, in the case of rotated constellations, the classical demapper must be replaced by a two-dimensional LLR demapper. The Implementation Guideline of DVB-T2 [24] describes the main concepts of this demapper and proposes different implementation methods, as the 2D LLR demapper applying the Max-Log approximation, or the 2D LLR demapper with iterative demapping (see section 3.3). The impact on computational complexity is very noticeable due to the need of a 2D demapper, as it will be shown in subsection 3.3.4.

The constellation rotation technique improves the performance of a DVB-T2 receiver in all propagation scenarios, except in Gaussian channels: this kind of channels don't present fading or erasures events and this makes rotated constellations to show no gain nor loss of performance.

3.2.2 Rotation angle in DVB-T2

The rotation angles applied in DVB-T2 standard are chosen trying to have a good trade off in every possible scenario, obtaining a noticeable gain respect to the case when RQD is not used.

The study in which the choice of the rotation angles for DVB-T2 was based is presented in [25]. As a summary, the most important factors taken into account in the selection process are the ones listed below.

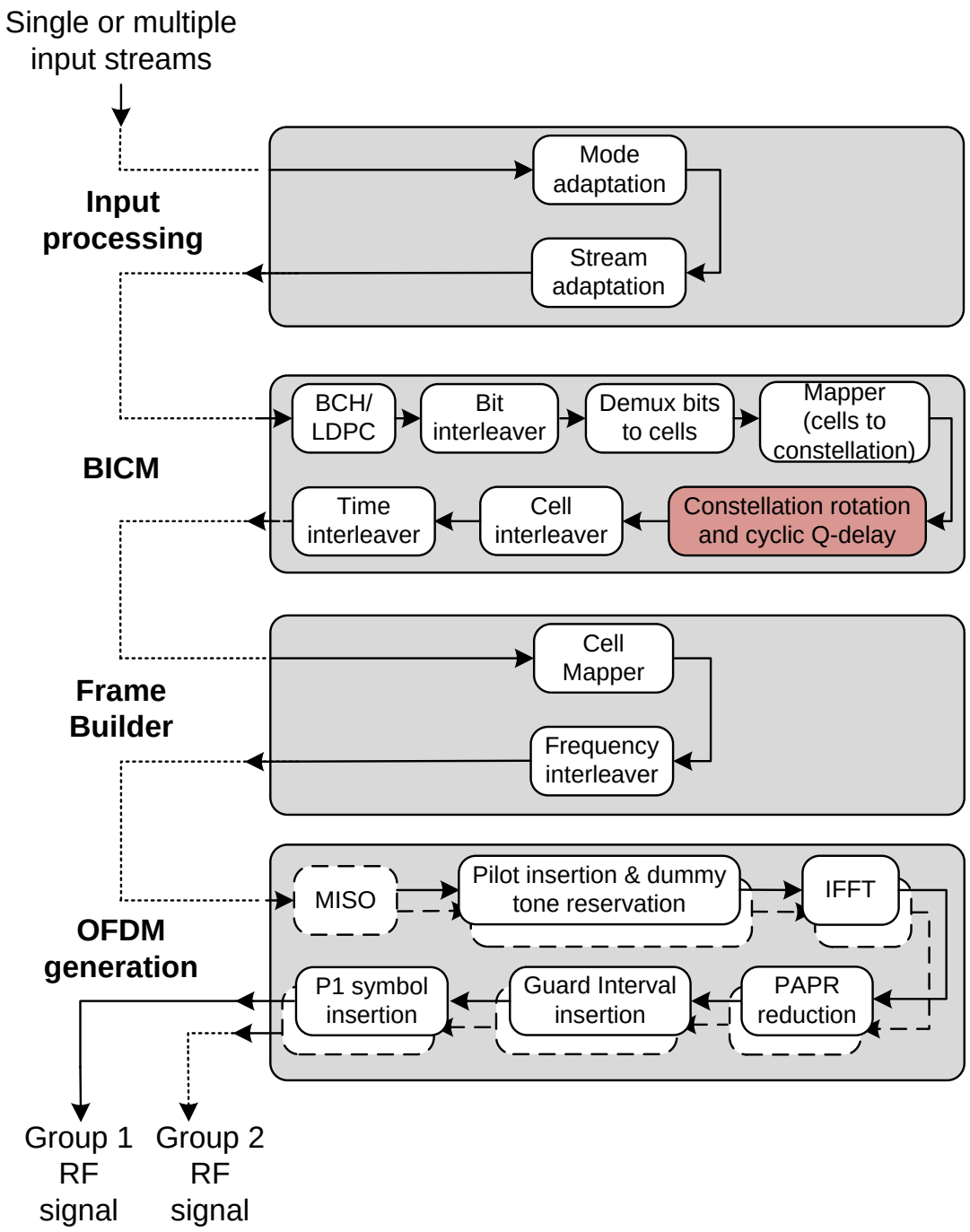

Figure 3.3: DVB-T2 transmission chain block scheme

- Distance Product-L: gives an internal vision of the asymptotic behaviour of the BER curves without coding for channels with fadings. Is a function of the measurement of the 2D distance.
- Minimum 1D distance: It has an important role in the asymptotic behavior of the uncoded BER curves in channels with fadings.
- Minimum bit difference between two neighbor symbols of the constellation with a minimum 1D distance: when the mean bit difference is increased, if an error occurs at the demapper the number of erroneous bits at the output increases leading to a worse performance of the LDPC decoder.
- Mean bit difference between two neighbor symbols of the constellation with a minimum 1D distance after projecting over the axis: when the mean bit difference is increased, if an error occurs at the demapper the number of erroneous bits at the output increases leading to a worse performance of the LDPC decoder.

As a result of the study in [25] the rotation angles used in DVB-T2 are the ones shown in Table 3.1.

Modulation	QPSK	16-QAM	64-QAM	256-QAM
$\theta(^{\circ})$	29	16.8	8.6	atan(1/16)

Table 3.1: Rotation angles in DVB-T2

In Table 3.1, atan(1/16) represents the arctangent of 1/16 expressed in degrees.

3.3 Demapping rotated constellations

In section 3.2 the constellation rotation technique has been introduced, and its main principles explained from the transmitter point of view. In this subsection it will be studied how the detection process is carried out when RQD is used in DVB-T2.

3.3.1 Removing the cyclic delay

The first step to be carried out when demapping rotated constellations is to remove the one cell cyclic delay applied to the Q component at the transmitter side. This can be easily done at the receiver by delaying the I component by a cell. By doing this, the I and Q components of the symbols generated at the transmitter's mapper are allocated again in the same cell.

3.3.2 2D LLR demapping

In the case of traditional QAM constellations with Gray mapping, approximations based on I/Q separation were available to simplify the detection process and its hardware implementation [26]. On the contrary, the use of rotated constellations requires at the receiver side to compute LLRs that are a 2 dimensions function. The scheme of the demapper is as the one presented in Figure 3.4.

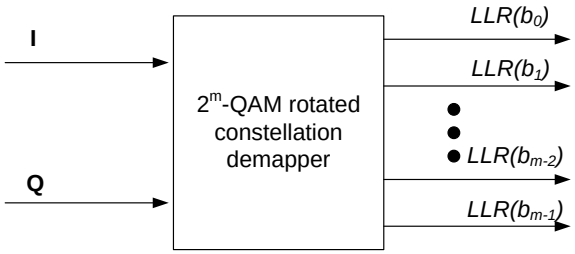

Figure 3.4: Demapper scheme

3.3.2.1 Exact LLR calculation

In order to obtain the LLRs at the output of the demapper (as shown in Figure 3.4) form the received points (I,Q) Equation 3.1 is applied, where b_i represents the i-th bit of the 2^m-QAM symbol and $Pr(b_i = 0|I, Q)$ the probability of the i-th bit being equal to 0 being I and Q received.

$$LLR(b_i) = \ln\left(\frac{Pr(b_i = 1|I, Q)}{Pr(b_i = 0|I, Q)}\right) \tag{3.1}$$

A positive LLR indicates that the bit b_i is more likely to be a "1" whereas a negative LLR indicates that the bit is more likely to be a "0". The problem is how to measure the likelihood level and then how to calculate the LLRs. A certain point of the constellation, x, is transmitted with values I_x and Q_x in its real and imaginary components respectively. Ideally the same values should be found at the receiver, but in a real communications scenario this is far from being true. The carriers that bear I and Q are affected by amplitude fading with factors ρ_I and ρ_Q respectively and noise is added, decreasing considerably the quality of the signal. Taking this into account the conditional probability density function (*pdf*), having transmitted x, can be expressed as shown in Equation 3.2, where σ^2 represents the noise variance.

$$p(I,Q|x) = \frac{1}{2\pi\sigma^2} e^{-\frac{(I-\rho_I I_x)^2 + (Q-\rho_Q Q_x)^2}{2\sigma^2}} \tag{3.2}$$

Considering the reception of a particular bit, b_i, if it was transmitted as "1" implies that any of the 2^{m-1} possible symbols with $b_i = 1$ could had been transmitted. The set of points of the constellation whose i-th bit takes the value j ("0" or "1") will be denoted C_i^j.

The conditional *pdf* for the received values I,Q supposing b_i transmitted as "1" is given in Equation 3.3, where it is supposed that the 2^m possible constellation points are transmitted with the same probability.

$$p(I,Q|b_i = 1) = \frac{1}{2^m \pi\sigma^2} \sum_{x \in C_i^1} e^{-\frac{(I-\rho_I I_x)^2 + (Q-\rho_Q Q_x)^2}{2\sigma^2}} \tag{3.3}$$

The conditional *pdf* for the received I, Q supposing b_i transmitted as "0" has the same aspect as Equation 3.3 but in this case $x \in C_i^0$. Making use of the Bayes theory and supposing the same probability for b_i to take the value "0" or "1", the LLR can be expressed as in Equation 3.4.

$$LLR(b_i) = \ln\left(\frac{Pr(b_i = 1|I,Q)}{Pr(b_i = 0|I,Q)}\right) = \ln\left(\frac{Pr(I,Q|b_i = 1)}{Pr(I,Q|b_i = 0)}\right) = \\ = \ln\left(\frac{\frac{1}{2^m\pi\sigma^2}\sum_{x\in C_i^1} e^{-\frac{(I-\rho_I I_x)^2+(Q-\rho_Q Q_x)^2}{2\sigma^2}}}{\frac{1}{2^m\pi\sigma^2}\sum_{x\in C_i^0} e^{-\frac{(I-\rho_I I_x)^2+(Q-\rho_Q Q_x)^2}{2\sigma^2}}}\right) \tag{3.4}$$

3.3.2.2 Approximate LLR calculation

The calculus of the LLR can be simplified by using the Max-log approximation, that consists in approximating the natural logarithm of the addition of exponentials by the natural logarithm of the maximum exponential in the sum, this is mathematically expressed in Equation 3.5.

$$\ln(e^{a_0} + e^{a_1} + ... + e^{a_n}) \approx \max_{i=0...k}(a_i) \tag{3.5}$$

Applying Equation 3.5 to Equation 3.4 the simplified expression shown in Equation 3.6 can be obtained.

$$LLR(b_i) \approx \min_{x\in C_i^0}((I-\rho_I I_x)^2 + (Q-\rho_Q Q_x)^2)) - \\ \min_{x\in C_i^1}((I-\rho_I I_x)^2 + (Q-\rho_Q Q_x)^2)) \tag{3.6}$$

This method is already proposed in [24].

3.3.3 Iterative demapping

When iterative demapping is used, the scheme shown in Figure 3.4 must be modified to use the extrinsic bit information coming from the LDPC decoder, as shown in Figure 3.5. As it can be seen, the information obtained from the LDPC decoding is used to recalculate the LLRs in a new iteration.

Genie-aided demapping represents iterative demapping when the number of

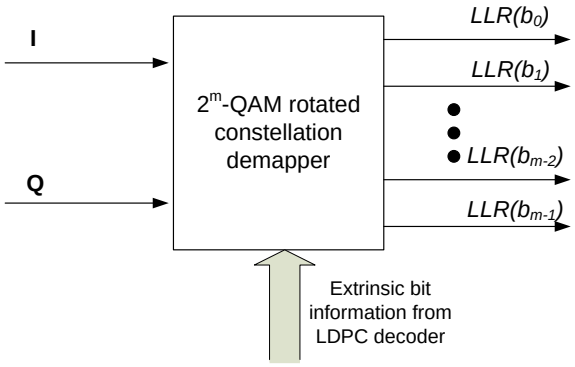

Figure 3.5: Iterative demapper scheme

iterations is infinite, reaching its maximum performance. In this ideal case, it is supposed that there are no errors in the LDPC decoder except in b_i bit. In this situation there are only 2 possible transmitted constellation points, these two points depend on the values of the other bits in the symbol. One of the possible candidates corresponds to $b_i = 1$ and the other with $b_i = 0$. In Figure 3.6 this situation is described for the case of a 16-QAM constellation and $b_3 = 0$, $b_2 = 0$ and $b_1 = 0$.

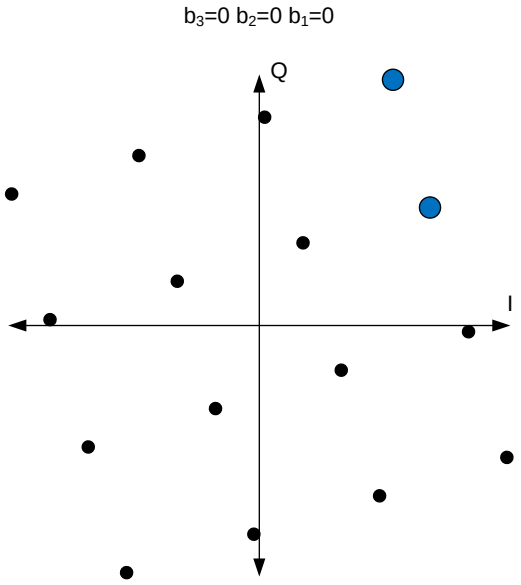

Figure 3.6: Two possible candidates in a genie aided demapping process

Having this conditions the expression for the LLRs can be simplified (Equation 3.7).

$$LLR(b_i) = \ln\left(\frac{e^{-\frac{(I-\rho_I I_1)^2+(Q-\rho_Q Q_1)^2}{2\sigma^2}}}{e^{-\frac{(I-\rho_I I_0)^2+(Q-\rho_Q Q_0)^2}{2\sigma^2}}}\right) \tag{3.7}$$

3.3.4 Complexity problem

As stated in section 3.2, the in-phase (I) and quadrature (Q) components of a transmitted symbol are sent in different carriers and even in different time slots, and thus, affected by independent fadings. As a consequence, many approximations that simplify the traditional QAM detection (as decomposing the QAM signal in 2 independent orthogonal PAMs [26]) cannot be applied because the I and Q components are not uncorrelated any more.

In the case of rotated constellations each LLR is a function of both I and Q components, and they require the calculation of two-dimensional (2D) distances

from the received point to all the selected M-QAM constellation points. For instance, if we consider the highest order constellation in DVB-T2 (256-QAM), 256 Euclidean distances must be calculated for each LLR metric. This is translated into a hardware complexity increase of the demapping process when compared with non-rotated constellations, even when the Max-log approximation is employed.

3.4 Performance improvement

In this section, by means of BER curves simulation results, the performance improvement that can be achieved with the use of the rotated constellation technique will be exposed.

3.4.1 Performance simulations

In order to show the performance improvement of the system that can be obtained when using rotated constellation the whole DVB-T2 transmission chain is used. The simulation model employed is the one provided for the DVB technical module to check the performance of the systems that meet the DVB-T2 standard, known as Common Simulation Platform [7].

Simulations are carried out for different kinds of channels: AWGN, Rayleigh P1, and Rayleigh Memoryless with Erasures (RME).

Rayleigh P1 channel is defined in [4] and also in [24]. It is used to describe the portable indoor or outdoor reception conditions. The channel does not include any Doppler and should therefore be considered as a snapshot of the real time-variant Rayleigh channel.

RME propagation scenario is described in [24] and describes an OFDM system with perfect frequency synchronization over a multipath channel with an arbitrary probability of carrier loss. The gain of the channel is modeled as a Rayleigh process followed by a random erasure with a determinate probability.

In these simulations all the elements are supposed ideal, this means, all the elements work with floating point and infinite precision. To have a wide view of the performance improvement the DVB-T2 system is configured in the two

extreme coding rates available for the LDPC decoder (1/2, the lowest one, and 5/6, the higher) and an intermediate case (3/4 coding rate). Results are shown for 2k mode, guard interval 1/8, and all the constellations available in DVB-T2 (QPSK, 16-QAM, 64-QAM and 256-QAM) except in the case of AWGN scenario, where only QPSK and 256-QAM are presented. Genie-aided provides the best possible performance because of being an ideal case iterative demapping, as stated in subsection 3.3.3, that is why it is used in all the simulations in this subsection. The performance is evaluated by means of BER (measured at the LDPC decoder output) versus C/N curves. For each point of the curves at least 100 erroneous FEC blocks need to be found with a maximum of 50 LDPC iterations.

3.4.1.1 Simulation results for AWGN channel

As it can be seen in Figure 3.7 and Figure 3.8, the gain that can be achieved in this kind of channels is null, as exposed in section 3.2. This is due to the fact that no erasure events occur in this kind of propagation scenarios, only AWGN is added at the receiver.

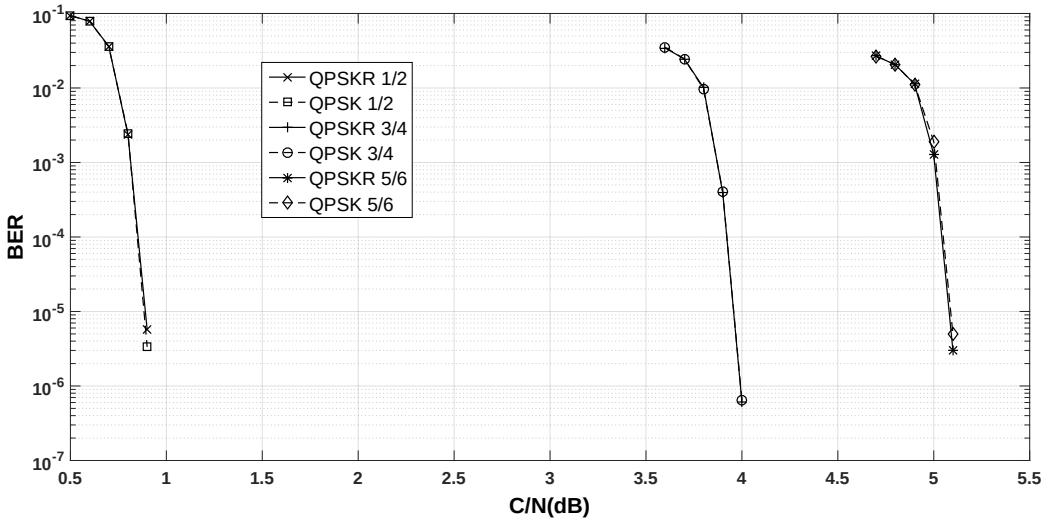

Figure 3.7: Rotated and not rotated constellation performance comparison in AWGN channel for QPSK constellation

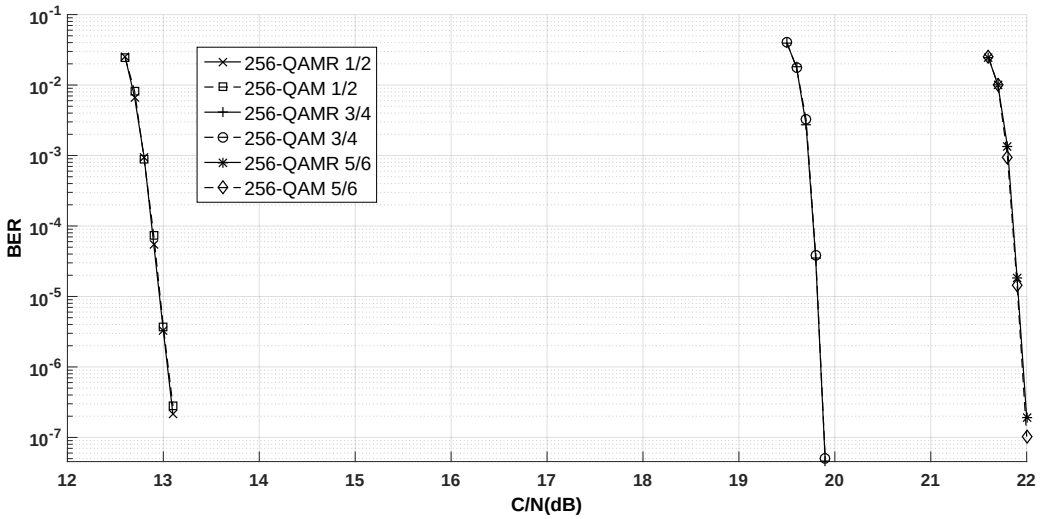

Figure 3.8: Rotated and not rotated constellation performance comparison in AWGN channel for 256-QAM constellation

For the sake of clarity the difference in performance between the traditional QAM constellations and RQD is numerically shown in Table 3.2. As it has been already stated, the performance in an AWGN scenario is practically the same, no gain nor loss is obtained by using RQD.

Constellation	QPSK			256-QAM		
Coding rate	1/2	3/4	5/6	1/2	3/4	5/6
$CN_{QAM+RQD}$	0.9	4.0	5.1	13.0	19.80	21.9
CN_{QAM}	0.9	4.0	5.1	13,0	19,9	21,9
Gain(dB)	0.0	0.0	0.0	0.0	0.1	0.0

Table 3.2: Performance gain in AWGN channel

3.4.1.2 Simulation results for Rayleigh P1 channel

This channel presents flat fading events and according to the theory exposed in section 3.2 RQD should show a performance gain, this can be observed in Figure 3.9, Figure 3.10, Figure 3.11 and Figure 3.12.

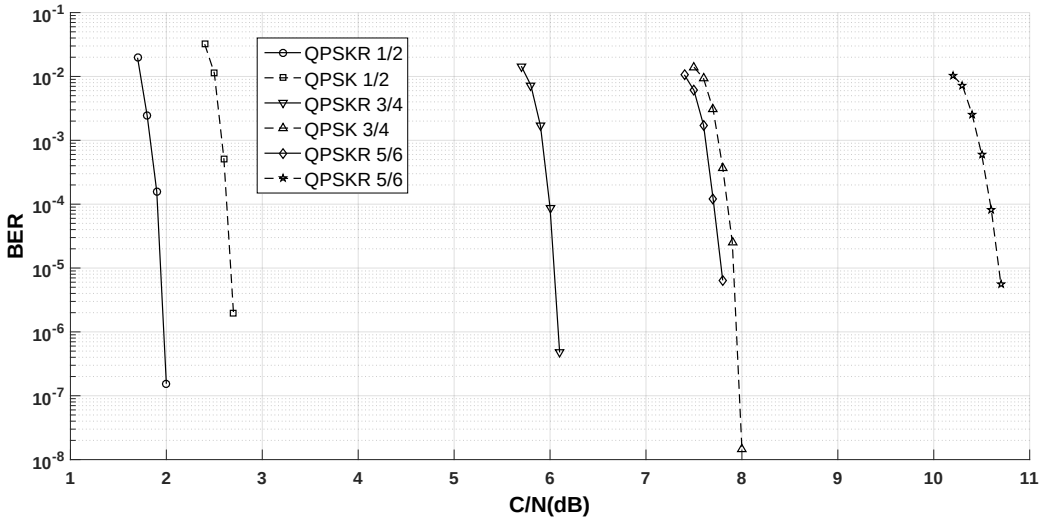

Figure 3.9: Rotated and not rotated constellation performance comparison in Rayleigh channel for QPSK constellation

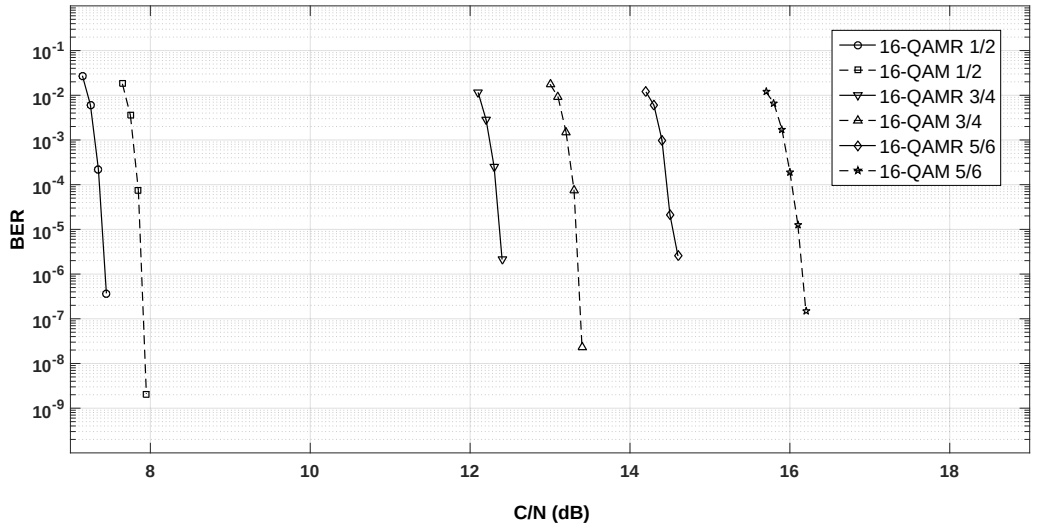

Figure 3.10: Rotated and not rotated constellation performance comparison in Rayleigh channel for 16-QAM constellation

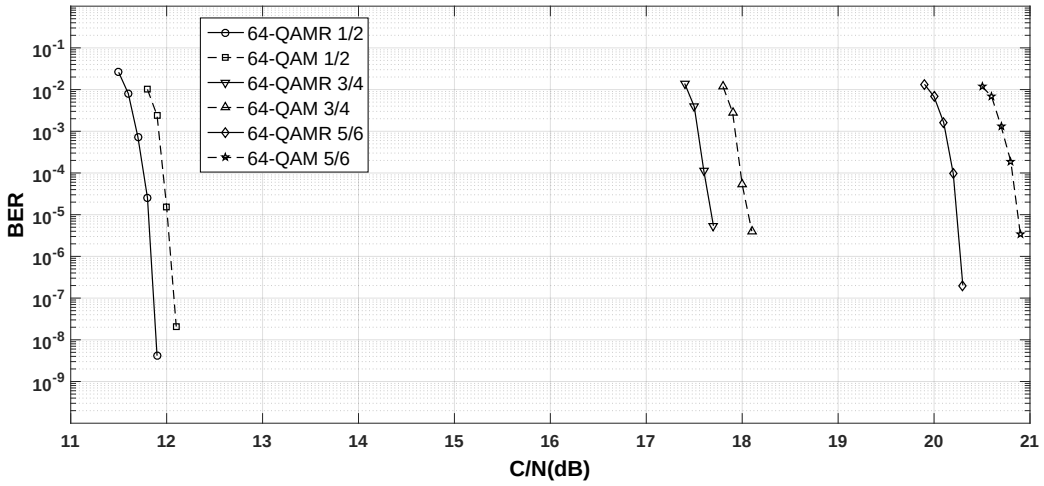

Figure 3.11: Rotated and not rotated constellation performance comparison in Rayleigh channel for 64-QAM constellation

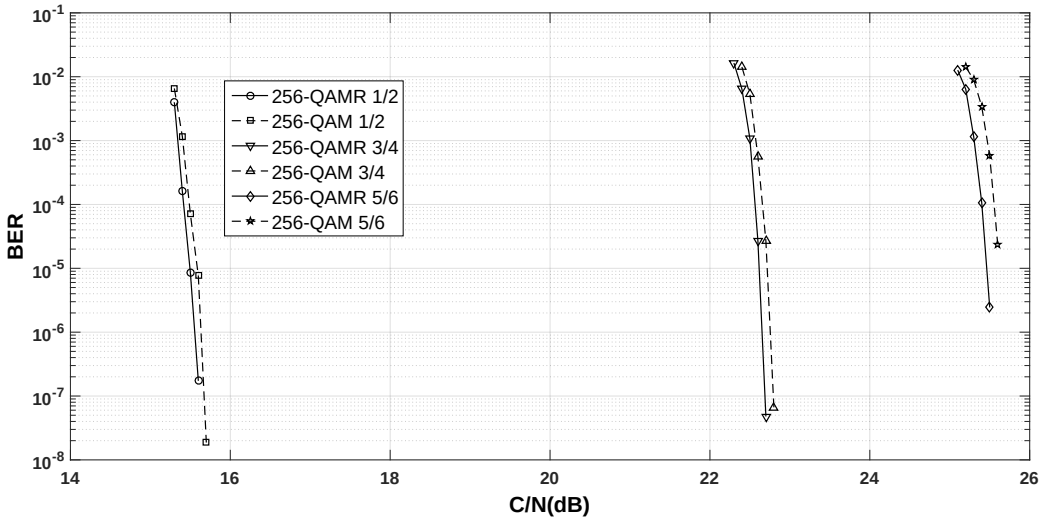

Figure 3.12: Rotated and not rotated constellation performance comparison in Rayleigh channel for 256-QAM constellation

Table 3.3 summarizes the performance improvement that can be achieved in P1 channel measured at a BER of 10^{-5}. A maximum gain of 1.9dB can be obtained.

Constellation	QPSK			16-QAM		
Coding rate	1/2	3/4	5/6	1/2	3/4	5/6
$CN_{QAM+RQD}$	2.0	6.1	7.8	7.5	12.4	14.6
CN_{QAM}	2.7	8.0	10.7	8.0	13.3	16.1
Gain(dB)	0.7	1.9	2.9	0.5	0.9	1.5
Constellation	64-QAM			256-QAM		
Coding rate	1/2	3/4	5/6	1/2	3/4	5/6
$CN_{QAM+RQD}$	11.9	17.7	20.3	15.5	22.7	25.5
CN_{QAM}	12.0	18.1	20.9	15.6	22.8	25.6
Gain(dB)	0.1	0.4	0.6	0.1	0.1	0.1

Table 3.3: Performance gain in Rayleigh channel

3.4.1.3 Simulation results for RME channel

Due to the random carrier loss that emulates this channel model, the gain obtained by using rotated constellations compared to traditional QAM constellations is very appreciable, and more when the carrier lost ratio increases. In the simulations results shown below, the carrier loss ratio has been set to 0.2 (a 20% carrier loss). In these simulation results it can be observed that some configurations cannot reach the BER target of 10^{-5}. This always applies to configurations that don't use RQD, so when comparing them to the ones using RQD the gain will be represented as infinity.

Table 3.4 summarizes the performance improvement that can be achieved in RME channel measured at a BER of 10^{-5}. A maximum gain of 9.8dB can be obtained when the reception is still possible not using RQD. In some cases the reception cannot be performed without RQD in those cases the gain has been represented using ∞.

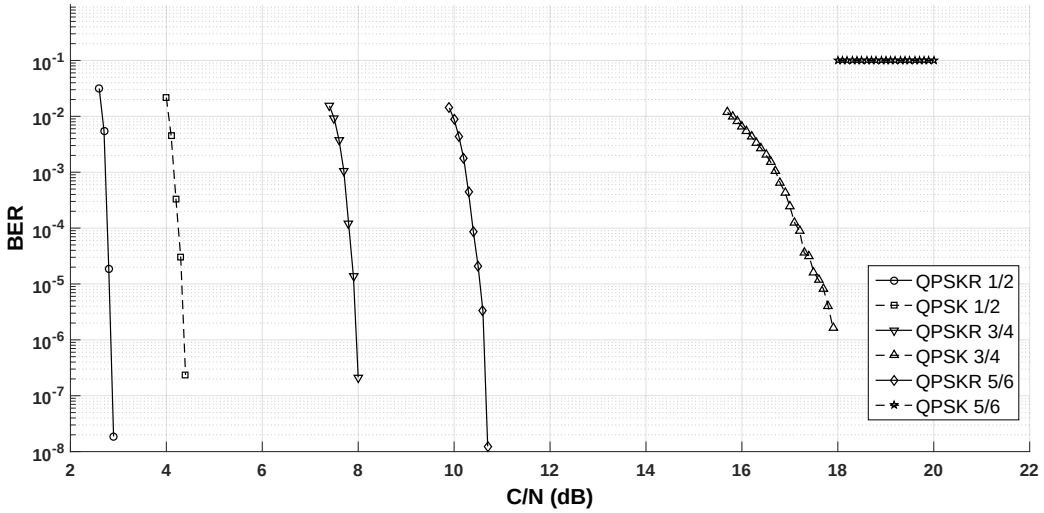

Figure 3.13: Rotated and not rotated constellation performance comparison in RME channel for QPSK constellation

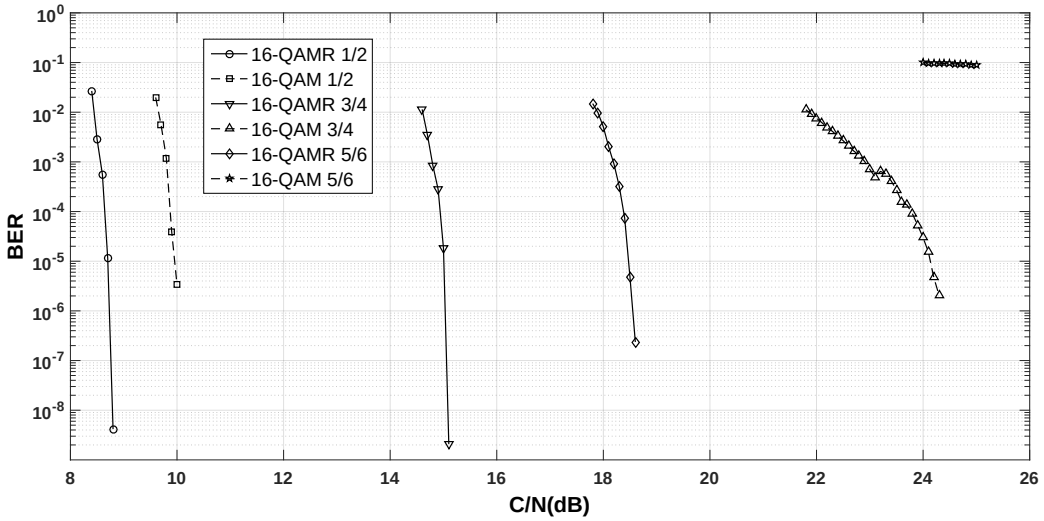

Figure 3.14: Rotated and not rotated constellation performance comparison in RME channel for 16-QAM constellation

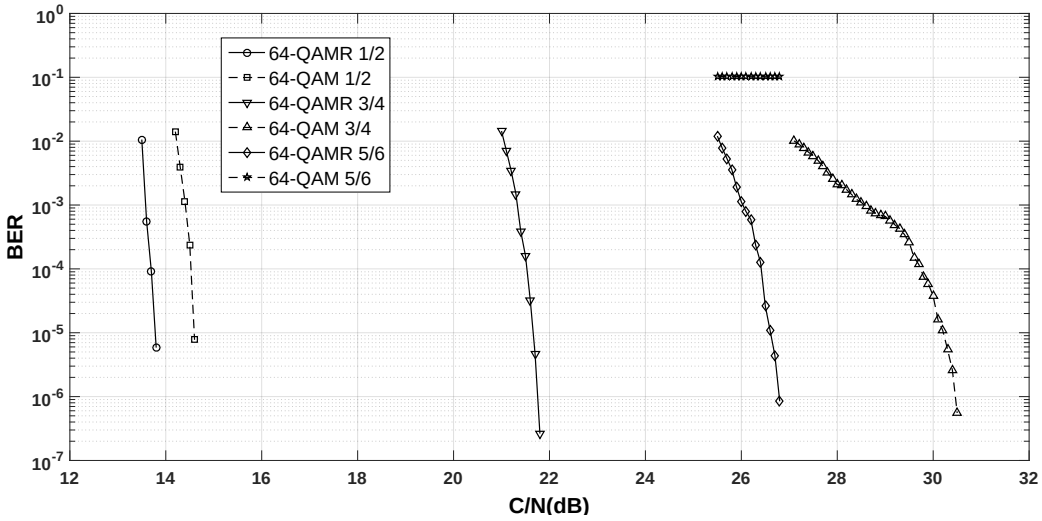

Figure 3.15: Rotated and not rotated constellation performance comparison in RME channel for 64-QAM constellation

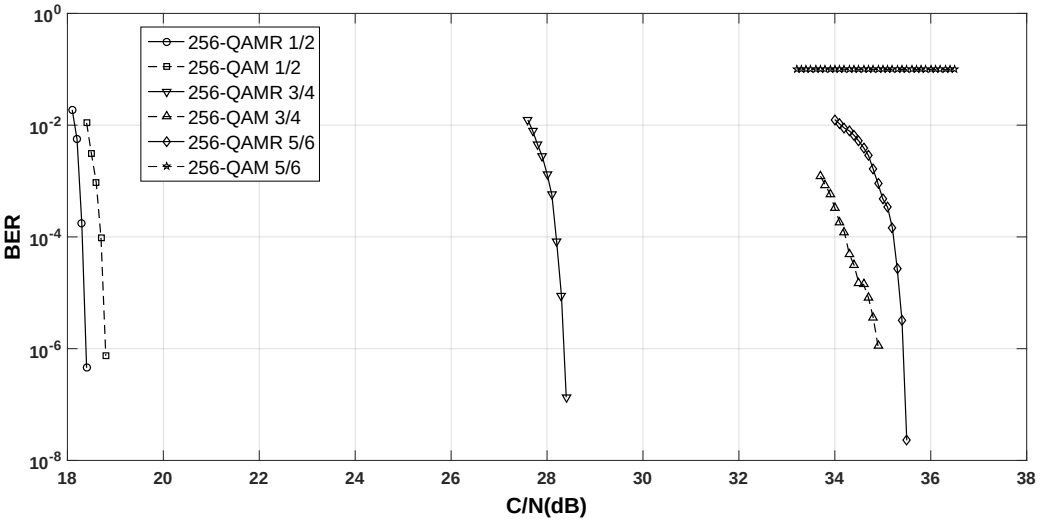

Figure 3.16: Rotated and not rotated constellation performance comparison in RME channel for 256-QAM constellation

Constellation	QPSK			16-QAM		
Coding rate	1/2	3/4	5/6	1/2	3/4	5/6
$CN_{QAM+RQD}$	2.9	7.9	10.6	8.7	15.0	18.5
CN_{QAM}	4.4	17.7	∞	10.0	24.2	∞
Gain(dB)	1.5	9.8	∞	1.3	9.2	∞
Constellation	64-QAM			256-QAM		
Coding rate	1/2	3/4	5/6	1/2	3/4	5/6
$CN_{QAM+RQD}$	13.8	21.7	26.7	18.4	28.3	35.4
CN_{QAM}	14.6	30.2	∞	18.8	34.7	∞
Gain(dB)	0.8	8.5	∞	0.4	6.4	∞

Table 3.4: Performance gain in RME channel

3.4.1.4 Results summary

As it has been shown in section 3.4, the use of rotated constellations only brings advantages in performance terms. In order to achieve a same BER level, if rotated constellations are used, the required C/N is lower (up to 9.72dB improvement can be obtained, when the gain can be numerically expressed). This gain can be translated into a wider coverage area or in the possibility of selecting a less robust LDPC coding rate and then achieving a higher capacity (more data is transmitted instead of redundancy).

From the simulation results it can be concluded that the lower corrector capacities the selected coding rate has the higher gain can be obtained by using rotated constellations. The other factor that influences the gain achieved is the constellation order, the higher the constellation density is, the lower gain can be obtained.

3.5 RQD demapping simplification

As shown in this chapter, the RQD technique adopted by the DVB-T2 standard [3] increases the robustness of the receiver in severe multipath propagation scenarios. The main drawback of the RQD technique is the high complexity of the

required LLR demapper. As shown in section 3.3, for each received point, the demapper must compute the Euclidean distances to all the M-QAM constellation points.

In this section simplification methods based on different approaches will be exposed. In the first approach the number of distance to compute will be reduced based on statistical properties, whereas the second will focus on approximating the Euclidean distance calculation for a more simple function in terms of hardware implementation.

3.5.1 Constellation candidates reduction

This first approach is based on reducing the amount of constellation points to which an Euclidean distance must be calculated in order to compute de LLRs needed by the LDPC decoder.

3.5.1.1 Quadrant division

Depending on the quadrant in which the received point lies in the complex plane, the 2D distances are computed to a reduced subset of the entire constellation, decreasing the number of required operations and so the hardware complexity of the demapper. It will be shown that, if the subsets are carefully selected, this method will have a negligible impact on the system performance while still reducing the hardware complexity.

In the case of a Max-log LLR demapper, the subsets can be easily determined analysing the histogram of the minimum 2D distances (see Figure 3.17). The histogram is constructed as follows: for all the points received in a particular quadrant (the number of received points is set to ten millions), the constellation symbols that are more likely to be at the minimum distance are determined, also the probability of occurrence of each of them. The subset for this particular quadrant will be determined by the N symbols with greatest occurrence probability, where N is the number of constellation points in the subset.

The resulting histogram for a 256-QAM constellation and a point belonging to the first quadrant is shown in Figure 3.17 (the same analysis can be carried out for all the quadrants). For the sake of clarity, the first, second and fourth quadrants

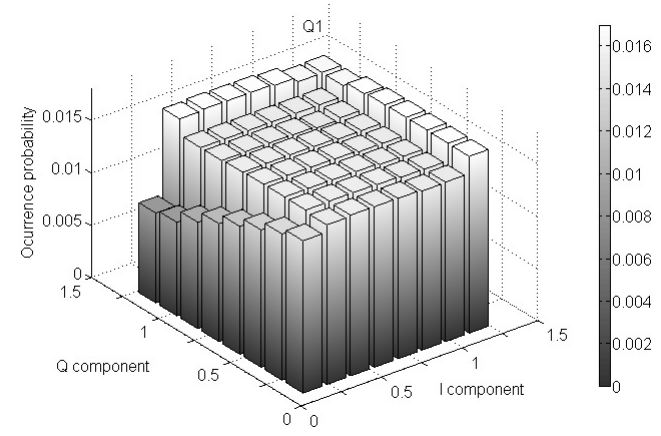

(a)

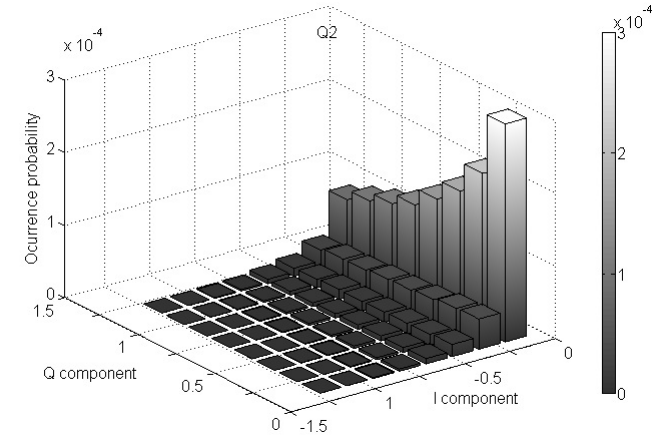

(b)

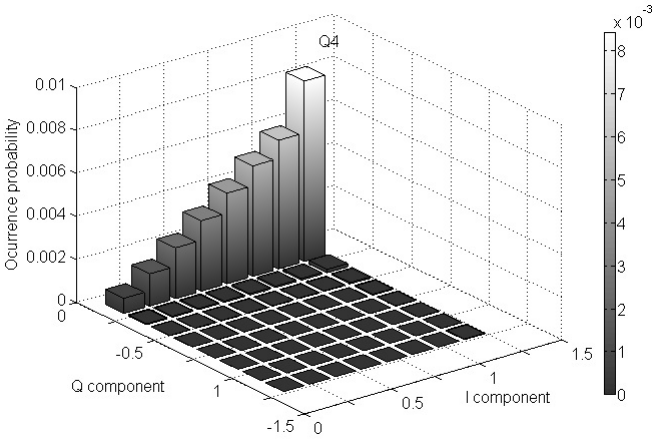

(c)

Figure 3.17: 1rst quadrant(a), 2nd quadrant(b) and 4th quadrant(c) histograms

(Q1, Q2 and Q4 respectively) have been depicted separately. The histogram of the third quadrant (Q3) has been omitted because, in this case, the occurrence probability is close to 0.

Consequently, in the case a point in Q1 is received, it is clear that the constellation points of Q3 may be ignored in the computation of the LLRs, which means a 25 % reduction in the number of operations. Moreover, we will see in the following section that some points of Q2 and Q4 can be also removed from the subset, having a negligible impact on the system performance.

3.5.1.1.1 Performance results

The impact of the proposed demapper on the system performance has been analyzed via BER curves at the output of the LDPC decoder of a DVB-T2 system. The results have been obtained by using the DVB-T2 CSP [7].

All the simulations presented here have been obtained for a 256 QAM, a LDPC block size of 64.800 bits, ideal channel estimation, different code rates (CR), and the worst case channels defined in [24], a Rayleigh memoryless channel, setting the erasure events to a 15% of the carriers. Figure 3.18 shows the five reduced subsets that have been evaluated for the proposed demapper. These subsets correspond to different reductions in the number of required operations (see Table 3.5). The losses have been obtained comparing the BER curves to the ideal Max-log demapper performance and measuring the difference in terms of C/N at a BER of 10-4.

Subset	1	2	3	4	5
Reduction in the number of operations	25%	31%	37.5%	44%	50%

Table 3.5: Subset reductions(%)

Figure 3.19 shows the BER curves for the five subsets and the ideal Max-log LLR demapper in the case of a CR of 3/4. It can be seen that the subset number 2, which corresponds to a 31% reduction, has a negligible impact on the system performance. In the case of the subset number 4, a 44% reduction can be obtained, but the losses are increased to 0.5dB.

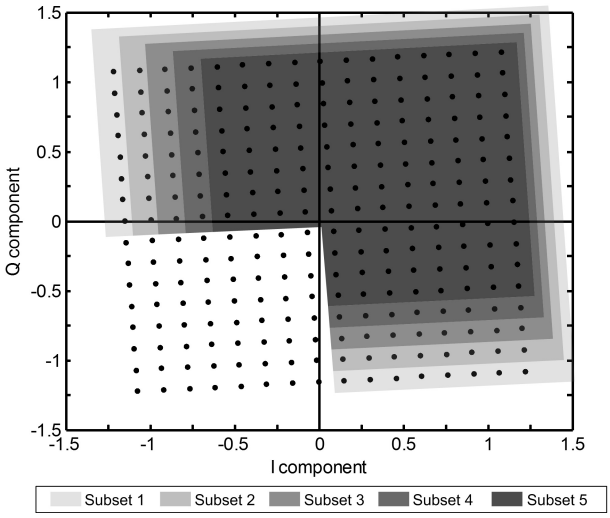

Figure 3.18: Used subsets for the 256-QAM constellation

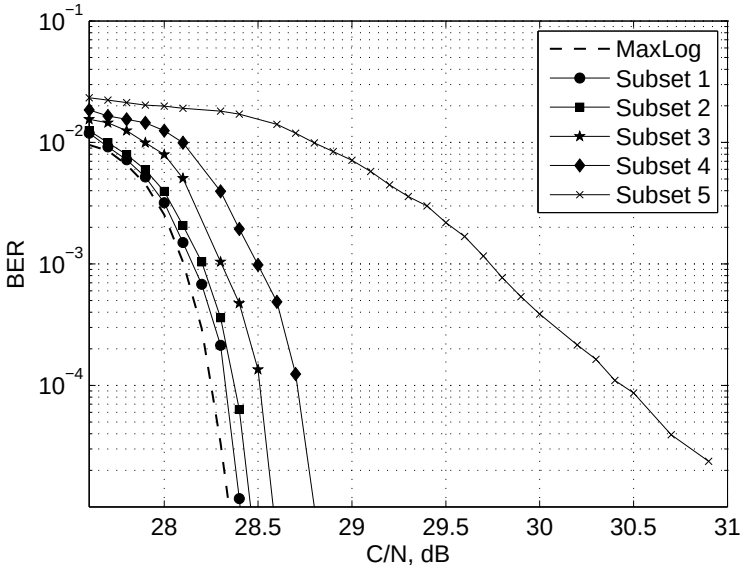

Figure 3.19: Performance of the studied subsets for 3/4 LDPC code rate

Figure 3.20 shows the losses compared to the ideal Max-log demapper for different code rates and for the five proposed subsets. For the most robust code rates, CR=1/2 and CR=2/3, the losses are always below 0.2dB for all the subsets. However, in the case of the less robust code rates, CR=4/5 and CR=5/6, only the first and second subsets have losses below 0.2dB. That is, for optimum performance, a 31% reduction in the number of operations can be obtained by using the subset number 2. For more realistic scenarios (like a Rayleigh) simulations have shown that the reduction can be even higher with no loss in system performance.

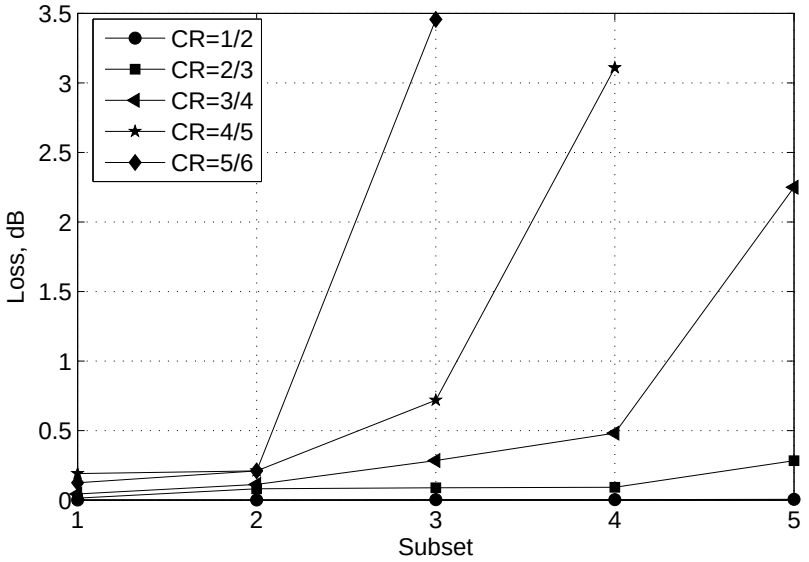

Figure 3.20: Performance loss for each subset and coding rate

The results shown in this subsection were published in [27].

3.5.1.2 Subquadrant division

In subsubsection 3.5.1.1, depending on the quadrant in which the received point lies in the complex plane, the 2D distances are computed to a reduced subset of the entire constellation, decreasing the number of required operations and so the hardware complexity of the demapper. Making a good choice of the subsets will lead to a complexity reduction with almost no performance loss, as simulations

results will show. These subsets are easily determined by analyzing the histogram of the minimum 2D distances. That is, for all the points received in a particular subquadrant, the constellation symbols that are more likely to be at the minimum distance are determined. Then, the subset for this particular subquadrant is composed of the symbols with greater occurrence probability.

In this section a technique similar to the one proposed in subsubsection 3.5.1.1 is used, but applied to subquadrants instead of quadrants. That is, depending on the subquadrant where the symbol is received a subset is selected and used to compute the LLR values.

Note that the quadrant is easily determined using the sign of the in-phase and quadrature components of the received point. Once the quadrant is known, the subquadrant can be obtained performing a simple subtraction and analysing the resulting sign.

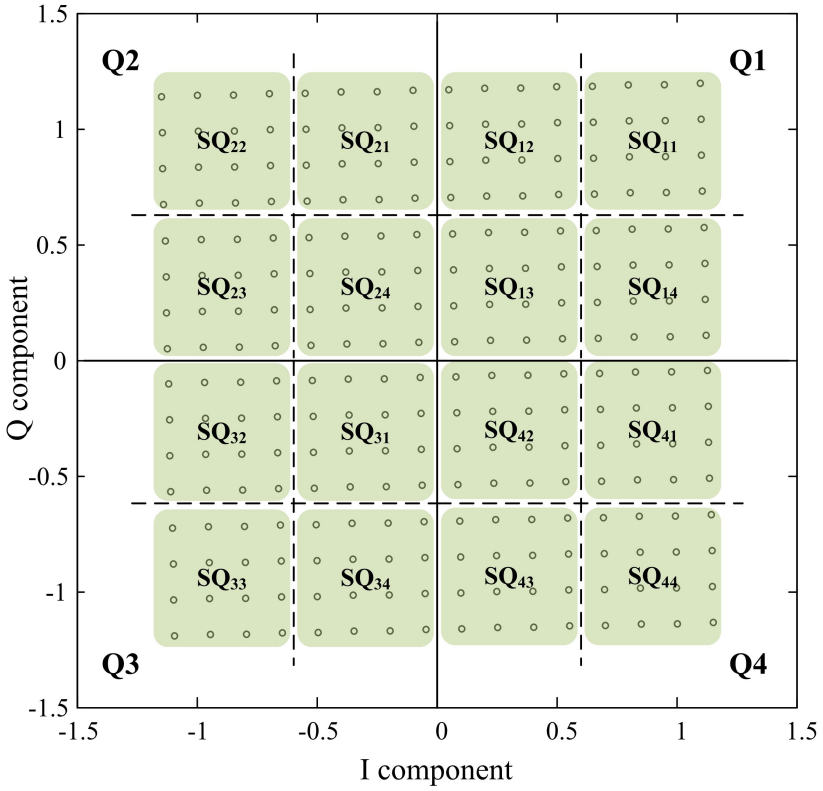

Figure 3.21: Subquadrants division

Figure 3.21 depicts the quadrants (Q) and subquadrants (SQ) assignment for a 256-QAM rotated constellation. Although there are 16 subquadrants, only 4 subsets are actually required, which correspond to the four subquadrants of any quadrant. The rest can be derived from these four due to the symmetries of the constellation.

In order to determine these four subsets, 4 histograms have to be computed, one for each subquadrant of a quadrant. An example of these histograms is shown in Figure 3.22 for the particular case of a point received in SQ11 subquadrant. For the sake of brevity only the histograms of the subquadrants with more significant occurrence probability are shown. In the particular case of the quadrant Q3 and the subquadrant SQ13 these probabilities were almost zero.

Therefore, when receiving a point in SQ11, the probability that the closest point falls in Q3 is almost zero. That is, it seems that all the points belonging to this quadrant can be ignored in the computation of the LLRs with a negligible performance loss. This means a reduction of a 25% in the number of distances to be calculated. Additionally, from the analysis based in subquadrants, points in SQ13 also seem to be negligible which would be an additional reduction of a 6.25%. However, the size of the subsets can have a big impact on the system performance. The definition of these subsets will be analysed carefully by means of system simulations in the following section.

3.5.1.2.1 Performance analysis

The impact of the proposed demapper on the system performance has been analyzed via bit error rate (BER) curves at the output of the LDPC decoder of a DVB-T2 system. The results have been obtained by using the DVB-T2 Common Simulation Platform [7]. All the simulations presented here have been obtained for a 256 QAM, a LDPC block size of 64.800 bits, ideal channel estimation, and all the code rates specified in DVB-T2 standard.

The procedure we have used to determine the optimum subsets is as follows. First, the histograms for the four subquadrants have been computed transmitting 10^9 constellations points over an ideal Rayleigh channel. This number is more than enough to have an appropriate resolution. Note that from Equation 3.4

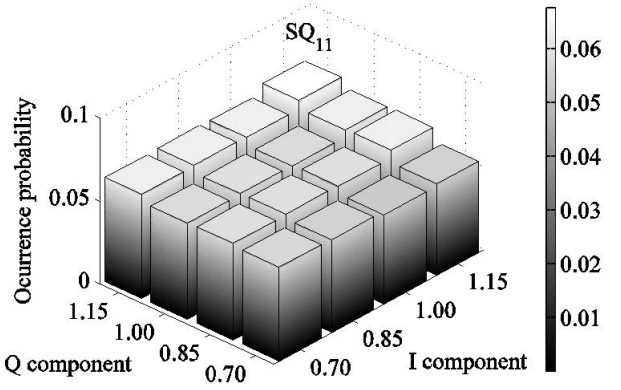

(a)

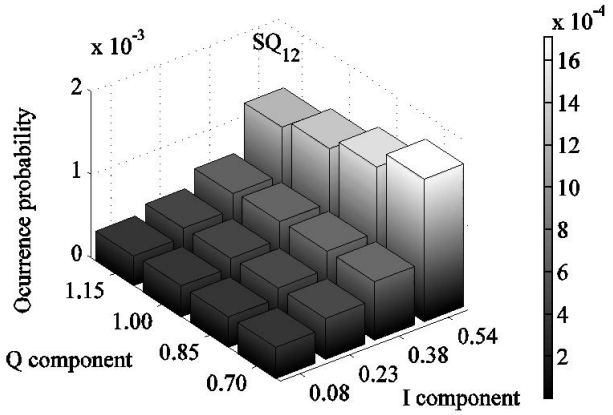

(b)

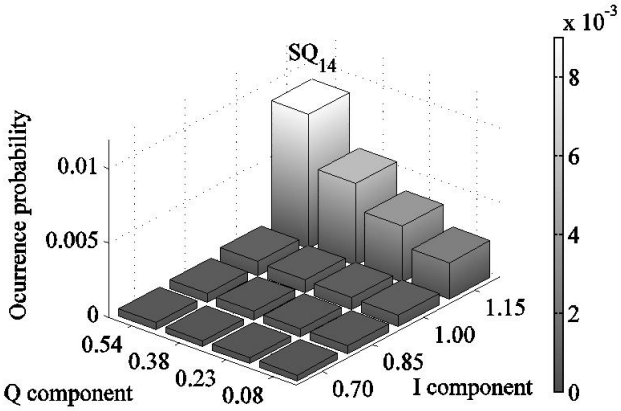

(c)

Figure 3.22: 1rst subquadrant(a), 2nd subquadrant(b) and 4th subquadrant(c) histograms

these histograms have to take into account not only the closest symbol but the closest symbol with a "1" in the bit under study and also the closest one with a "0". Second, for each subquadrant, the constellation points are sorted based on the results of the histograms. That is, for each subquadrant we now have a vector with all the points of the constellation, 256 points in the case of a 256-QAM, sorted by their occurrence probability. Finally, the subsets are defined from these vectors keeping the N points with a higher probability.

In order to determine the minimum value of N, simulations have been run for different channel scenarios and different coding rates, although the results presented here are the ones corresponding to the worst coding rate case. All the loss results presented in this Ph.D. dissertation have been measured at a BER of 10^{-6}.

For the sake of simplicity, the same number of points for each subset has been used. However, after a deeper analysis of the histogram and the simulation results, it has been found that the optimum value of N varies depending on the subquadrant. Nevertheless, in a real receiver, the complexity of the demapper will be determined by the maximum value of N so it would have no benefits to use a different value for each subquadrant.

The results have been divided in three subsections: the first one for the more realistic channels like the typical P1 channel defined in [4] or even the 0dB echo channel, the second one for the worst case scenario defined in [24], a Rayleigh memoryless channel with erasures, and finally, in the third subsection the impact of a real channel estimator is analyzed.

Results for the P1 and the 0dB echo channels

Figure 3.23 shows the BER curves of the system for different values of N, a CR of 5/6, and the P1 channel. The results for the ideal Max-log demapper are also shown for comparison purposes. From this figure it can be seen that with only 36 points, the performance degradation of the system in terms of C/N is negligible (under 0.1dB). Just for illustrating purposes, the resulting subset for SQ11 and N=36 is depicted in Figure 3.24.

Figure 3.25 and Figure 3.26 show the BER curves for the code rates 3/4 and

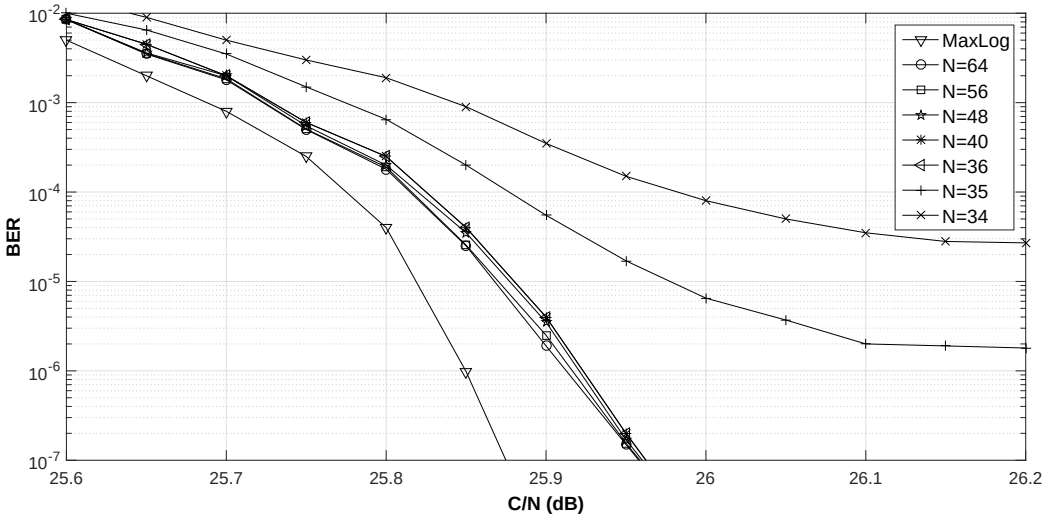

Figure 3.23: Performance for 5/6 CR in the P1 channel

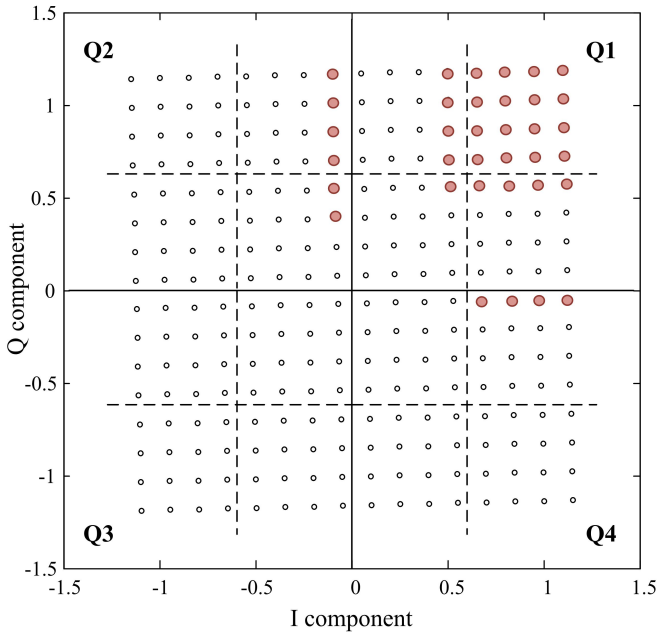

Figure 3.24: Subset example

1/2 respectively, both for the P1 channel. Each figure shows the curves for N=36 and N=34. Comparing these figures to Figure 3.23, it can be seen that the losses are lower, that is, the lower the code rate the less the difference between the Maxlog approximation and the proposed method.

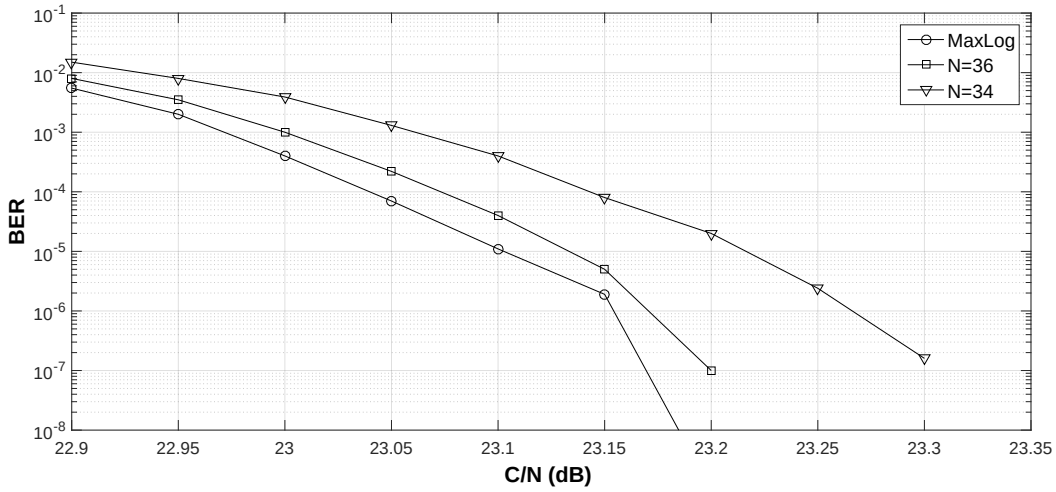

Figure 3.25: Performance for 3/4 CR in the P1 channel

Figure 3.27 shows the same results but for a 0db echo channel with a 95% echo delay. In this case it can be seen that with only 56 points, the performance degradation of the system in terms of C/N is as before, under 0.1dB.

Figure 3.28 and Figure 3.29 show the BER curves for the code rates 3/4 and 1/2 respectively, both for the 0dB echo channel. Each figure shows the curves for N=56 and N=36. As in the P1 channel case, when comparing these figures to Fig. 9 it can be seen that the lower the code rate the less the difference between the Max-log approximation and the proposed method.

In conclusion, in the case of these channels, the size of the subsets can be reduced to only 56 points, a 22% of the total number of points of the constellation. In terms of complexity reduction, the number of 2D Euclidean distances are reduced a 78%, which outperforms the results already presented in [1] and [27].

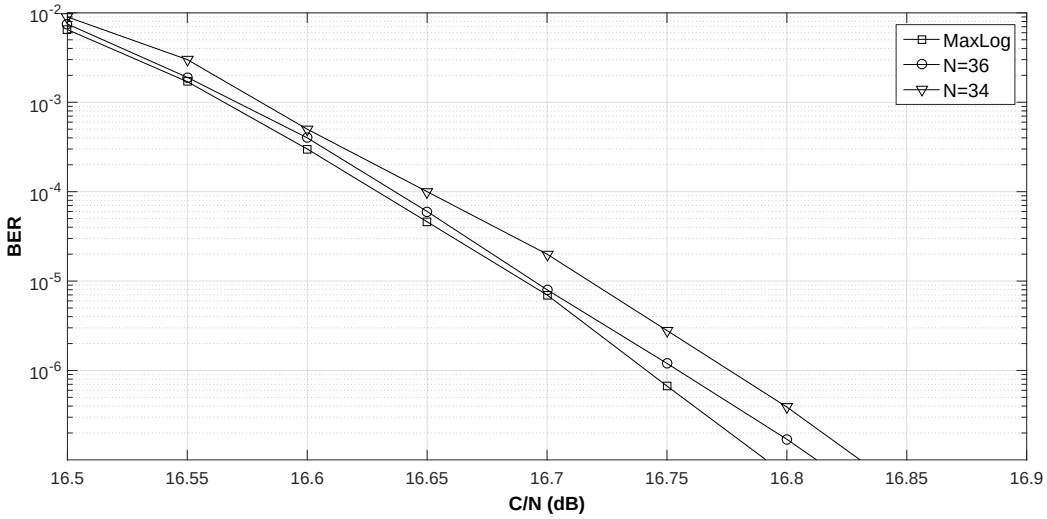

Figure 3.26: Performance for 1/2 CR in the P1 channel

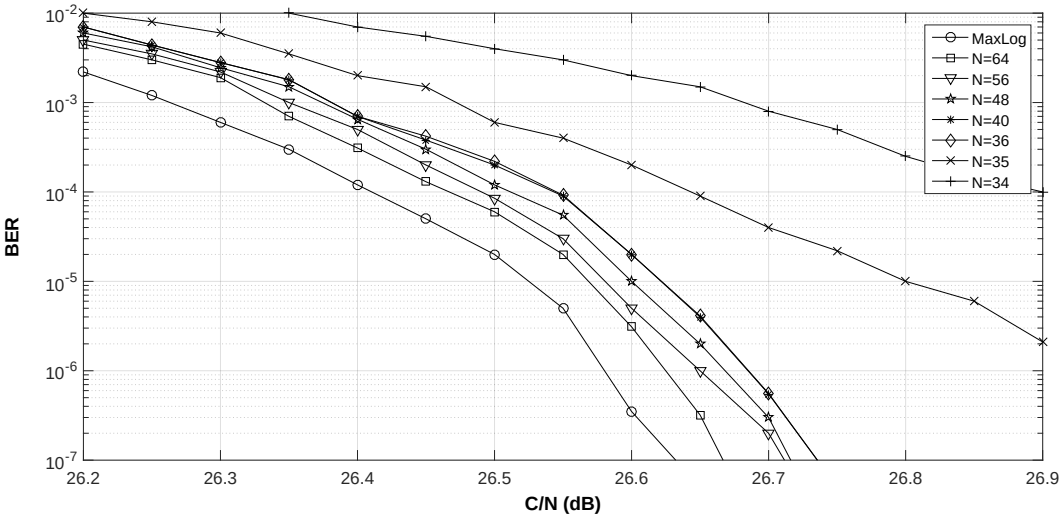

Figure 3.27: Performance for 5/6 code rate in the 0dB Echo channel

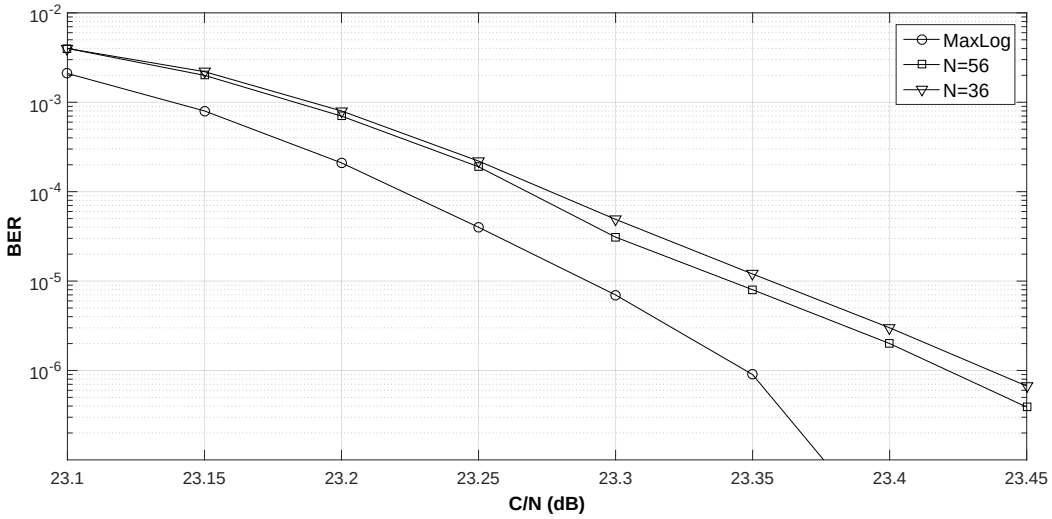

Figure 3.28: Performance for 3/4 code rate in the 0dB Echo channel

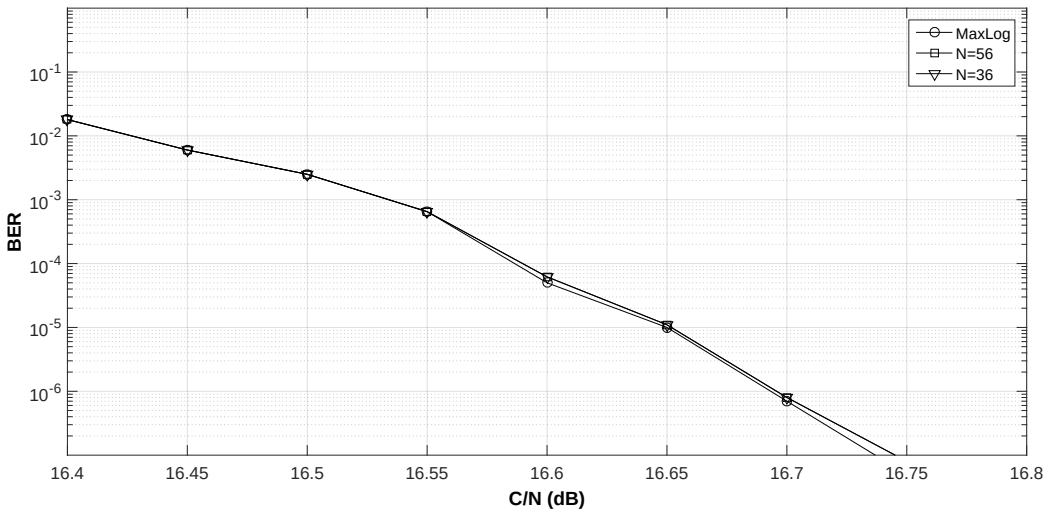

Figure 3.29: Performance for 1/2 code rate in the 0dB Echo channel

Results for RME channel

Figure 3.30 shows the BER curves of the system for different values of N and for an RME channel with 15% of erasure events. The results for the ideal max-log demapper are also shown for comparison purposes. From this figure it can be seen that for a performance degradation under 0.1dB this channel require subsets with a minimum of 152 points.

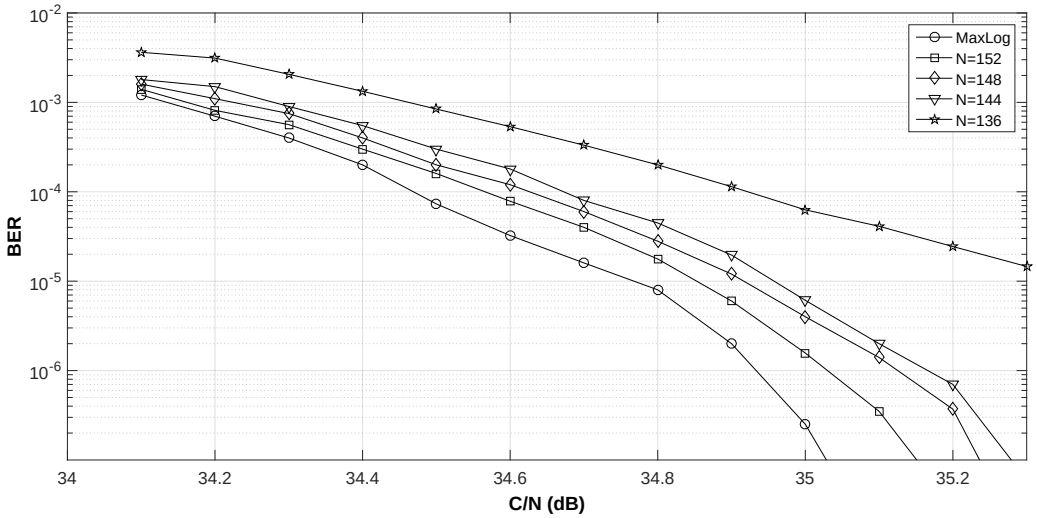

Figure 3.30: Performance for 5/6 CR in the RME channel

Due to the harder propagation conditions of the RME channel, the subsets need more points in order to show a negligible performance loss. Anyway, in terms of complexity reduction, the required number of 2D Euclidean distances is still greatly reduced; a 41% reduction is obtained.

Figure 3.31 and Figure 3.32 show the BER curves for the code rates 3/4 and 1/2 respectively, both for the RME channel. Each figure shows the curves for N=152 and N=144. As in the previous subsection, it can be seen that these more robust code rates show lower losses so the optimization of the subsets can be done focusing on the worst case code rate, that is, CR 5/6.

As stated earlier, the RME channel is clearly the worst case propagation

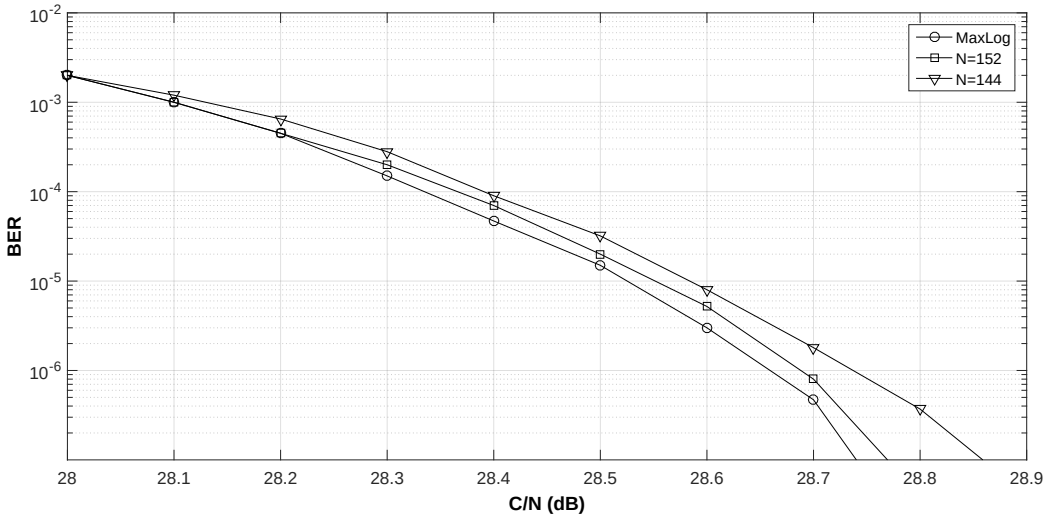

Figure 3.31: Performance for 3/4 CR in the RME channel

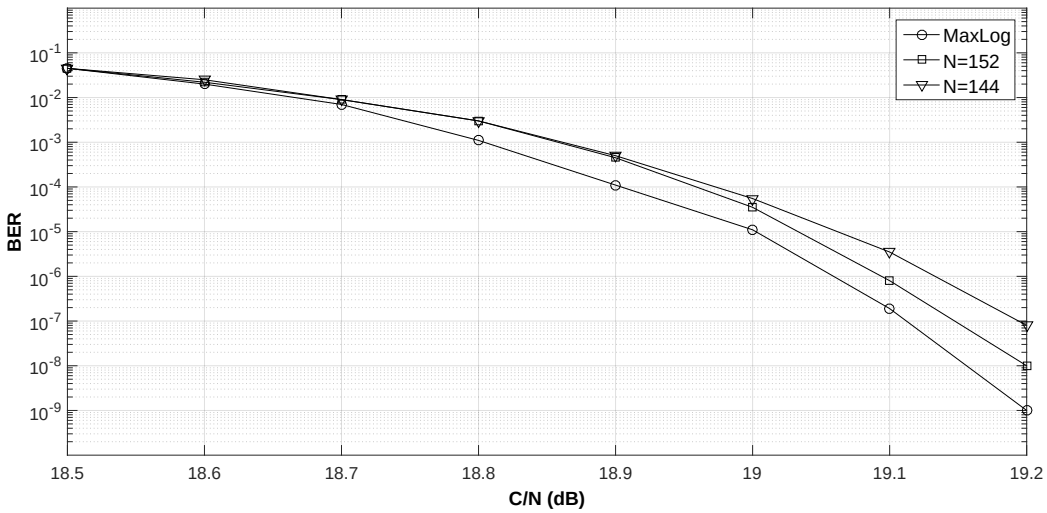

Figure 3.32: Performance for 1/2 CR in the RME channel

scenario defined in [24]. In fact, it does not correspond to a real channel but it allows testing the DVB-T2 systems in very hard propagation conditions. That is, this channel is very unlikely to occur, so a low cost receiver could use the subsets found for the P1 or the 0dB echo channels.

Real channel estimation effect

The aim of this subsection is to show the impact of the real channel estimation on the proposed method. A 2D pilot aided channel estimator based on Wiener filters [28] has been added to the CSP. Simulations have been run for the P1 channel, different code rates (5/6, 3/4 and 1/2) and the PP1 pilot pattern [3].

Figure 3.33 shows two BER curves for CR 5/6, one for the ideal max-log demapper and one for our proposed scheme with N=36. In both curves the receiver uses the 2D channel estimator. When compared with the results of Fig. 5 (ideal channel estimation) a loss of 0.65dB can be denoted. According to [24] a performance loss of 0.41dB can be expected due to the pilot boosting, so the losses of the real channel estimator can be estimated to be 0.24dB.

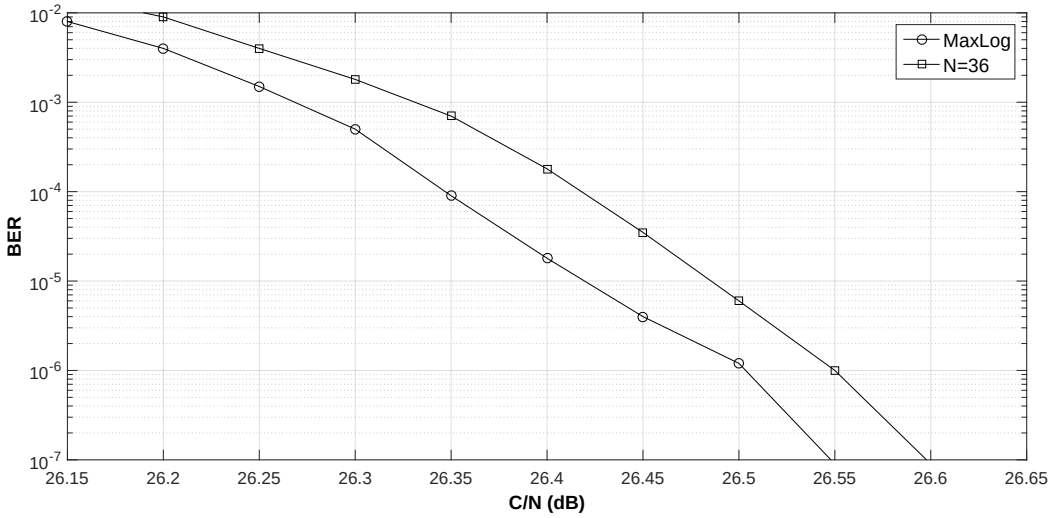

Figure 3.33: Performance for 5/6 CR in DVBT-P channel with real channel estimation

From Figure 3.33 it can be seen that the performance loss between the max-log demapper and the proposed scheme is almost the same as the one with ideal channel estimation shown in Figure 3.23. The same conclusions can be drawn from Figure 3.34 and Figure 3.35 where the same curves are depicted for CR 3/4 and 1/2 respectively.

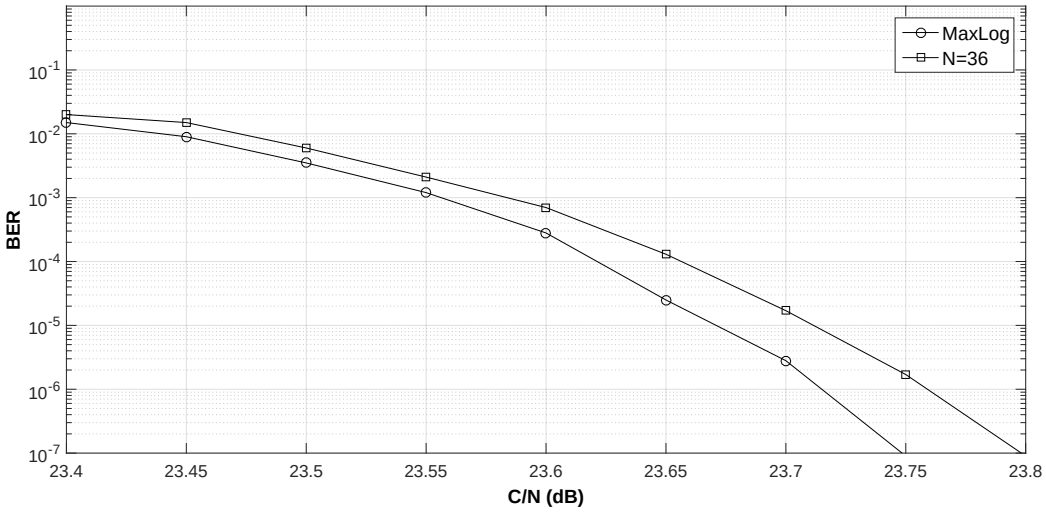

Figure 3.34: Performance for 3/4 CR in DVBT-P channel with real channel estimation

The results presented in this subsection were published in [29]

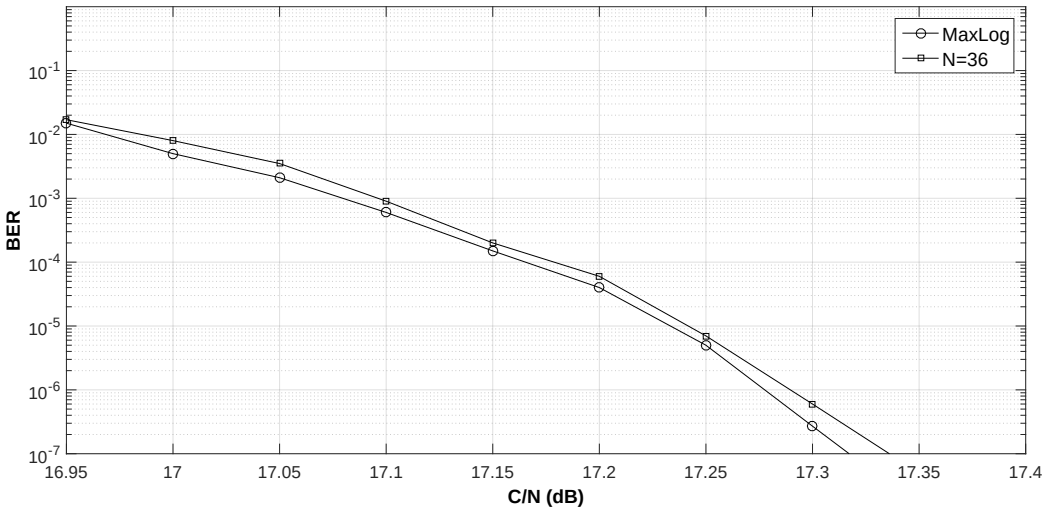

Figure 3.35: Performance for 1/2 CR in DVBT-P channel with real channel estimation

3.5.2 Metrics simplification

In order to reduce the complexity introduced by the use of the RQD technique, other approaches have been proposed in the literature. In [30], the authors propose to decorrelate the received signal in order to be able to detect it as two independent PAM modulations, obtaining a great complexity reduction. However, this method already shows a performance loss of 0.3 dB in some configurations for a BER level of only 10^{-3}.

The second approach is the one suggested in [27],[29] (these two explained in the pervious subsections),[1],[31],[32]. In them the authors show that, using different subsets of the original constellation, the number of distances to be calculated can be considerably reduced. Depending on the accuracy of the chosen subset the performance will be more or less affected by the reduction of the number of distances to be computed.

Mathematically, the expression for the LLR metrics for the i-th bit (b_i) of the received symbol ($I + jQ$) when the max-log approximation is used is shown in Equation 3.6.

From Equation 3.6, 2^m terms like the one shown in Equation 3.8 must be calculated in the case of a 2^m-QAM constellation. Note that D represents the Euclidean distance between the received complex value and the ideal constellation point propagated through the channel ($\rho_I I_x + j\rho_Q Q_x$).

$$D^2 = (I - \rho_I I_x)^2 + (Q - \rho_Q Q_x)^2) \tag{3.8}$$

In the DVB-T2 standard, m can take values up to 8 in the case of a 256-QAM constellation. This means that for each received constellation point, 256 terms as the one in Equation 3.8 must be calculated, which makes the detection process very complex in terms of hardware implementation.

The third approach, which is compatible with the previous one, consists in simplifying Equation 3.8 by using an approximation. This approach has been used in [1], where the authors propose to use Equation 3.9 as a simplification when calculating Equation 3.8. This approximation leads to the scheme shown in Figure 3.36, which avoids the use of multipliers for the squared terms in Equation 3.8, and leads to a negligible performance loss.

$$D \approx \begin{cases} \max(a,b) & \text{if } \min(a,b) \leq \dfrac{\max(a,b)}{4} \\ \max(a,b) - \dfrac{\min(a,b) - \dfrac{\max(a,b)}{4}}{2} & \text{if } Otherwise \end{cases} \tag{3.9}$$

In Equation 3.9 $a = \text{abs}(I - \rho_I I_x)$ and $b = \text{abs}(Q - \rho_Q Q_x)$.

In this subsection a technique that follows this approach and further reduces the hardware complexity will be shown. As it will be shown by means of simulation results, the performance loss will remain negligible.

3.5.2.1 Proposed method: Abs approximation

When max-log approximation is used as shown in Equation 3.6 it is needed to find the point of the constellation that minimizes the distance between the received signal and the subset of constellation points in which i-th bit value is "0" or

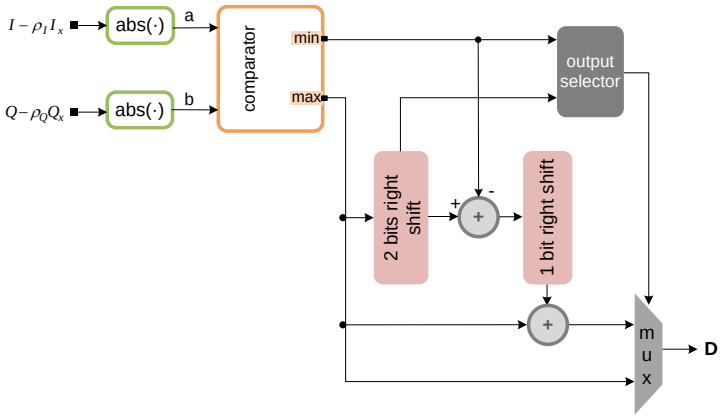

Figure 3.36: Method proposed in [1]

"1". It can be found many distance metrics in the literature different from the traditional Euclidean distance; however all of them need to accomplish some conditions. Being D the distance between the points i and j these restrictions are:

$$D(i,j) >= 0 \tag{3.10}$$

$$D(i,i) = 0 \tag{3.11}$$

$$D(i,j) = D(j,i) \tag{3.12}$$

$$D(i,j) <= D(i,h) + D(h,j) \tag{3.13}$$

Equation 3.13 expresses what is known as triangle inequality.

The main target of this work is to obtain a method that can reduce the hardware implementation complexity of the soft bit decision detection as the used in standards as DVB-T2. So the proposed used distance metric needs to be as simple as possible keeping a good performance. Manhattan distance for an n-dimensional space can be formulated as indicated in Equation 3.14.

$$D(i,j) \approx |x_{i1} - x_{j1}| + |x_{i2} - x_{j2}| + ... + |x_{in} - x_{jn}| \tag{3.14}$$

This approximation has a much simpler implementation than the traditional Euclidean one, and one of the most simple among the distance metrics that meet Equation 3.10-Equation 3.13.

To reduce the complexity of the RQD demapper, the simplicity of Equation 3.8 leads us to propose using the 2 dimensions expression of the Manhattan distance, where a and b represent the absolute value of the difference between the I and Q components of the ideal constellation point propagated through the channel and the received one respectively:

$$D \approx a + b \tag{3.15}$$

This approximation will be used instead of Equation 3.9 when looking for the minima of the distances needed in Equation 3.6.

Focusing in the case of QAM constellations used in DVB-T2 standard it can be found that with traditional non rotated constellations the decision area for every constellation takes the shape of a square mesh when the Euclidean distance is used. When non rotated constellations are used the aforementioned grid represents also the decision regions for the Manhattan distance approximation. This means that either using the Euclidean distance or Manhattan approximation leads to the same result when looking for the constellation point that minimizes the distance with a received signal, so the performance loss is null. Note that the value of this minimum is not the same for both but the constellation point that produces it is. However in DVB-T2, the use of the rotated constellation technique changes the decision regions as shown in Figure 3.37 where the decision regions for the Euclidean distance are bounded with dashed lines and the decision regions for the Manhattan approximation are limited by continuous lines (for the sake of simplicity the same channel gain has been assumed for I and Q components, if not the shape of the regions would be not square but rectangular depending on the power gain ratio between ρ_I and ρ_Q).

As it can be easily noticed, the regions for the two distance metrics are different, but they are coincident in the majority of the area. The grey marked zones represent the non coincident areas, thus the points where the Euclidean distance

and the Manhattan approximation would give a different result when looking for the constellation point that minimizes the distance.

As a proof of this, Figure 3.38 shows the mismatch rate when comparing the minimum obtained with the exact Euclidean distance and the Manhattan approximation for all the available constellations in DVB-T2 standard in presence of AWGN. Depending on the code rate and constellation used, the C/N needed to perform the detection process varies, and so the BER level at the output of the demapper that the LDPC needs to be able to correct the errors; the mismatch rate shown in Figure 3.38 always remains under the required uncoded BER level. To clarify this, in Table 3.6 it is shown a comparison of the BER at the output of the demapper and the mismatch rate presented by the proposed approximation at the same C/N level. The C/N level has been chosen to have a BER level after the LDPC under 10^{-6} for a 16-QAM constellation in a Rayleigh channel (as it will be seen in paragraph 3.5.2.1.1, the worst work case studied for the proposed method). However, this mismatch will lead to a very slight performance loss as it will be shown in paragraph 3.5.2.1.1.

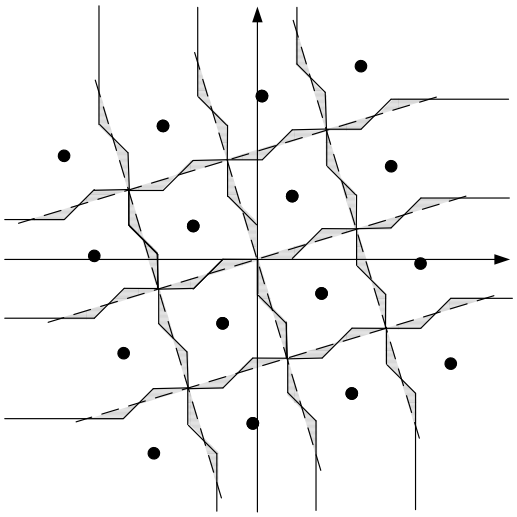

Figure 3.37: Decision areas for Manhattan approximation and Euclidean distances with rotated constellations

Focusing on the complexity reduction, in the case of a 256-QAM, the proposed

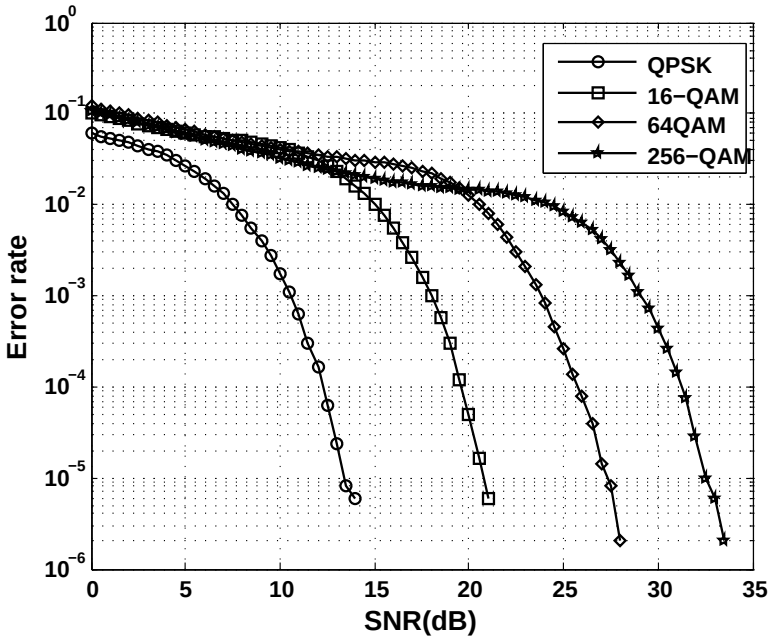

Figure 3.38: Mismatch rate between Manhattan approximation and Euclidean distance

Code Rate	C/N(dB)	BER	Mismatch rate
1/2	8.45	0.157	0.048
3/5	10.2	0.118	0.040
2/3	11.65	0.093	0.033
3/4	13.3	0.068	0.020
4/5	14.45	0.053	0.013
5/6	15.35	0.043	0.008

Table 3.6: Mismatch and BER after the demapper comparison

simplification requires only the calculation of additions per each received point instead of multiplications when compared to Equation 3.8 and it avoids the use of comparators when compared to Equation 3.9.

From a digital implementation point of view, the absolute values can be computed by using one's complement arithmetic instead of two's complement, obtaining even a higher complexity reduction.

In order to avoid performance loss, once the minimum distances have been found, Equation 3.8 is still used to compute the LLRs. Note that Equation 3.8 is only used two times per LLR instead of 2^m. The scheme of the hardware implementation of this approximation is shown in Figure 3.39. The proposed method is compared with the exact Euclidean calculation by using the number of additions and multiplications needed in Table 3.7. In the case of DVB-T2 m can take values up to 8 (256-QAM), that means that the number of multiplications needed by the proposed scheme represents the 0.8% of the ones needed for the exact Euclidean calculation of the distance maintaining almost the same amount of additions.

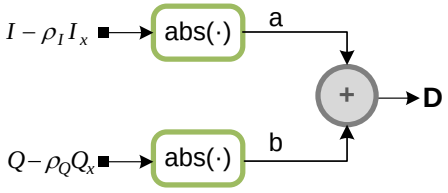

Figure 3.39: Proposed method

	Exact calculation	Proposed method
Additions	2^m	$2^m + 2$
Multiplications	2^{m+1}	4

Table 3.7: Complexity comparison

3.5.2.1.1 Performance evaluation

Simulations have been run to determine the impact of the proposed detection technique on the system performance. For that purpose, BER curves at the output of the LDPC decoder of a DVB-T2 system have been obtained.

Simulations have been run for a LDPC block size of 64.800 bits and all the CR included in the DVB-T2 standard: 1/2, 3/5, 2/3, 3/4, 4/5, and 5/6, and three propagation scenarios: a P1 Rayleigh channel, a 0dB Echo channel with an echo delay set to 95% of the guard interval, and the worst case defined in [24], the RME, in this case with a 15% erasure event rate. Ideal channel estimation has been used. For the sake of brevity only some of the results obtained will be explicitly shown in this chapter. However, for all the possible CR and constellations (QPSK, 16-QAM, 64-QAM, and 256-QAM), the simulation results show a performance loss for the proposed method always under 0.1dB measured at a BER level of 10^{-6}. To illustrate this, Figure 3.40, Figure 3.41and Figure 3.42 show the BER curves against the C/N for a CR of 3/4 (an intermediate CR) in the three aforementioned propagation scenarios. In each figure, three different approximations have been represented: the max-log approximation, the method presented in [1] by Telecom Bretagne (TB), and the proposed method. From these figures it can be followed that the performance loss is negligible in all the simulated propagation scenarios.

In Table 3.8 it is shown a summary of the performance loss obtained when using the proposed method. The table contains the simulation results of all the constellations and code rates available in DVB-T2 for a RME (15% erasure events) propagation scenario (as stated before the worst case proposed in the implementation guidelines). It can be seen that the performance loss is negligible for all the possible cases. From Table 3.8 it can be also followed that the proposed approximation finds its worst work case for a 16-QAM constellation. The performance of the proposed method for a 16-QAM constellation in every studied propagation scenario can be seen in Table 3.9. In both tables < 0.05 indicates that the performance loss when compared with Max-log is under 0.05 dB and < 0.1 indicates that this loss is between 0.1 and 0.05 dB.

In conclusion, the main benefit of the proposed method is that it has a negligible impact on the system performance having a much simpler hardware implementation than the one presented in [1].

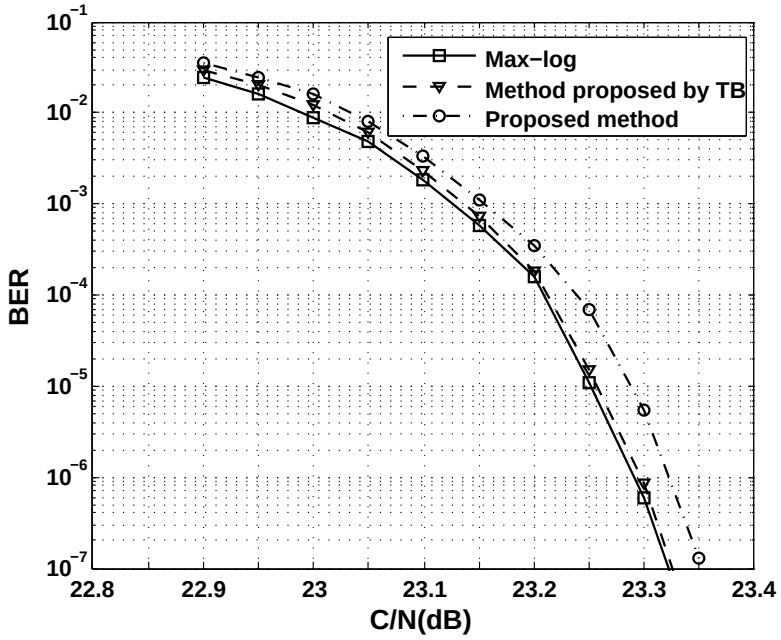

Figure 3.40: BER against C/N for 256-QAM, CR=3/4, in 0dB Echo channel

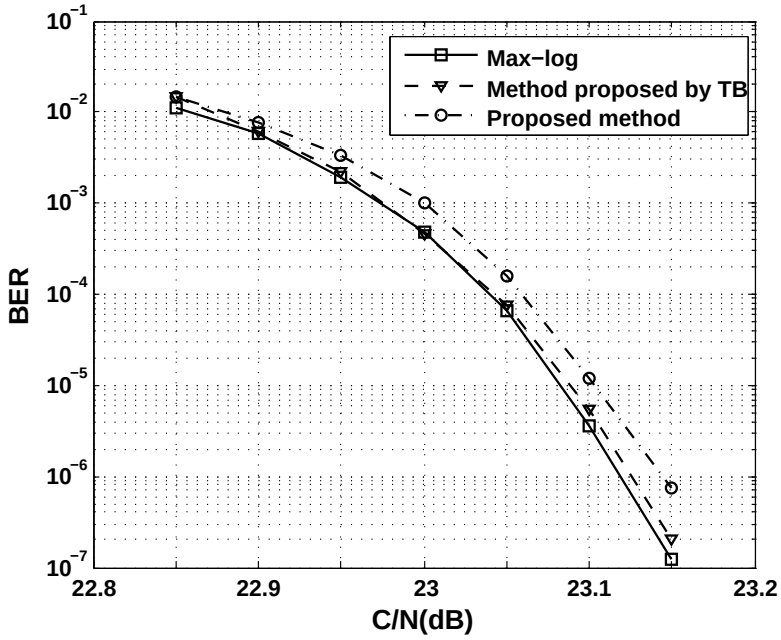

Figure 3.41: BER against C/N for 256-QAM, CR=3/4, in Rayleigh channel

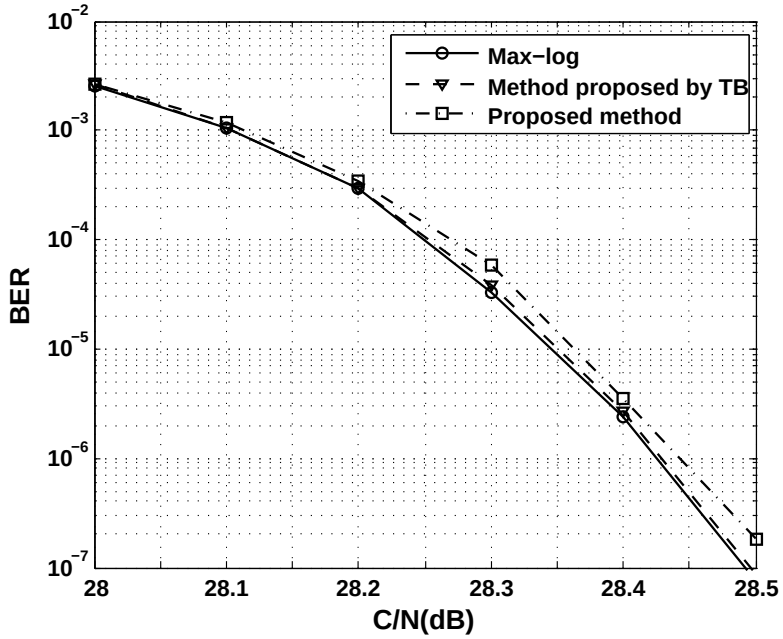

Figure 3.42: BER against C/N for 256-QAM, CR=3/4, in RME(15%) channel

Code rate	QPSK	16-QAM	64-QAM	256-QAM
1/2	< 0.05	< 0.1	< 0.05	< 0.05
3/5	< 0.05	< 0.1	< 0.05	< 0.05
2/3	< 0.05	< 0.1	< 0.1	< 0.1
3/4	< 0.05	< 0.1	< 0.05	< 0.05
4/5	< 0.05	< 0.05	< 0.05	< 0.05
5/6	< 0.05	< 0.1	< 0.05	< 0.05

Table 3.8: RME (15% erasure events) performance loss(dB)

Code rate	0dB echo	Rayleigh	RME(15%)
1/2	< 0.05	< 0.1	< 0.1
3/5	< 0.05	< 0.1	< 0.1
2/3	< 0.05	< 0.1	< 0.1
3/4	< 0.05	< 0.1	< 0.1
4/5	< 0.05	< 0.1	< 0.05
5/6	< 0.05	< 0.1	< 0.1

Table 3.9: 16-QAM performance loss(dB)

3.6 Conclusions

In this chapter one of the most promising diversity techniques included in DVB-T2, RQD, has been presented. This technique has been widely explained, showing its theoretical principles and how it is implemented in DVB-T2 systems.

The performance of the RQD technique has been evaluated by means of computer simulations. These simulations results show a very noticeable performance improvement as shown in section 3.4, making the communication feasible in very adverse propagation environments in which without using RQD the communication would not be possible.

The main drawback of using RQD has been studied, that is, the hardware complexity increase at the receiver side. The rotation and cyclic delay implies that the information of the in phase and quadrature components are transmitted in different subcarriers, that makes both to suffer different fadings, that's why simplifications based on decomposing real and imaginary components to have 1D distances instead of 2D ones are not suitable when rotated constellations are applied, 2D Euclidean distances must be computed.

In order to reduce the complexity problem two different strategies have been followed. The first one consists in selecting a subset of points of the original constellation as candidates to compute the distances needed at the receiver side. With this approach a 78% reduction can be achieved, in terms of distances to be computed per received symbol. The second approach focuses in using an approximation when calculating the 2D distances needed at the receiver. With

the proposed method the use of multipliers is almost avoided, instead just adders are needed reducing the consumed silicon area.

The two shown approaches are compatible, so they can be combined to obtain a higher complexity reduction.

Chapter 4

MIMO

4.1 Introduction

To increase the data rate in power, bandwidth and complexity constrained systems is a very challenging target. To this aim DVB-NGH adopts one of the most promising techniques nowadays, MIMO which consists in using several transmitter and receiver antennas. The use of MIMO allows to greatly increase the available capacity for the system. The first works on this unexplored field were carried out by Winters [15], Foschini [16], and Telatar [17] and they brought a very high interest on what by the time was known as Smart Antenna Technologies. This interest was due to the high spectral efficiency that can be obtained when the propagation channel has a high dispersion level and its variations can be estimated accurately. All this promising results were the starting point for hundreds of investigations about MIMO in order to characterize theoretical and practical issues related to the wireless MIMO channels.

The aforementioned high spectral efficiency is based on the fact that a channel with enough dispersion offers independent propagation paths for the information transmitted by every antenna in the system. For MIMO systems a capacity of $\min(M, N)$ channels can be achieved, where M represents the number of transmitter antennas and N the number of receiver ones. This makes the capacity to be scaled by $\min(M, N)$ when compared with the SISO equivalent system.

This capacity gain requires a scattered propagation environment so that the

channel matrix has full range and it can be estimated perfectly at the receiver side. The capacity of a MIMO channel strongly depends on the statistical and correlation properties of the propagation paths between antennas. Exhaustive works have been carried out to characterize the MIMO channel properties and develop analytical models as the ones used in the DVB-NGH standardization process [33]. The correlation of the paths between antennas varies drastically with the distance between transmitter and receiver and the Doppler dispersion.

4.2 MIMO scenario definition

A generic MIMO scenario presents M transmitter antennas and N receiver antennas as depicted in Figure 4.1.

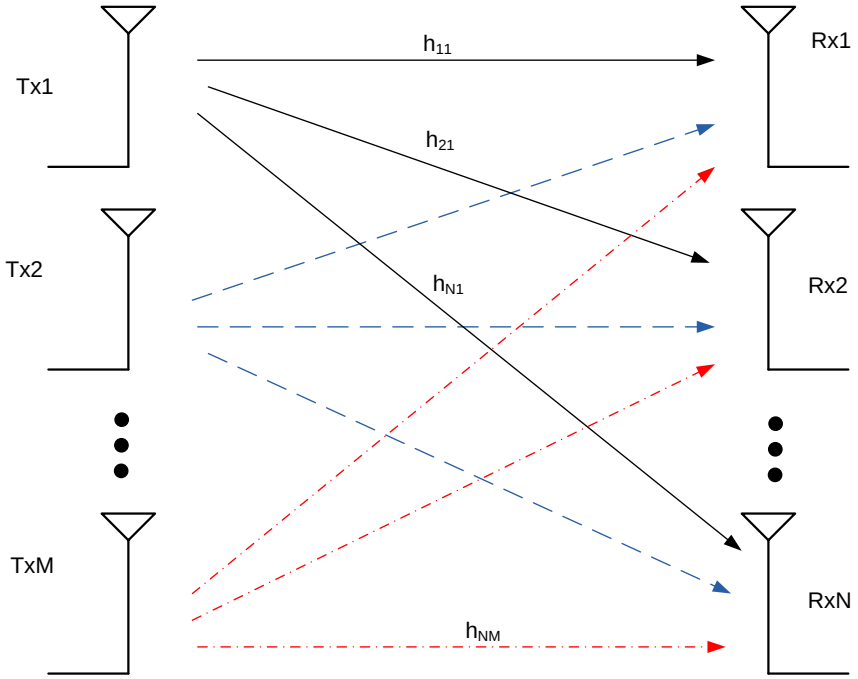

Figure 4.1: MIMO generic scenario

In this case the channel can be expressed mathematically as a NxM matrix. The propagation process can be then modeled in the frequency domain as shown in Equation 4.1.

$$y = \mathbf{H}x + n \tag{4.1}$$

Where y is a Nx1 vector representing the received signal, x a Mx1 vector representing the transmitted data, n a Nx1 vector representing the noise at the receiver's antenna and $\mathbf{H}$ a NxM matrix representing the propagation channel. $\mathbf{H}$ can be described as follows in Equation 4.2.

$$\mathbf{H} = \begin{bmatrix} h_{11} & \cdots & h_{1M} \\ \vdots & \ddots & \vdots \\ h_{1N} & \cdots & h_{NM} \end{bmatrix} \tag{4.2}$$

Where h_{ij} models the channel response between the j-th transmitter antenna and the i-th receiver antenna. This value can be taken as an instantaneous sample of the channel in a determinate frequency and time instant. When there is multipath in the communication with a high spread because of the delays, $\mathbf{H}$ changes with the frequency. If the transmitter or the receiver are mobile elements Doppler spread will appear and the elements of $\mathbf{H}$ vary with the time. If the transmitter antennas are sufficiently separated and the same occurs with the receiver ones, h_{ij} can be modeled as independent complex Gaussian variables with zero mean, unity variance (Rayleigh fading). This model is known as identically distributed Gaussian MIMO channel. In general, if the antennas are separated by more than the half of the wavelength, the channel fadings can be modeled as Gaussian random variables.

From this generic scenario different systems can be derived: SISO ($M = 1$, $N = 1$), SIMO ($M = 1$, and any entire number different from 1 for N), and MISO ($N = 1$, and any entire number different from 1 for M).

4.3 MIMO channel capacity

The science that studies the limits of the achievable capacity in communication systems is known as Information Theory. The basic measurement of the per-

formance of a communication process is known as channel capacity; this can be defined as the maximum data rate which allows to obtain an arbitrarily low error rate. Along this section this channel capacity will be studied for different scenarios, beginning with the simplest one, a SISO AWGN channel, that will be used as a starting point for the analysis of other fading channels which don't have a unique definition of the channel capacity. However, several different notions of it are developed and can be used to carry out a systemic analysis of the capacity limits. These different notions can be used to distinguish the different resources available for the system planning.

4.3.1 AWGN channel capacity

The first principles of the Information Theory were settled by Claude Shannon in 1948 [2] trying to characterize the the limits of a reliable communication process. Before Shannon developed his theory it was believed that the only way to reach a reliable communication in a noisy channel was to reduce the data rate, for example using a repetition code. Shannon showed that this was not right, and that using a more efficient coding a reliable communication could be obtained. Although, as stated before, it exists a maximum data rate known as channel capacity, above which the error rate cannot be reduced to zero.

In order to carry out the aforementioned study the expression in Equation 4.3 will be taken as the communication system model.

$$y[m] = x[m] + n[m] \tag{4.3}$$

Where $x[m]$ and $y[m]$ represent the system input and output respectively, $n[m]$ is an additive white Gaussian noise with zero mean and unity standard deviation, and m the discrete time index.

4.3.1.1 Repetition codes

Using Bipolar Phase Shift Keying (BPSK) symbols, where $x[m] = \pm\sqrt{P}$, being P the power of the symbol, the error rate can be written as $Q(\sqrt{P/\sigma^2})$, being Q the tail probability function of the normal standard distribution, defined as

$Q(x) = \int_x^\infty \frac{1}{\sqrt{2\pi}} e^{\frac{-u^2}{2}} du$. In order to reduce the error rate the same symbol can be transmitted N times. That makes a code block with length N. The codewords would be then $x_A = \sqrt{P}[1, ..., 1]^t$ and $x_B = -\sqrt{P}[1, ..., 1]^t$. These codewords have a power of NP. If vector x_A is sent the received vector y will be as described in Equation 4.4, where $n = [n[1], ..., n[N]]$.

$$y = x_A + n \tag{4.4}$$

An error will occur when y is closer to x_B than to x_A. In this case, the error rate will follow the expression in Equation 4.5, where $\| \cdot \|$ represents the module operator.

$$Q\left(\sqrt{\frac{\|x_A - x_B\|}{2\sigma}}\right) = Q\left(\sqrt{\frac{NP}{\sigma^2}}\right) \tag{4.5}$$

This expression exponentially decreases with the value of N. Therefore, it can be concluded that the error rate can be reduced arbitrary just by increasing the block length. As a drawback, the data rate is reduced by an N factor.

The data rate can be increased by using a multilevel Pulse Amplitude Modulation (PAM). Repeating a M-PAM symbol, with the symbols equispaced $\pm\sqrt{P}$, the bit rate becomes $\log_2(M)/N$ bits per symbol time. In this case, the error rate for the internal points of the constellation is the one shown in Equation 4.6

$$Q\left(\frac{\sqrt{NP}}{(M-1)\sigma}\right) \tag{4.6}$$

As long as the order of the M-PAM modulation increases less than $\sqrt{N}$, a reliable communication can be assured. However, the data rate is limited by $\log_2(M)/N$. Even in this way the data rate tends to zero when the block length increases.

Geometrically, repetition codes align all the codewords in the same dimen-

sion. But the signal space has bigger space, in this case N. For a more efficient communication the codewords should be spread in the N dimensions.

An estimation of the maximum number of codewords that can cope with the power constraint P can be obtained applying the classic sphere packing problem. Because of the large numbers law, the N-dimensional received vector would be inside of a sphere of radius $\sqrt{N(P+\sigma^2)}$, so without loss of generality, only what happens inside the sphere must be studied, see Figure 4.2. If $N \to \infty$, it can be obtained that:

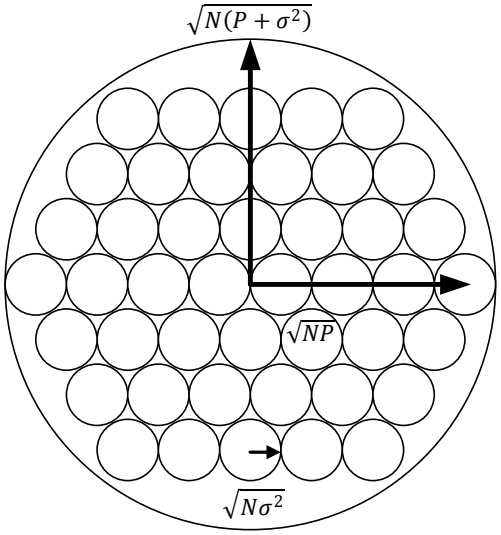

Figure 4.2: Sphere packing

$$\frac{1}{N}\sum_{n=1}^{N} n^2[m] \to \sigma^2 \tag{4.7}$$

For a high value of N, the received vector y will lie, with high probability, inside a sphere of radius $\sqrt{N}\sigma$ with center x, that is, the transmitted codeword. A reliable communication can be obtained if the spheres don't overlap. The maximum number of codewords that fit inside the sphere without overlapping is

the quotient between the volume of the sphere and the noise spheres, as shown in Equation 4.8

$$\frac{\sqrt{N(P+\sigma^2)}^N}{\sqrt{N\sigma^2}^N} \tag{4.8}$$

This implies that the maximum number of bits per symbol that can be reliably transmitted is the one shown in Equation 4.9

$$\frac{1}{N}\log_2\left(\frac{\sqrt{N(P+\sigma^2)}^N}{\sqrt{N\sigma^2}^N}\right) = \frac{1}{2}\log_2\left(1+\frac{P}{\sigma^2}\right) \tag{4.9}$$

The expression shown in Equation 4.9 is what is known as AWGN channel capacity. This reasoning is based only in the number of codewords that can be packed assuring a reliable communication.

Taking into account that $\frac{P}{\sigma^2} = SNR$ Equation 4.9 can be rewritten as in Equation 4.10.

$$C_{awgn} = log_2\left(1+SNR\right) bits/s/Hz \tag{4.10}$$

From the engineering point of view, the difficult task is to find codes that make coding and decoding process as simple as possible with a performance close to the channel capacity.

The AWGN channel capacity is probably one of the most known results of the Information Theory, but it is not more than the application of the Shannon theory to a concrete scenario.

4.3.1.2 SIMO channel

A transmission scenario with a transmitter antenna and N receiver antennas can be described as in Equation 4.17, where y_n represents the received signal at the n-th receiver antenna, h_n the complex gain of the path between the transmitter

antenna and the n-th receiver antenna, and n_n the aditive white Gaussian noise.

$$y_n[m] = h_n x[m] + n_n[m] \tag{4.11}$$

In order to perform the detection of the received signal it will be enough to apply Equation 4.12, where $h = [h_1, ..., h_N]^t$, $n = [n_1, ..., n_N]^t$, and $y = [y_1, ..., y_N]^t$.

$$\check{y}_n[m] := h^* y[m] = \|h\|^2 x[m] + h^* n[m] \tag{4.12}$$

This represents an AWGN channel with a SNR at the receiver side of $P\|h\|^2/\sigma^2$, where P represents the average energy per transmitted symbol, and σ the noise power. Thus, the channel capacity for a SIMO scenario can be expressed as:

$$C_{SIMO} = log_2\left(1 + \frac{P\|h\|^2}{\sigma^2}\right) bits/s/Hz \tag{4.13}$$

The usage of multiple antennas increases the effective SNR, leading to a performance improvement in terms of signal power level.

4.3.1.3 MIMO channel capacity

The aim of this section is to show how MIMO can improve the available system capacity, but to obtain a closed expression for a MIMO scenario is very complicated. Due to this, several hypothesis will be taken into account to achieve a closed expression for the MIMO channel capacity in order to compare the different performances that can be obtained with the different schemes proposed in this section.

For the sake of simplicity a 2x2 MIMO channel will be used (the simplest MIMO scenario). The channel can be modelled in this case as a complex 2x2 matrix, Equation 4.14, where h_{ij} represents the attenuation between transmitter

j and receiver i.

$$\mathbf{H} = \begin{bmatrix} h_{11} & h_{12} \\ h_{21} & h_{22} \end{bmatrix} \tag{4.14}$$

The capacity in this case can be expressed as in Equation 4.15, as can be followed from [34].

$$C_{MIMO2x2} = log_2 \left(det(I_2 + \frac{P\mathbf{H}\mathbf{H}^*}{2\sigma^2}) \right) bits/s/Hz \tag{4.15}$$

If more constraints are added, as perfect polarization in the antennas and that propagation doesn't cause depolarization, the result is a too idealistic model that should be used only to give an idea of how the capacity of the channel can be increased with a MIMO system. According with the previous suppositions the channel matrix is diagonal and time invariant, this implies that the transmission channel could be modelled as two independent fixed channels h_{11} and h_{22}. In this case, the expression for a MIMO channel capacity can be expressed as follows:

$$C_{MIMO2x2} = log_2 \left(1 + \frac{P\|h_{11}\|^2}{2\sigma^2} \right) + log_2 \left(1 + \frac{P\|h_{22}\|^2}{2\sigma^2} \right) bits/s/Hz \tag{4.16}$$

If Equation 4.16 is compared to Equation 4.10, supposing that both channel coefficients, h_{11} and h_{22}, have an equivalent attenuation, the result is the one shown in Table 4.1 (note that $\frac{P\|h_{22}\|^2}{2\sigma^2}$ represents the SNR).

SNR (dB)	SISO capacity (bits/s/Hz)	MIMO capacity (bits/s/Hz)	MIMO capacity increase
5	2.06	2.74	33%
10	3.46	5.17	49%
20	6.66	11.34	70%

Table 4.1: Capacity increase(%)

As it can be seen in Table 4.1 the capacity that offers a MIMO system surpasses the SISO equivalent considerably when working with high SNR.

4.4 MIMO data coding

As studied in section section 4.3, the channel capacity that can be achieved with MIMO systems surpasses greatly the one offered by the equivalent SISO system, but to reach this capacity gain many "optimistic" simplifications have been adopted. In a real wireless communication scenario different propagation paths appear, see Figure 4.1, and depending on the correlation properties of these propagation paths the capacity that can be achieved can be far from the one shown in Table 4.1. In order to reduce the effect that the non ideal conditions cause to the achievable capacity in a MIMO system it is capital to choose an appropriate data coding. In this section the properties of the MIMO systems that are used to design different MIMO codes will be briefly explained, as well as some of the better performance offering codes known nowadays.

4.4.1 Principles and characteristics

The different antenna configurations provide different benefits that can be classified in array gain, diversity gain, multiplexing gain, and interference reduction. The coding plan at the transmitter side and the corresponding processing at the receiver are based in the link's requirements (data rate, span, reliability, etc.). For MIMO coding it is not necessary to know the channel status information at the transmitter, but if it is known, it leads to a better performance.

In the following subsections the main advantages of using MIMO will be explained.

4.4.1.1 Array gain

For the sake of clarity a SIMO system will be used as an example. This kind of configurations has a transmitter antenna and more than one receiver antenna, for our example 2 receiver antennas will be used. Both receiver antennas receive different signals, y_1 and y_2, coming from the same transmitted x propagated through

different paths. If the channel is known at the receiver side, the corresponding processing can be applied to combine y_1 and y_2 in a coherent way. In this case the achieved SNR would be higher, in concrete 3dB higher. This result can be extended to systems with more than one receiver antenna as shown in Equation 4.17, where the linear optimum filter would be $w = \mathbf{H}^*$, and the maximum SNR would be proportional to the channel norm, $\|h\|^2 = \sum_m^N |h_m|^2$.

$$wy = w\mathbf{H}x + wn \tag{4.17}$$

The average increase of power at the receiver side is called array gain and it is proportional to the number of receiver antennas.

The array gain also appears in systems with several transmitter antennas. To obtain the maximum profit from this configuration is mandatory to know at the transmitter side the channel status information. If a system with several (M) transmitter antennas is considered the reception can be described as shown in Equation 4.18.

$$y = \mathbf{H}(wx) + n \tag{4.18}$$

In this case, the optimum filter is $w = \mathbf{H}/\|\mathbf{H}\|$. As in the SIMO configuration the gain obtained is proportional to the number of antennas available, in this case at the transmitter side.

4.4.1.2 Diversity gain

The signal power in a wireless channel dissipates in time, frequency and space. When the signal power decreases drastically it is said that a fading has occurred in the channel. The diversity can be used in wireless channels to avoid this to happen. The basic principle is to offer to the receiver different versions of the transmitted signal propagated through independent paths. The higher the number of independent paths is, the higher probability of one of them not to suffer a fading. This is translated into a higher stability of the channel.

Diversity also appears in SISO systems with the use of time and frequency. This frequency and time diversity leads generally to a reduction of data rate due to the usage of time or frequency to add redundancy, the RQD technique studied in chapter 3 is a clear example of frequency/time diversity. The use of several antennas at the transmitter or receiver introduces a new diversity source, in addition to the the array gain explained in subsubsection 4.4.1.1. Two different kinds of spatial diversity can be described: reception and transmission.

Reception diversity is applied to the systems with several receiver antennas (SIMO, MIMO). Without loss of generality a SIMO system as the one depicted in Figure 4.3 will be taken as an example . There is only one transmitter antenna and both receiver antennas receive an independent version of the transmitted signal. With the proper data processing, at the receiver the two versions of the transmitted signal are combined in a way that the resulting signal is much more robust than the original ones. The diversity order is measured as the number of independent paths that the transmitted signal propagates through, in SIMO systems it is equal to the number of receiver antennas.

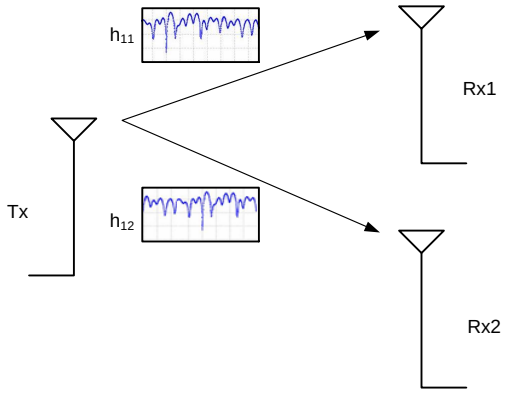

Figure 4.3: Reception diversity example

Transmission diversity can be applied when multiple antennas are used at the transmitter side. The use of this diversity doesn't imply the knowledge of the channel status at the receiver. However, a good design of the transmitted signal is needed to obtain all the possible performance of this kind of diversity. In figure Figure 4.4 an order 2 transmission system is represented, the order corresponds

with the number of transmitter antennas.

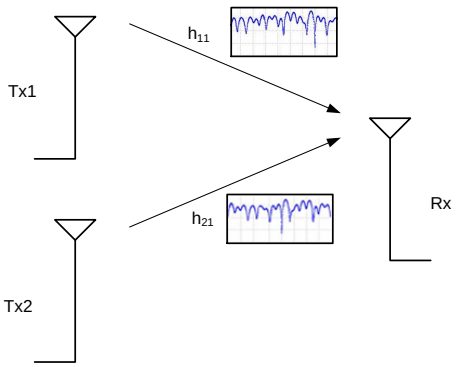

Figure 4.4: Transmission diversity example

The use of diversity in MIMO systems combines the two kinds of diversity described in this section. As shown in Figure 4.1 the MIMO system consists of MxN (number of transmitter and receiver antennas respectively) SISO equivalent paths. Due to this fact, the diversity order in MIMO systems is scaled linearly with the product of N and M. Mathematically the diversity can be described as the slope of the curve that characterizes the system by means of a SER (Symbol Error Rate) versus SNR curve.

4.4.1.3 Multiplexing gain

The main advantage of the MIMO systems is the rise of the output data rate, that is not offered by SIMO and MISO systems. This increase is referred as multiplexing gain. This effect can be easily observed using a well known technique, Spatial Multiplexing (SM) consisting in transmitting (in the case of a 2x2 MIMO sytem) a subset of symbols of the original stream by one antenna and the remaining by the other as depicted in Figure 4.5.

In favourable transmission conditions the transmitted data vectors will be quite geometrically separated, ideally they will be orthogonal. At the receiver side we can extract each of the substreams and reconstruct the original data.

To have a mathematical approach of the total gain that can be achieved with the use of MIMO, lets consider that we have a MxM configuration. The available

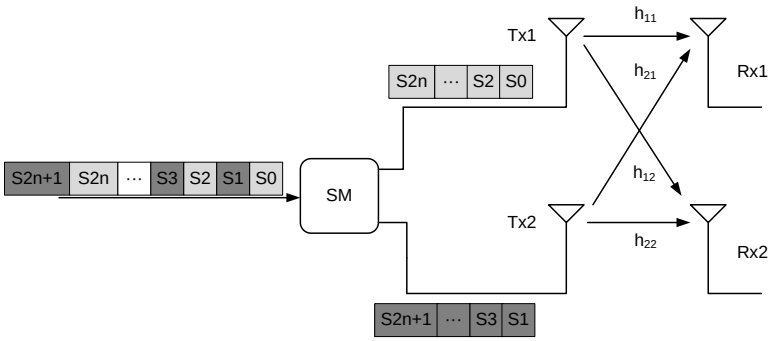

Figure 4.5: Spatial Multiplexing scheme

capacity is expressed in Equation 4.19[35].

$$C_H = M \log_2(\det(\mathbf{I}_M + SNR\mathbf{H}\mathbf{K}_X\mathbf{H}^*)) \tag{4.19}$$

with $\mathbf{I}_M$ representing the identity matrix with dimensions MxM and $\mathbf{K}_X = \frac{1}{M}\mathbf{I}_M$.

When the channel matrix is square and orthogonal ($\mathbf{H}\mathbf{H}^* = \mathbf{I}$), then with an identically distributed data input Equation 4.19 can be rewritten as in Equation 4.20.

$$C_H = M \log_2(1 + \frac{SNR}{M}) \tag{4.20}$$

The capacity is linearly scaled with the number of transmitter antennas for an increasing SNR. In general it can be demonstrated that an orthogonal channel as the one used in the previous example maximizes the capacity in MIMO systems. In an identically distributed channel with flat fadings the channel matrix becomes almost orthogonal when the number of transmitter antennas is high. When the number of transmitter and receiver antennas is different, the capacity increase is limited to the minimum number of them.

4.4.1.4 Conclusions

In this subsection the principal advantages of the MIMO systems have been summarized, using illustrative examples with 2 transmitter and/or receiver antennas (the spatial diversity simplest case). It is important to remark that is not possible to obtain benefit of all the properties explained at the same time. This is because the spatial degrees of liberty are limited and it is needed to find a trade off between them. The optimal space time/frequency solution depends on the channel properties and on the network requirements.

Chapter 5

MIMO performance in DVB-NGH

5.1 Introduction

In chapter 4 the basic theory of MIMO systems was briefly exposed. In this chapter the main candidate technologies proposed for DVB-NGH [5] will be presented and the performance of all of them will be studied using MATLAB based simulations. The simulation results shown in this chapter were used during the DVB-NGH standardization process in order to select the most adequate MIMO codification, eSM.

The figure of merit used to compare the different MIMO codifications, SISO and SIMO will be its achievable capacity.

5.2 MIMO schemes proposed in DVB-NGH

As stated in subsection 4.4.1, MIMO systems have clear advantages over the traditional SISO systems. However to obtain the maximum profit of them it is essential to apply an efficient coding to the data transmitted. In this subsection the main target is to show the different techniques that were taken as possible candidates for MIMO data coding in DVB-NGH. Some of them well known, as Golden, Silver and Alamouti codes and other newly proposed for the standard as eSM.

5.2.1 Alamouti MIMO

This MIMO scheme was originally proposed by Siavash M. Alamouti in [14] and its MISO version was already included in DVB-T2. The aim of this technique is to obtain a higher robustness in 2x2 MIMO systems, it follows a scheme as the one shown in Figure 5.1.

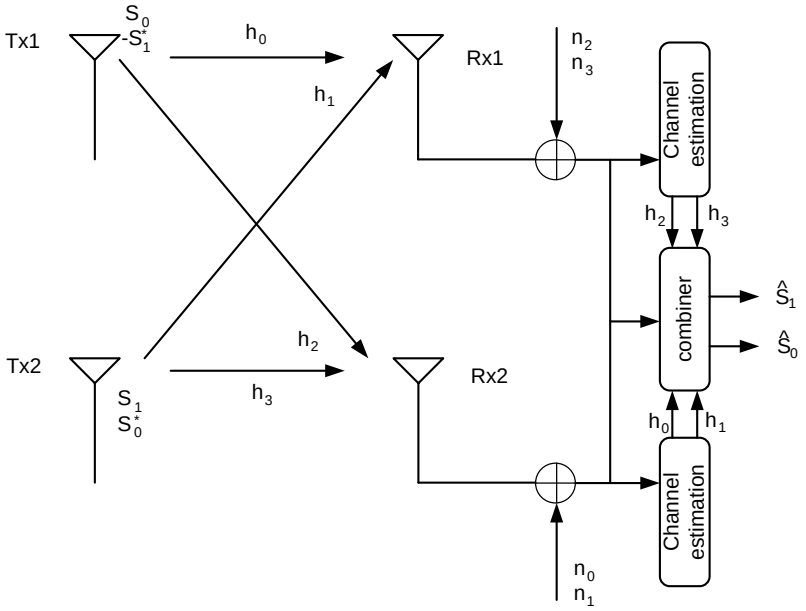

Figure 5.1: MIMO 2x2 Alamouti scheme

Mathematically it can be described as shown in Equation 5.1, where $\mathbf{X}$ represents the output of the MIMO coder and s_1, s_2 the two input M-QAM symbols.

$$\mathbf{X}(s_1, s_2) = \begin{bmatrix} s_1 & -s_2^* \\ s_2 & s_1^* \end{bmatrix} \tag{5.1}$$

This code uses diversity to enhance the system robustness, but reaches half the data rate available for a MIMO 2x2 configuration.

5.2.2 Golden Code

Golden Code [36] is a space-time code for MIMO systems with 2 transmitter and receiver antennas. The generation of the code follows the expression in Equation 5.2, where s_1,s_2,s_3 and s_4 represent four consecutive M-QAM constellation symbols to be transmitted, $\theta = (1+\sqrt{5})/2$ (the golden number that gives name to the codification), and $\sigma = 1-\theta$.

$$\mathbf{X}(s_1,s_2,s_3,s_4) = \frac{1}{\sqrt{5}}\begin{bmatrix}(1+\sigma i)s_1+(\theta-i)s_2 & (1+\sigma i)s_3+(\theta-i)s_4\\ (i-\theta)s_3+(1+\sigma i)s_4 & (1+\theta i)s_1+(\sigma-i)s_2\end{bmatrix} \quad (5.2)$$

The main properties of this code are:

- Full rank: The determinant of the difference of two codewords is always different from zero.
- Full rate: The four degrees of freedom in the system are used.
- No null determinant: the minimum determinant is $1/\sqrt{5}$.
- Reaches the frontier of diversity in multiplexing gain.
- The spectral efficiency is $2\log_2(M) bits/s/Hz$.
- The number of distances to be computed in ML detection is M^4

5.2.3 Silver Code

Silver Code [37] is a time-space code for MIMO 2x2 systems that allows a simpler detection than Golden Code. The codification of the codewords follows the expression indicated in Equation 5.3, where $\mathbf{X}_a$ is defined in Equation 5.4, $\mathbf{X}_b$ in Equation 5.5 and Equation 5.6 and $\mathbf{T}$ in Equation 5.7.

$$\mathbf{X} = \mathbf{X}_a(s_1,s_2) + \mathbf{T}\mathbf{X}_b(z_1,z_2) \quad (5.3)$$

$$\mathbf{X}_a(s_1,s_2) = \begin{bmatrix}s_1 & -s_2^*\\ s_2 & s_1^*\end{bmatrix} \quad (5.4)$$

$$\mathbf{X}_b(z_1, z_2) = \begin{bmatrix} z_1 & -z_2^* \\ z_2 & z_1^* \end{bmatrix} \tag{5.5}$$

$$\begin{bmatrix} z_1 \\ z_2 \end{bmatrix} = \mathbf{U} \begin{bmatrix} s_3 \\ s_4 \end{bmatrix} = \frac{1}{\sqrt{7}} \begin{bmatrix} 1+i & -1+2i \\ 1+2j & 1-i \end{bmatrix} \begin{bmatrix} s_3 \\ s_4 \end{bmatrix} \tag{5.6}$$

$$\mathbf{T} = \begin{bmatrix} 1 & 0 \\ 0 & -1 \end{bmatrix} \tag{5.7}$$

where s_i represents a M-QAM symbol to be transmitted. This codification technique has a very similar characteristics to the ones of the Golden Code, and the main ones are summarized below.

- Full rank: The determinant of the difference of two codewords is always different from zero.
- Full rate: The four degrees of freedom in the system are used.
- No null determinant: the minimum determinant is $1/\sqrt{7}$.
- Reaches the frontier of diversity in multiplexing gain.
- The spectral efficiency is $2\log_2(M) bits/s/Hz$.
- Fast decoding: In the worst case the number of distances to be calculated while detecting will be $2M^3$for a ML detection.

5.2.4 eSM

This technique is based in the well known SM (given as an example in subsubsection 4.4.1.3) and was originally proposed in [38]. This technique pretends to obtain a high multiplexing gain in uncorrelated channels and robustness in channels with a high correlation.

The eSM scheme proposed for DVB-NGH is described in Equation 5.8.

$$\begin{bmatrix} x_1 \\ x_2 \end{bmatrix} = \frac{1}{\sqrt{1+a^2}} \begin{bmatrix} 1 & a \\ a & -1 \end{bmatrix} \begin{bmatrix} s_1 \\ s_2 \end{bmatrix} \tag{5.8}$$

In Equation 5.8, s_1 and s_2 represent normalized QAM symbols, and x_1 and x_2 the codfied MIMO symbols. The a parameter is defined depending on the constellation used, as shown in Equation 5.9.

$$a = \begin{cases} (\sqrt{2}+3+\sqrt{5})/(\sqrt{2}+3-\sqrt{5}) & \text{if QPSK+QPSK} \\ (\sqrt{2}+4)/(\sqrt{2}+2) & \text{if 16-QAM+16-QAM} \end{cases} \tag{5.9}$$

Equation 5.8 can be also seen as a rotation between both of the transmitter antennas, and then to be rewritten as shown in Equation 5.10, where θ represents the aforementioned rotation angle.

$$\begin{bmatrix} x_1 \\ x_2 \end{bmatrix} = \begin{bmatrix} cos(\theta) & -sin(\theta) \\ sin(\theta) & cos(\theta) \end{bmatrix} \begin{bmatrix} s_1 \\ s_2 \end{bmatrix} \tag{5.10}$$

5.3 Effective bit per cell calculation

In order to be able to represent the capacity against the noise power it is necessary to calculate the effective bits per cell for each of the possible MIMO configurations. This calculation quantifies the effective number of data in every cell taking into account the following parameters:

- Bits per cell: this parameter depends on the chosen modulation and corresponds with the number of bits represented by the chosen M-QAM constellation point transmitted into the corresponding cell. The number of bits per cell is indicated in Table 5.1.
- Coding rate: this parameter refers to the proportion between the total number of bits of the codeword output of the forward error correction block

Modulation	QPSK	16-QAM	64-QAM	256-QAM
Bits per cell ($Bits_c$)	2	4	6	8

Table 5.1: Bits per cell

and the data bits in it. In this case LDPC codes are used.

$$CR = \frac{Bits_{data}}{Bits_{data} + Bits_{redundancy}} \tag{5.11}$$

- BCH header: this corresponds to the redundancy bits inserted by the BCH code. The number of redundancy bits depends on the LDPC code rate, as shown in Table 5.2.

Code rate	Data bits	Data+header bits
3/15	3072	3240
5/15	5232	5400
6/15	6312	6480
4/9	7032	7200

Table 5.2: BCH overhead

- Scattered pilots: they are added for channel estimation purpose. This pilots make the amount of effective bits per cell to decrease. The pilot pattern selected for MIMO study in DVB-NGH standardization process was PP1 [3]. Depending on what kind of configuration is used (MIMO, SIMO, SISO) the correction to apply will be 1/6 or 1/12. This is because in PP1 one cell in every 12 is a pilot and then this capacity is lost. For 2x2 MIMO twice the number of pilots are needed.

- Half/full rate MIMO coding (M): In the case of MIMO full rate coding the whole capacity that the channel offers is used to transmit different data, in half rate codes half of this available capacity is used to increase the robustness of the system with additional redundancy, so the capacity is

halved in comparison. In this document the only half rate MIMO code is Alamouti.

Taking into account all these parameters, the calculus of the number of effective cells is as shown in Equation 5.12.

$$EBPC = M \cdot Bits_c \cdot CR \cdot \frac{Bits_{data}}{Bits_{BCHoverhead}} \cdot (1 - PP1_{overhead}) \tag{5.12}$$

For all the configurations contemplated during the standardization process the calculus of the EBPC is shown in Table 5.3, Table 5.4, and Table 5.5.

Modulation	BPC	Code rate	Data bits	Data+header bits	EBPC
QPSK	2	3/15	3072	3240	0.35
		5/15	5232	5400	0.59
		6/15	6312	6480	0.71
		4/9	7032	7200	0.80
16-QAM	4	3/15	3072	3240	0.7
		5/15	5232	5400	1.18
		6/15	6312	6480	1.43
		4/9	7032	7200	1.59
64-QAM	6	3/15	3072	3240	1.04
		5/15	5232	5400	1.78
		6/15	6312	6480	2.14
		4/9	7032	7200	2.39
256-QAM	8	3/15	3072	3240	1.39
		5/15	5232	5400	2.37
		6/15	6312	6480	2.86
		4/9	7032	7200	2.18

Table 5.3: SISO and SIMO EBPC

Modulation	BPC	Code rate	Data bits	Data+header bits	EBPC
QPSK	2	3/15	3072	3240	0.32
		5/15	5232	5400	0.54
		6/15	6312	6480	0.65
		4/9	7032	7200	0.72
16-QAM	4	3/15	3072	3240	0.63
		5/15	5232	5400	1.08
		6/15	6312	6480	1.30
		4/9	7032	7200	1.45
64-QAM	6	3/15	3072	3240	0.95
		5/15	5232	5400	1.61
		6/15	6312	6480	1.95
		4/9	7032	7200	2.17
256-QAM	8	3/15	3072	3240	1.26
		5/15	5232	5400	2.15
		6/15	6312	6480	2.60
		4/9	7032	7200	2.89

Table 5.4: MIMO half rate EBPC

Modulation	BPC	Code rate	Data bits	Data+header bits	EBPC
QPSK	2	3/15	3072	3240	0.63
		5/15	5232	5400	1.08
		6/15	6312	6480	1.3
		4/9	7032	7200	1.45
16-QAM	4	3/15	3072	3240	1.26
		5/15	5232	5400	2.15
		6/15	6312	6480	2.60
		4/9	7032	7200	2.89

Table 5.5: MIMO full rate EBPC

5.4 Performance analysis

In this section the capacity curves obtained by means of computer simulations will be presented. In each subsection it will be shown first the system configuration and after the capacity curves that characterize the system performance for that given configuration.

The CSP [7] was taken as a basis for the simulation platform, being modified to add the MIMO simulation capability. As a result a system as the one shown in Figure 5.2 was obtained.

The simulation chain consists of 4 groups of blocks regarding the functionality that is carried out in them: data input porcessing, BICM, frame builder and OFDM signal generation.

To compare SISO and MIMO it should be taken into account that in the MIMO channel generation the resulting propagation scenario is normalized to have an unity gain. Due to this fact, when one of the paths of the MIMO channel is taken to generate the SISO propagation scenario it will have a gain different from the unity (lower in this case). This makes the noise power inserted at the receiver in the SISO scenario lower than in the case of MIMO resulting in a non fair comparison. As a solution for this problem a certain noise power is inserted independently to the signal level, this is the noise power is inserted referred to a normalized signal level.

In the graphics presented in this subsection it will be represented the noise power (dB) in the abscissa axis and in ordinate the effective bits per cell (calculated as shown in section 5.3). A BER target is fixed at the receiver side after the LDPC decoder ($10^{-5} generally$), the noise power will be the one that provides the fixed performance level. The curves with the same token and line represent the same MIMO technique or SISO and SIMO configurations.

In the following subsections the simulation results obtained for the different set of propagation scenarios will be presented, after that these results will be analysed.

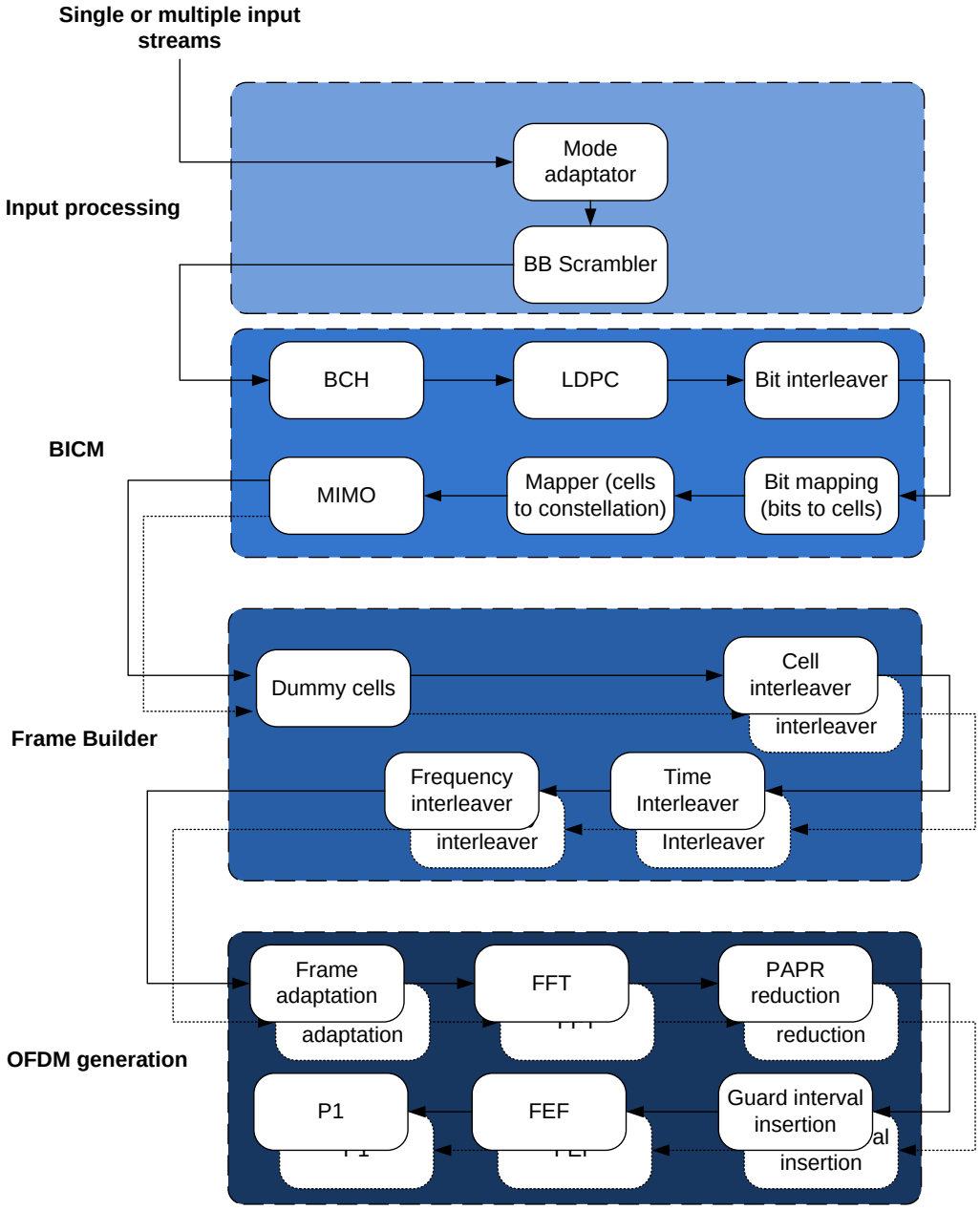

Figure 5.2: Transmitter block diagram

5.4.1 Results in snapshot scenarios

The snapshot scenarios are fixed realizations of the propagation channel, this means that the propagation scenario is time invariant. This gives a first approach of what MIMO coding gives a better performance, and also the gain that can be achieved when compared to other configurations as SISO or SIMO.

Note that this approximation is not very representative of a mobile communication, this configuration was used in the beginning of the standardization process because of the lack of a realistic and representative mobile channel model. However the simulations in this scenario can clarify whether there is difference of performance between the different proposed techniques, or not.

All the simulations in this subsection follow the system configuration listed below:

- C/N shown for a BER target of 10^{-5} after the LDPC decoder with a maximum of 50 iterations.
- Ideal channel estimation.
- Bit and frequency interleavers activated, time interleaver bypassed.
- 4k tranmission mode.
- 1/4 guard interval.
- 5Mhz bandwidth.
- Maximum likelihood detection.

First the simulation results will be presented, to be studied in detail afterwards.

5.4.1.1 Pessimistic Outdoor Channel

In this channel model described in [33] only a 10% of the channel realizations will be under its capacity. The simulation results obtained are shown in Figure 5.3.

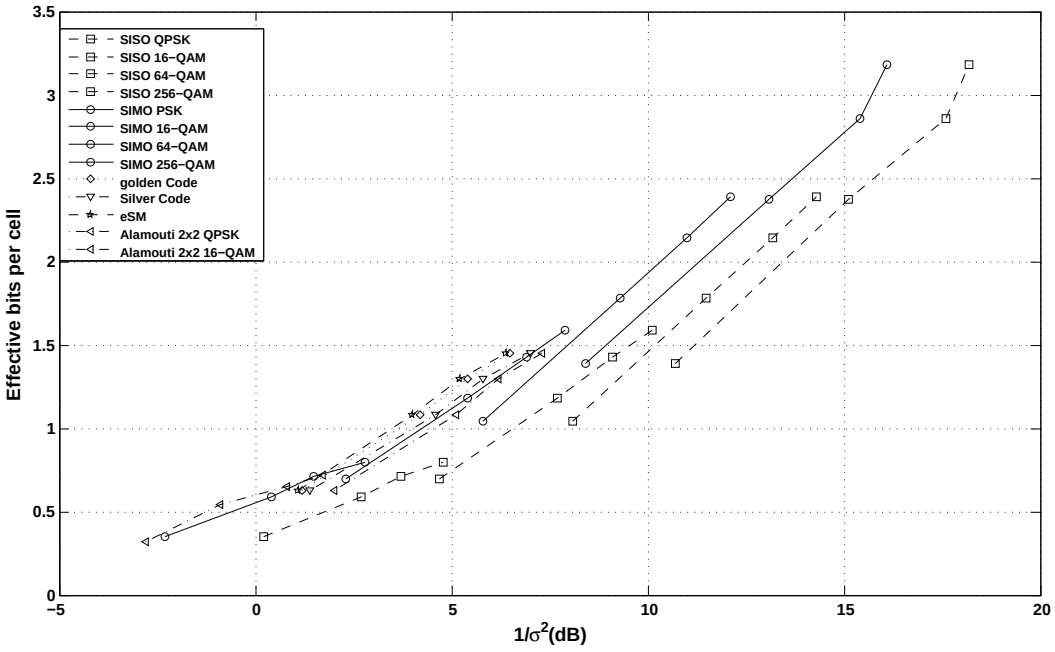

Figure 5.3: Pessimistic snapshot scenario simulation results

5.4.1.2 Typical Outdoor Channel

In this channel model described in [33] the 50% of the channel realizations will be under its capacity, and the 50% remaining will be over it. The simulation results obtained can be seen in Figure 5.4.

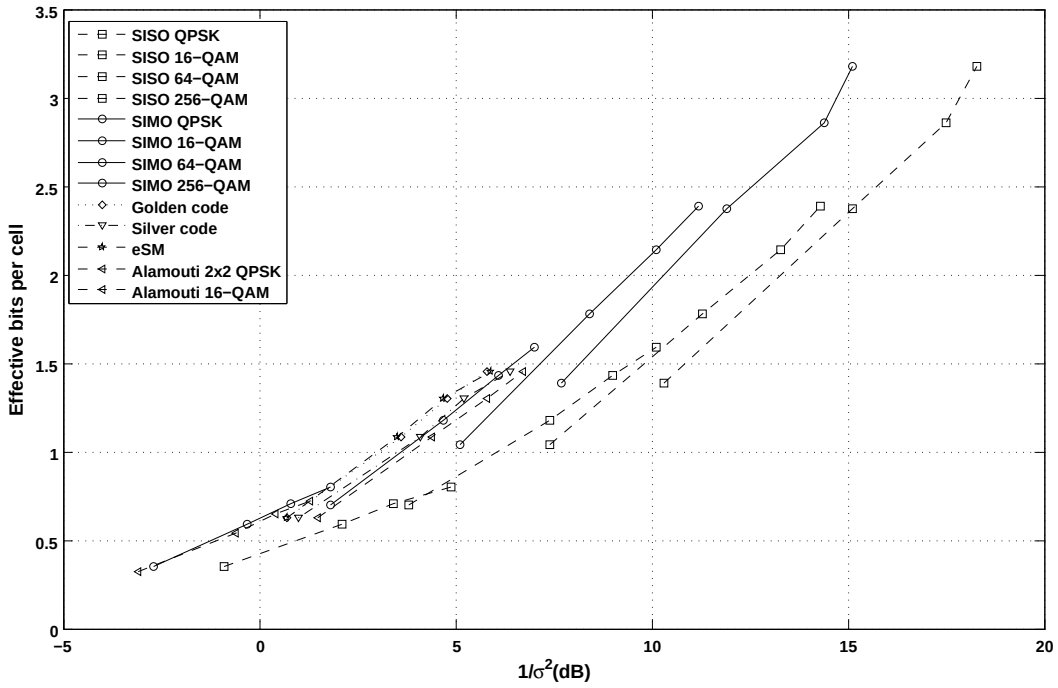

Figure 5.4: Typical snapshot scenario simulation results

5.4.1.3 Optimistic Outdoor Channel

In this channel model described in [33] only a 10% of the channel realizations will be over its capacity. The simulation results obtained can be seen in Figure 5.5.

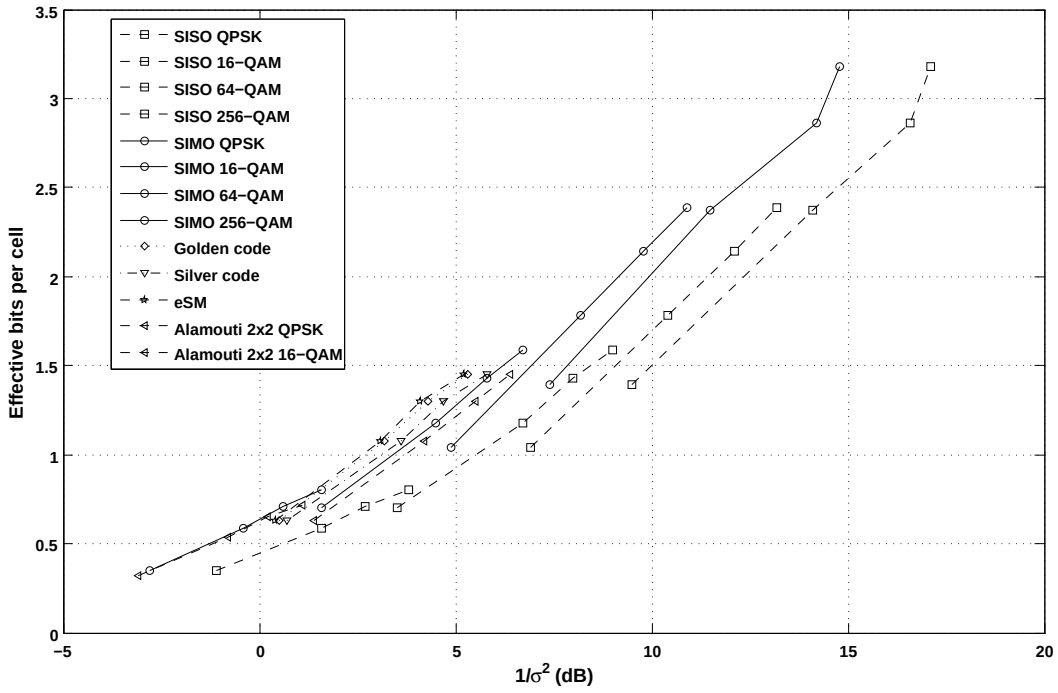

Figure 5.5: Optimistic snapshot scenario simulation results

5.4.1.4 Results analysis

A similar behavior in terms of relative performance between the studied techniques can be appreciated in the curves presented in the previous subsections. It can be observed that MIMO techniques have a better performance in the simulated cases. The performance difference between eSM, Golden code, and Silver code, is almost negligible. This could lead to the conclusion that these three techniques were all well suited to be adopted in DVB-NGH, however taking into account the detection process, as mentioned in section 5.2, Golden and Silver codes introduce a very high hardware complexity ($M^4 and M^3$ respectively) whereas eSM in comparison is much simpler (M^2). This makes eSM the best choice among the studied MIMO codifications.

A summary of the gain that can be obtained using eSM compared to the other studied configurations at different effective bits levels is presented in the following tables.

	eSM vs Golden Code		
EBPC	Pessimistic	Typical	Optimistic
0.63	0.1	0	0.1
1.08	0.2	0.1	0.1
1.30	0.2	0.1	0.2
1.45	0.1	0.1	0.1

Table 5.6: eSM gain (dB) referred to Golden code

	eSM vs Silver Code		
EBPC	Pessimistic	Typical	Optimistic
0.63	0.3	0.3	0.3
1.08	0.6	0.6	0.5
1.30	0.6	0.5	0.6
1.45	0.6	0.5	0.6

Table 5.7: eSM gain (dB) referred to Silver code

	eSM vs Alamouti 2x2		
EBPC	Pessimistic	Typical	Optimistic
0.63	0.9	0.8	1.0
1.08	1.1	0.9	1.1
1.30	0.9	1.1	1.4
1.45	0.9	0.8	1.2

Table 5.8: eSM gain (dB) referred to Alamouti 2x2

	eSM vs SISO		
EBPC	Pessimistic	Typical	Optimistic
0.63	3.2	2.6	2.7
1.08	3.0	3.1	2.9
1.30	3.2	3.4	3.2
1.45	2.8	3.2	2.9

Table 5.9: eSM gain (dB) referred to SISO

	eSM vs SIMO		
EBPC	Pessimistic	Typical	Optimistic
0.63	0.8	0.7	0.8
1.08	0.7	0.6	0.8
1.30	0.9	0.7	1.0
1.45	0.6	0.3	0.7

Table 5.10: eSM gain (dB) referred to SIMO

From Table 5.6, Table 5.7,Table 5.8, Table 5.9 and Table 5.10 it can be followed that eSM offers a better performance, in terms of capacity, than the rest of the studied schemes, presenting a maximum gain over them that can be found in Table 5.11. The minimum gain observed can be found in Table 5.12.

	Golden	Silver	Alamouti	SIMO	SISO
Max. gain (dB)	0.2	0.6	1.4	1.0	3.4

Table 5.11: eSM maximum gain (dB)

	Golden	Silver	Alamouti	SIMO	SISO
Min. gain (dB)	0.0	0.3	0.8	0.3	2.7

Table 5.12: eSM minimum gain (dB)

5.4.2 SFNs results

An SFN is the one in which several transmitters transmit the same information using the same frequency. The main target of the SFNs is the improvement of the spectral efficiency, allowing a higher performance when compared to the traditional MFNs. An SFN can increase the coverage area, this is because the total received power in the points between transmitters increases.

The SFN transmissions can be considered as multipath propagation cases in very adverse conditions. The receiver receives different echoes of the same signal and the delay between them can cause severe fadings in the communication channel.

In DVB-NGH the use of this kind of channels is contemplated and because of this during the standardization process the channel models described in [33] were developed.

The simulation conditions in SFN scenarios were set to:

- BER lower than 10^{-5} after the LDPC decoder with at least 200 erroneous FEC blocks and a máximum of 20000 LDPC blocks for each C/N.
- 16k length LDPC with code rates of 1/4, 1/3, 2/5, and 1/2.
- 8 MHz bandwidth
- Guard interval of 1/4.
- 4k FFT size.
- Relative power imbalance between paths of 9, 6, 3, and 0 dB.

In this subsection the same procedure as in the previous will be followed. First the simulation results will be presented and after they will be analysed.

5.4.2.1 SFN indoor simulation results

This kind of scenario models a SFN reception inside a typical building.

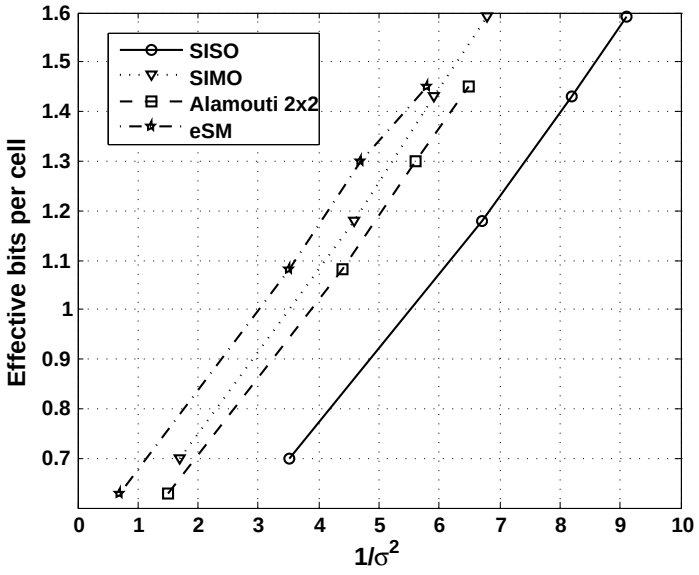

Figure 5.6: SFN indoor scenario results for 9 dB power imbalance

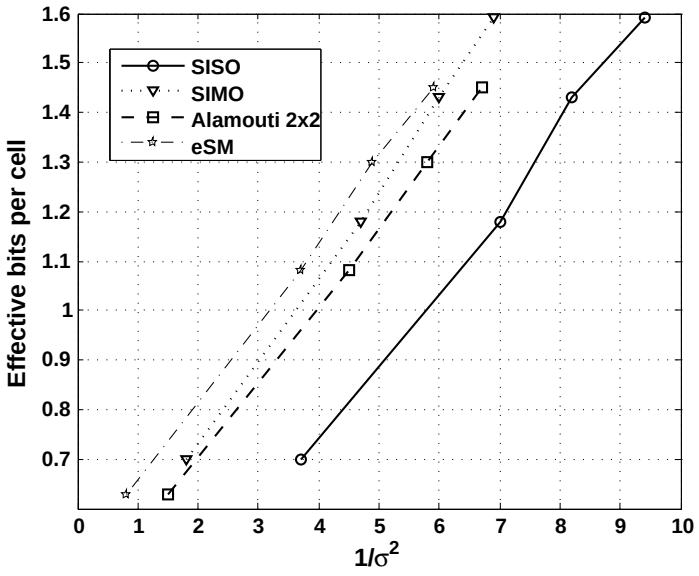

Figure 5.7: SFN indoor scenario results for 6 dB power imbalance

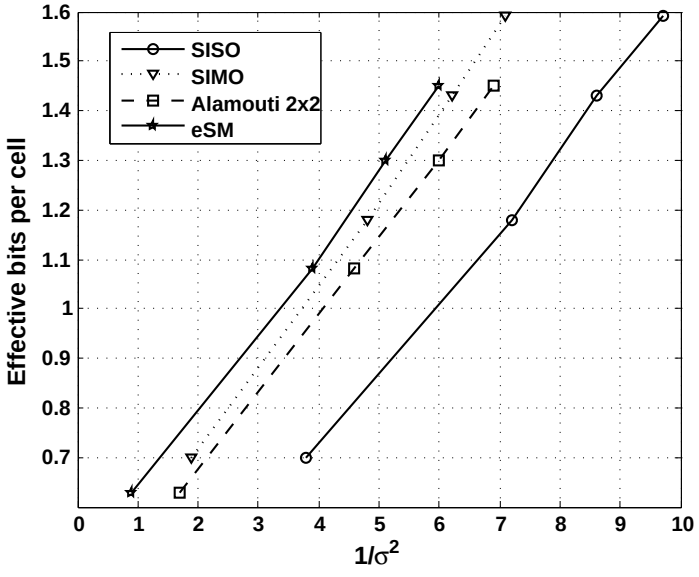

Figure 5.8: SFN indoor scenario results for 3 dB power imbalance

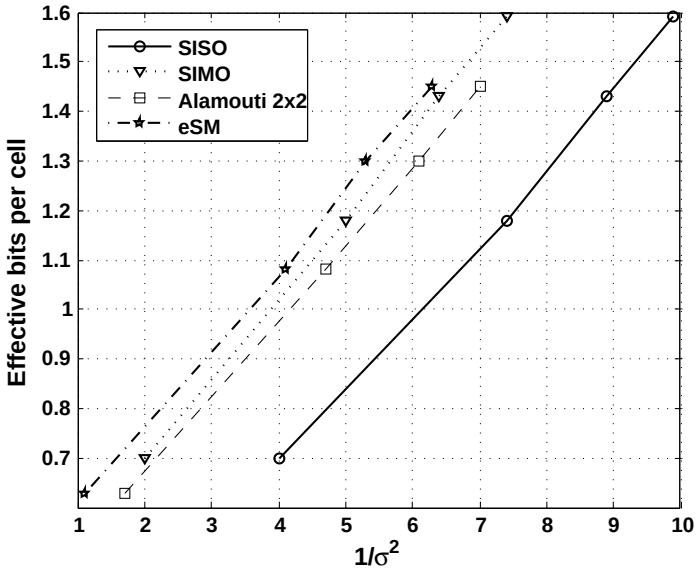

Figure 5.9: SFN indoor scenario results for 0 dB power imbalance

5.4.2.2 SFN outdoor simulation results

This kind of scenario models a SFN reception in an open area environment.

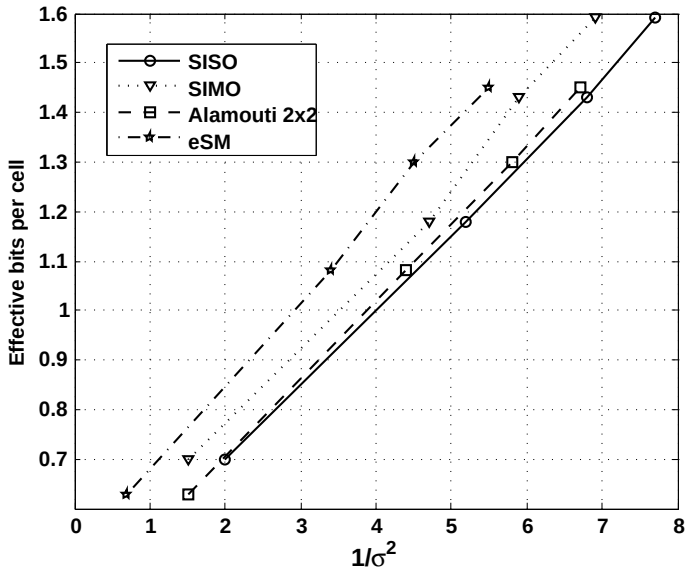

Figure 5.10: SFN outdoor scenario results for 9 dB power imbalance

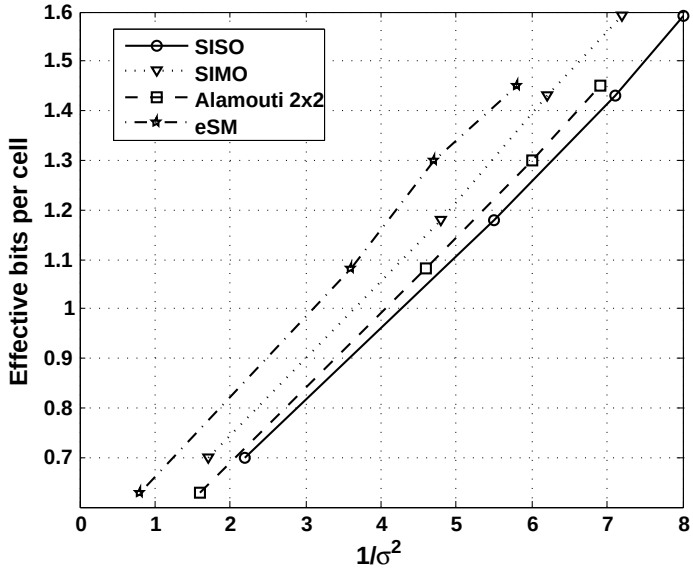

Figure 5.11: SFN outdoor scenario results for 6 dB power imbalance

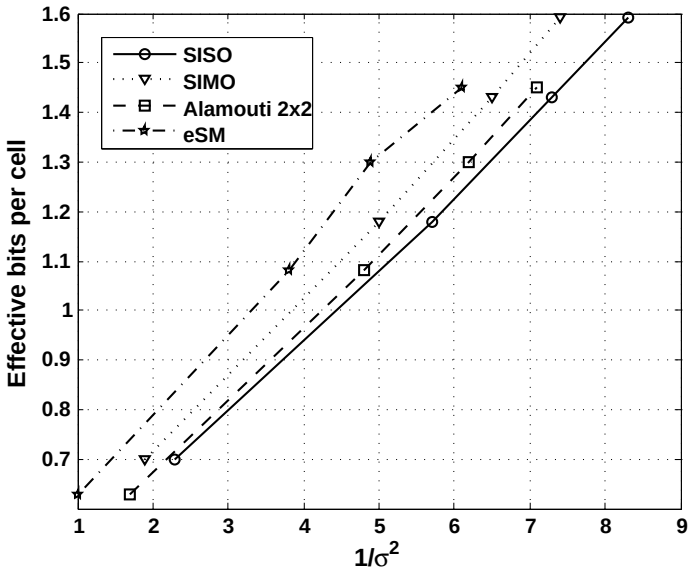

Figure 5.12: SFN outdoor scenario results for 3 dB power imbalance

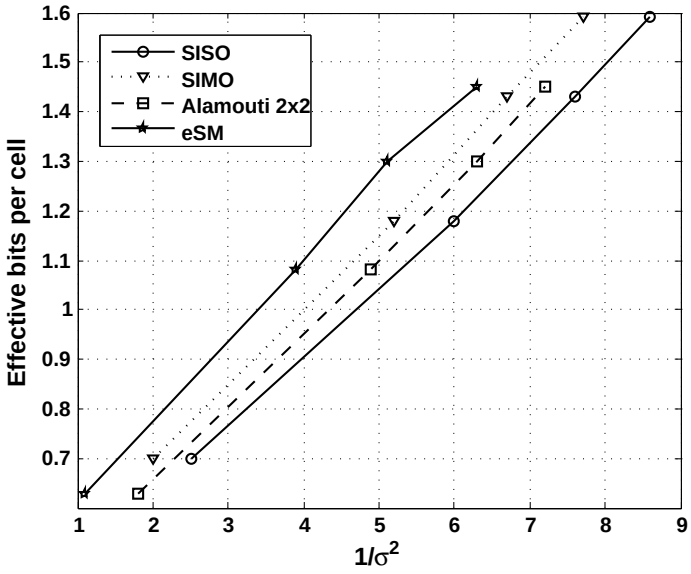

Figure 5.13: SFN outdoor scenario results for 0 dB power imbalance

5.4.2.3 Results analysis

All the results presented in subsubsection 5.4.2.1 and subsubsection 5.4.2.2 show a very similar behavior, eSM presents a better performance in every case. Also it is remarkable that SIMO and Alamouti 2x2 show a very similar performance in the case of not having a very big power imbalance but when the power imbalance increases SIMO offers better performance.

To have a quantitative idea of the performance gain obtained in terms of $1/\sigma^2$(dB) the following tables show a comparative between the different codes for the studied cases.

	eSM Vs SISO Indoor			
PI \ EBPC	0.63	1.08	1.30	1.45
9	2.30	2.53	2.72	2.51
6	2.31	2.61	2.68	2.25
3	2.33	2.59	2.77	2.34
0	2.35	2.59	2.82	2.43

Table 5.13: eSM gain (dB) referred to SISO in SFN indoor scenario

	eSM Vs SISO Outdoor			
PI \ EBPC	0.63	1.08	1.30	1.45
9	0.82	1.13	1.47	1.41
6	0.89	1.21	1.57	1.41
3	0.77	1.19	1.57	1.33
0	0.84	1.37	1.67	1.43

Table 5.14: eSM gain (dB) referred to SISO in SFN outdoor scenario

These tables show the difference in performance existing between eSM and the rest of configurations and codes contemplated in the DVB-NGH standardization process. The capacity is measured with a BER level of 10^{-5} and the measurements

	eSM Vs SIMO Indoor			
PI \ EBPC	0.63	1.08	1.30	1.45
9	0.53	0.50	0.52	0.21
6	0.53	0.40	0.42	0.01
3	0.55	0.30	0.37	-0.09
0	0.43	0.28	0.37	-0.08

Table 5.15: eSM gain (dB) referred to SIMO in SFN indoor scenario

	eSM Vs SIMO Outdoor			
PI \ EBPC	0.63	1.08	1.30	1.45
9	0.23	0.63	0.78	0.53
6	0.40	0.55	0.77	0.53
3	0.42	0.55	0.82	0.51
0	0.40	0.63	0.82	0.53

Table 5.16: eSM gain (dB) referred to SIMO in SFN outdoor scenario

	eSM Vs Alamouti indoor			
PI \ EBPC	0.63	1.08	1.30	1.45
9	0.80	1.00	0.90	0.70
6	0.70	0.80	0.90	0.60
3	0.80	0.70	0.90	0.50
0	0.60	0.60	0.90	0.40

Table 5.17: eSM gain (dB) referred to Alamouti 2x2 in SFN indoor scenario

	eSM Vs Alamouti outdoor			
PI \ EBPC	0.63	1.08	1.30	1.45
9	0.80	1.00	1.30	1.20
6	0.80	1.00	1.30	1.10
3	0.70	1.00	1.30	1.00
0	0.70	1.00	1.20	0.90

Table 5.18: eSM gain (dB) referred to Alamouti 2x2 in SFN outdoor scenario

are taken with different EBPC and different power imbalance between paths. The maximum gain that eSM presents is shown in Table 5.19. The minimum gain found is presented in Table 5.20.

	SISO	SIMO	Alamouti 2x2
Maximum Gain (dB)	2.82	0.82	1.3

Table 5.19: Maximum eSM gain (dB) in SFN scenarios

	SISO	SIMO	Alamouti 2x2
Minimum Gain (dB)	0.82	0.23	0.4

Table 5.20: Maximum eSM gain (dB) in SFN scenarios

5.4.3 Mobile channel model results

The mobile channel used is a 6 taps model and is defined in [33]. The model takes into account effects as the polarization rotation and power asymmetry between the two used polarizations. Doppler frequencies of 33.3 and 194.8 Hz (corresponding with speeds of 60 and 350 km/h at the work frequency of 600 MHz) are contemplated, defined as representative of vehicular movements of low and high speed. The models mean to be representative in the UHF band.

The system has been set as listed bellow:

- 4k FFT size.
- 1/4 guard interval.
- LDPC code rates of 1/4, 1/3, 2/5, and 1/2.
- Ideal channel estimation.
- 16-QAM constellation.
- $1/\sigma^2$ values are measured at a BER level of 10^{-5} after the LDPC decoder.

5.4.3.1 33.3 Hz Doppler results

In these simulations the maximum Doppler frequency is set to 33.3 Hz (as stated before corresponding with a vehicular movement of 60 km/h at the working frequency of 600 MHz).

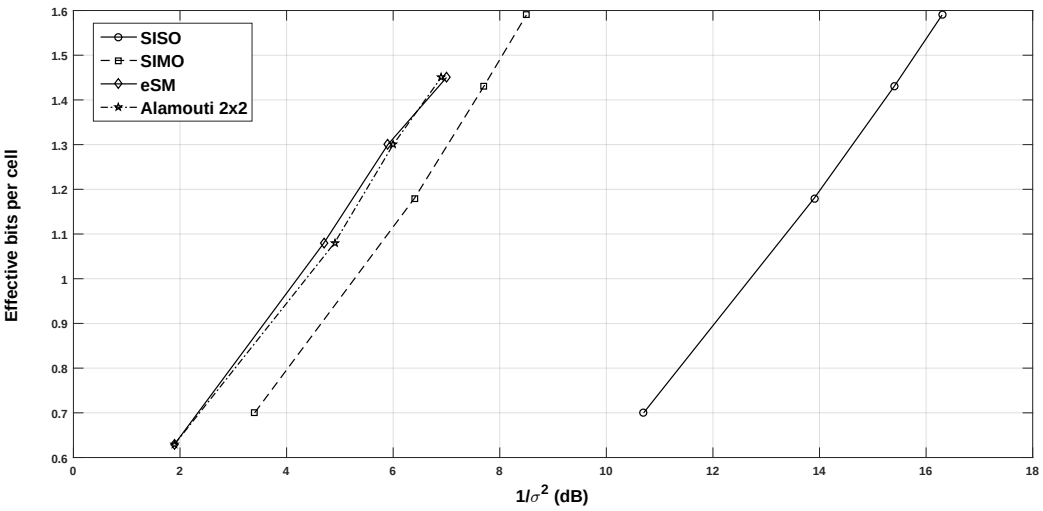

Figure 5.14: Simulation results for 33.3 Hz Doppler

As appreciated in Figure 5.14 the proposed codification has a considerable gain when compared with the SISO scheme, and over a diversity scheme as SIMO. The gain in dB observed is summarized in Table 5.21.

33.3 Hz Doppler	EBPC=1.18		
Coding	Alamouti 2x2	SIMO	SISO
eSM gain (dB)	0.2	1.7	9.2

Table 5.21: eSM gain (dB) in 33.3 Hz Doppler scenario

5.4.3.2 194.8 Hz Doppler results

In these simulations the maximum Doppler frequency is set to 194.8 Hz. As it can be seen in Figure 5.15 the behaviour found is very similar to the one found in the previous subsection, and a numeric summary of the gain can be found in Table 5.22.

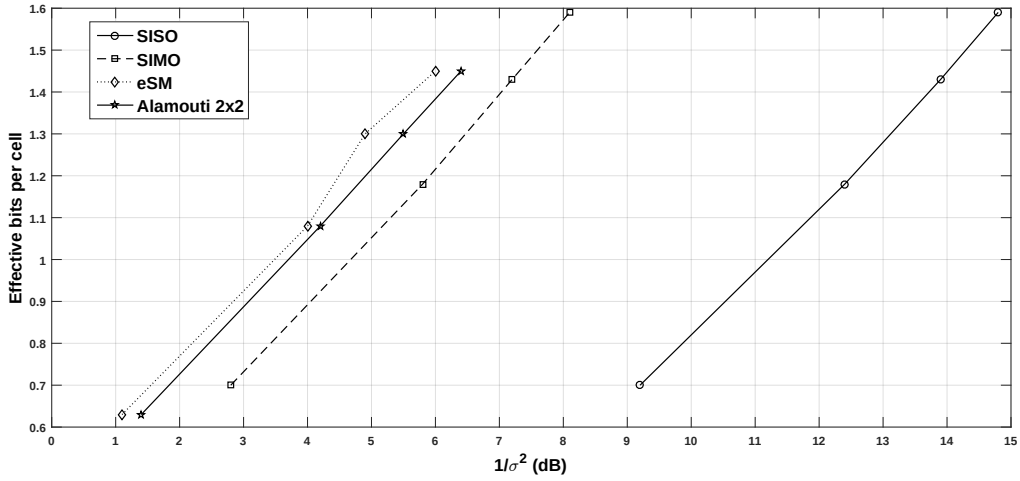

Figure 5.15: Simulation results for 194.8 Hz Doppler

5.4.3.3 Results analysis

From previous figures it can be seen that when Doppler affects the communication the gain gap between traditional SISO systems and MIMO ones increases notably (over 9 dB). However the difference between MIMO codes decreases, eSM and

194.8 Hz Doppler	EBPC=1.18		
Coding	Alamouti 2x2	SIMO	SISO
eSM gain (dB)	0.2	1.7	8.4

Table 5.22: eSM gain (dB) in 194.8 Hz Doppler scenario

Alamouti have a performance gap of about 0.2dB instead of the about 1dB that could be found in the static channel realizations.

5.4.4 Overall results analysis

In this chapter it has been shown the huge gain introduced in the system because of the use of MIMO when compared with other possible configurations as SIMO and SISO. This gain increases greatly when the Doppler spread affects the communication reaching over 9dB performance gain when compared with SISO.

5.5 Contributions derived from the DVB-NGH study

In this section the two main contributions that were achieved during the study of DVB-NGH will be presented. The first one is a simplification method for the DVB-NGH MIMO decoder that follows the same philosophy as the second approach presented in chapter 3. The second contribution is the application of eSM to SISO systems as DVB-T2.

5.5.1 Detection process complexity

For an optimal detection and calculation of the LLR metrics, the Max-log approximation can be used leading to the expression in Equation 5.13, where b_i represents the i-th bit of the received symbol, σ^2 is the noise variance, C_i^k is the subset of symbols of the ideal MIMO constellation in which the i-th bit's value is k (0 or 1), $\widetilde{\mathbf{H}}$ is the estimated channel matrix, Y is the received signal, and S is

the ideal transmitted MIMO symbol.

$$LLR(b_i) \approx \frac{1}{2\sigma^2} \min_{x \in C_i^0} \left(\left\| Y - \widetilde{\mathbf{H}} S \right\| \right) - \min_{x \in C_i^1} \left(\left\| Y - \widetilde{\mathbf{H}} S \right\| \right) \tag{5.13}$$

In the case of MIMO, the symbols are vectors of M components that increase the number of possible candidates in the C_i^k subsets when compared to the SISO equivalent scheme (same number of bits per QAM constellation symbol). For a generic M component MIMO codification vector, the number of possible candidates is 2^{mM}, where m represents the number of bits of the used QAM constellation (supposing the same constellation order in all the components of the transmitted vector). Note that for eSM M=2. Therefore, in order to find the minimums of Equation 5.13, for every possible candidate we need to calculate the expression shown in Equation 5.14, where y_j represents the j-th component (with j taking the values 0 or 1) of the received vector Y, and hs_j is the j-th component of the vector result of the multiplication.

$$\begin{aligned} \left\| Y - \widetilde{\mathbf{H}} S \right\|^2 = (Re(y_0) - Re(hs_0))^2 + (Im(y_0 - Im(hs_0))^2 \\ + Re(y_1) - Re(hs_1))^2 + (Im(y_1 - Im(hs_1))^2 \end{aligned} \tag{5.14}$$

As an example example, for two 16-QAM (nbpcu=8) there will be 256 possible candidates. Therefore, according to the expression in Equation 5.14, the number of multiplications needed to perform the detection of one received symbol, without taking into account the $\widetilde{\mathbf{H}}S$ product, is 1024. In the case of nbpcu=8 (16-QAM and 64-QAM combination) the number of possible candidates is 1024, increasing the number of distances to be calculated to 4096, this represents the worst case in DVB-NGH.

At the decoder, the $\widetilde{\mathbf{H}}S$ product is also required in order to compute Equation 5.14, Table 5.27 shows the total amount of operations to be performed for each received symbol when the exact squared Euclidean distance calculation is used.

Table 5.23: Total amount of operations to perform in the detection process for each received symbol

n_{bpcu}	Real products	Additions/Subtractions	Complex products
6	256	704	256
8	1024	2816	1024
10	4096	11264	4096

All the multiplications required to find the minimum distances represent a considerable problem when facing the hardware implementation of receivers and this becomes critical when applied to mobile devices as DVB-NGH ones.

5.5.2 Simplification method

As exposed in the previous section, the use of MIMO implies a high complexity decoder. In order to minimize this important drawback (and more taking into account that DVB-NGH is a mobile communications standard), it is proposed to apply an approximation for the calculation of Equation 5.14. The proposed method is an extension of a 2D distance approximation described in [39] and already used in chapter 3 to simplify the hardware complexity of the DVB-T2 reception process.

The distance computation will be now substituted by Equation 5.15 where a_0, b_0, a_1, b_1 are defined by Equation 5.16 and Equation 5.17, and f_0 and f_1 are expressed as Equation 5.18. In Equation 5.16, Equation 5.17, and Equation 5.18, the subscript i takes the values 0 and 1. In Equation 5.18, w and z represent any real value. Finally, λ_i and γ_i are constants that shall be selected to minimize the error of the approximation in Equation 5.15.

$$\left\| Y - \widetilde{\mathbf{H}} S \right\|^2 \approx f_1\left(f_0(a_0, b_0), f_0(a_1, b_1)\right)) \tag{5.15}$$

$$a_i = abs\left(Re(y_i) - Re(hs_i)\right) \tag{5.16}$$

$$b_i = abs\left(Im(y_i) - Im(hs_i)\right) \tag{5.17}$$

$$f_i(w,z) = \lambda_i max(w,z) + \gamma_i min(w,z) \tag{5.18}$$

Note that the simplification proposed is only used when looking for the minimums that appear in Equation 5.13, once the two minimums required are found two exact distances are calculated to avoid any error on their values and hence minimize the performance loss.

In subsection 5.5.1, the number of multiplications and additions for the exact distance calculation were presented, for comparison purpose the same analysis for the proposed method is shown in Table 5.24. Comparing both tables it can be seen that the number of complex multiplications, which belong to the unchanged $\widetilde{\mathbf{H}}S$ product, remains the same. The number of additions or subtractions have slightly increased due to the comparators of our proposed simplification (comparisons can be seen as subtractions where the sign indicates which value is higher). Note however that the number of real multiplications have been drastically reduced, having a big impact in the hardware complexity as will be seen in subsubsection 5.5.2.2.

5.5.2.1 Parameters optimization (λ_i,γ_i)

The values of λ_i and γ_i in Equation 5.18 are selected to obtain the minimum root mean square error (RMSE) of the proposed method applied to the decoder output LLRs. To illustrate this, Figure 5.16 shows the normalized mean square error of the proposed approximation in [39] where only 2 parameters are optimized (λ, γ). The same process is followed to obtain the values in the case with 4 parameters to be optimized.

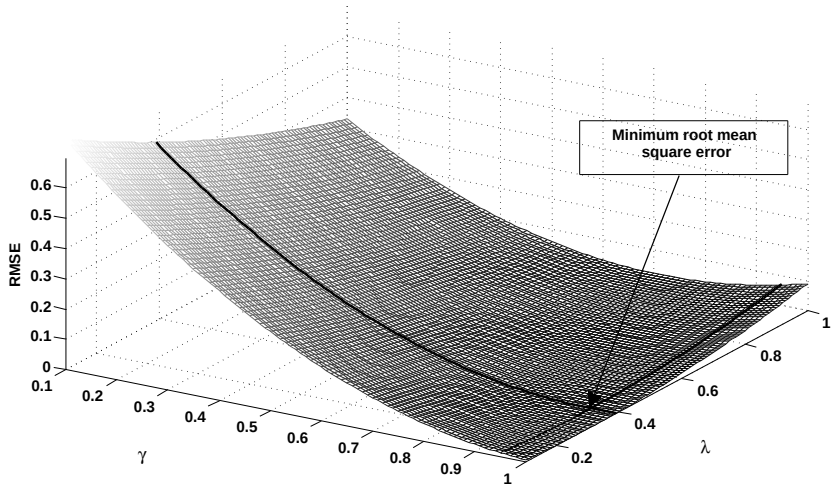

Figure 5.16: Parameters λ and γ optimization

Table 5.24: Total amount of operations to perform in the detection process applying the proposed method for each received symbol

n_{bpcu}	Real products	Additions/Subtractions	Complex products
6	48	980	256
8	64	3696	1024
10	80	14476	4096

The simulations show that the optimum values are $\lambda_0 = 0.7$, $\gamma_0 = 0.3$, $\lambda_1 = 0.9$, and $\gamma_1 = 0.4$. However, in order to further reduce the hardware complexity, these values have been rounded to the nearest power of 2 so the hardware implementation consists of bits shifts instead of multiplications. As result of this constraint, the chosen values are finally $\lambda_0 = 0.5$, $\gamma_0 = 0.25$, $\lambda_1 = 1$, and $\gamma_1 = 0.5$. As it will be shown in next section, these values lead to a negligible impact on the system performance. A block diagram of the proposed solution can be seen in Figure 5.17.

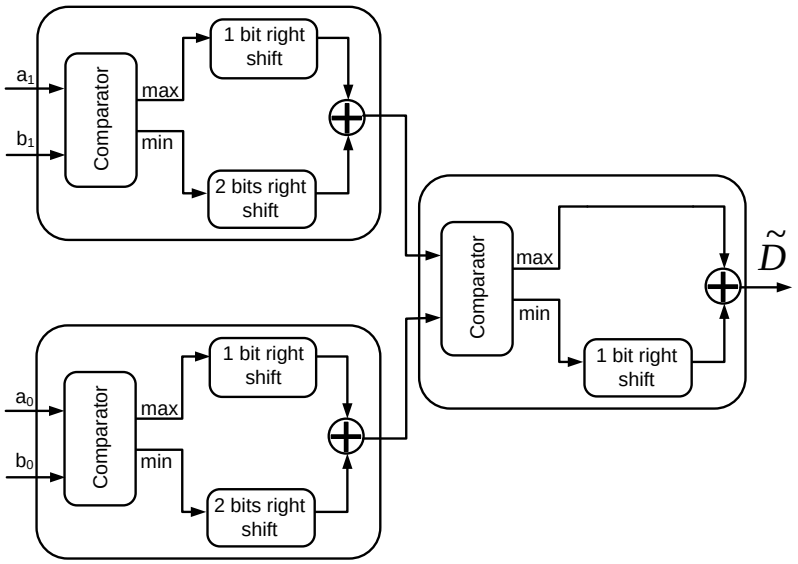

Figure 5.17: Proposed method for MIMO demapper simplification

5.5.2.2 Performance simulation results

The impact of the proposed method on the system performance has been analyzed via BER curves at the output of the LDPC decoder of a DVB-NGH system. In order to obtain these results the same simulation platform as the one developed during the DVB-NGH standardization process was used (see Figure 5.2).

In order to evaluate the performance of the proposed method, the channel model used during the DVB-NGH standardization process and obtained after a measurement campaign held in Helsinki [33] was chosen. As already stated in subsection 5.4.3 , this model represents a characteristic mobile outdoor channel by using an 8 taps propagation scheme, furthermore effects as polarization rotation and power asymmetry between polarizations are added. The variation range of Doppler frequencies is set between 33.3 Hz and 194.8Hz (corresponding to speeds of 60 and 350 km/h for the carrier frequency of 600 MHz). This channel model is supposed to be representative in the UHF frequency band (from 500 to 1000 MHz approximately). All the simulations presented in this paper have been obtained for a LDPC block size of 16.200 bits (16k), code rates form 3/15 to 11/15, and a Doppler frequency of 33.3 Hz. The eSM configuration has been set to 0dB PI and 16-QAM+16-QAM (nbpcu=8) input modulations.

The performance of the aforementioned scheme is characterized by means of BER curves versus C/N after the LDPC decoder at the receiver side. The proposed method is compared to the Max-log approximation.

It can be followed from all the curves that the performance loss due to the use of the proposed method is almost negligible, being under 0.1 dB in every code rate.

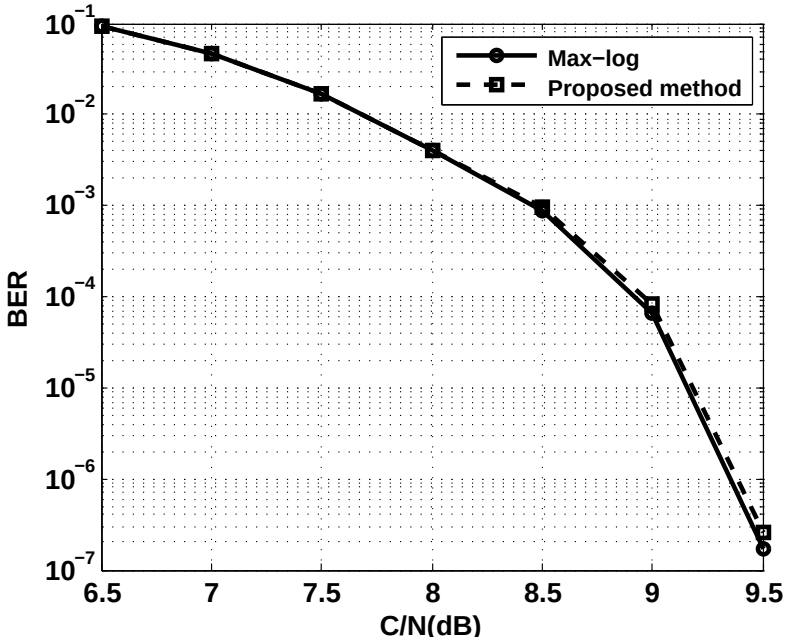

Figure 5.18: Simulation results for 3/15 code rate

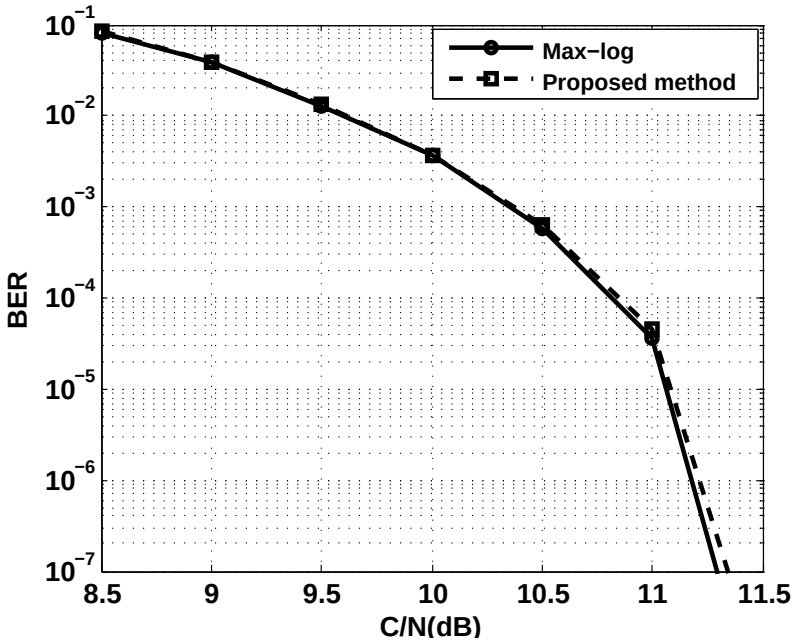

Figure 5.19: Simulation results for 4/15 code rate

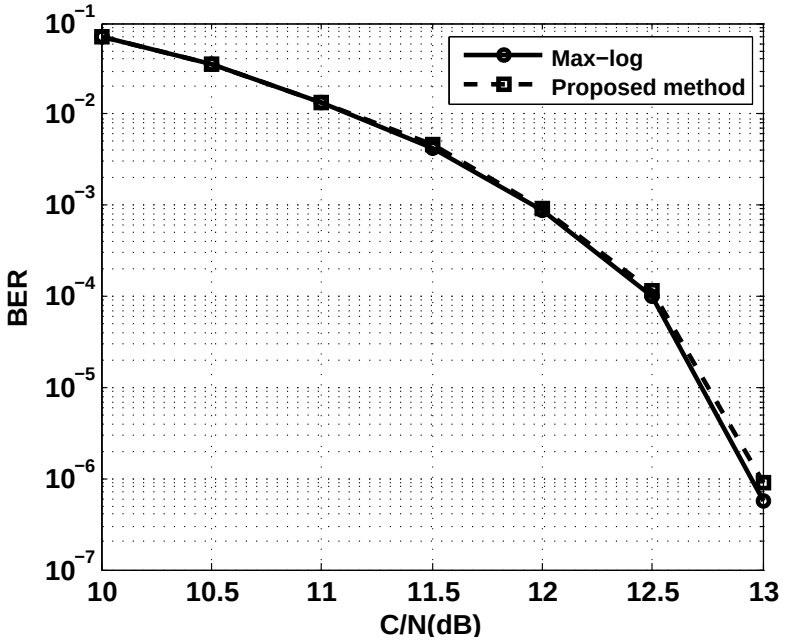

Figure 5.20: Simulation results for 5/15 code rate

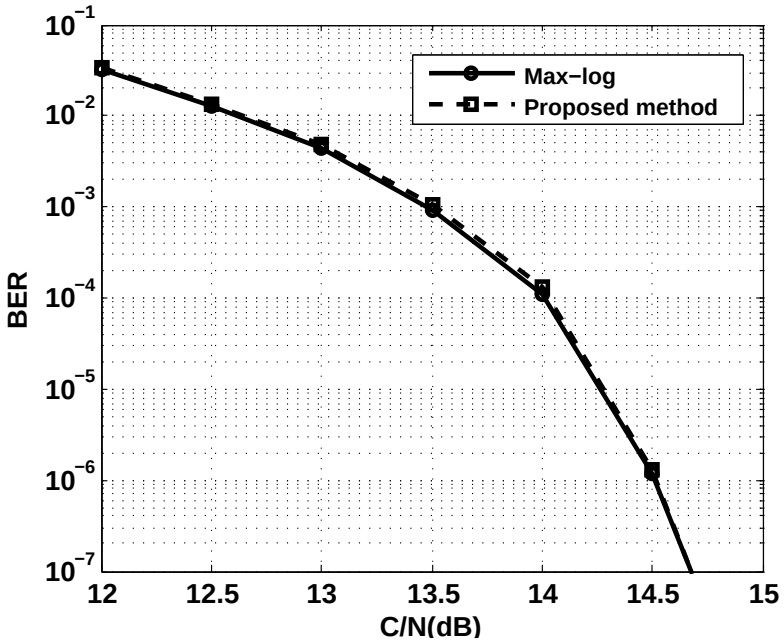

Figure 5.21: Simulation results for 6/15 code rate

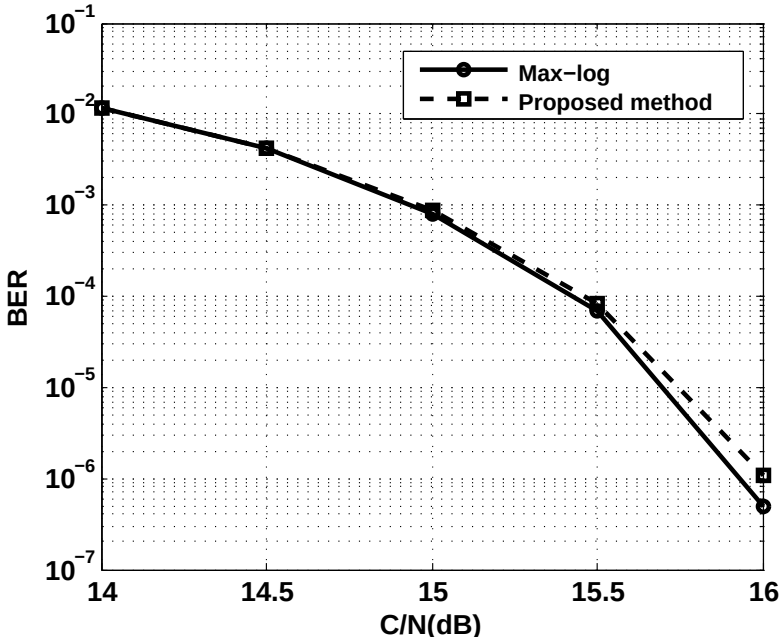

Figure 5.22: Simulation results for 7/15 code rate

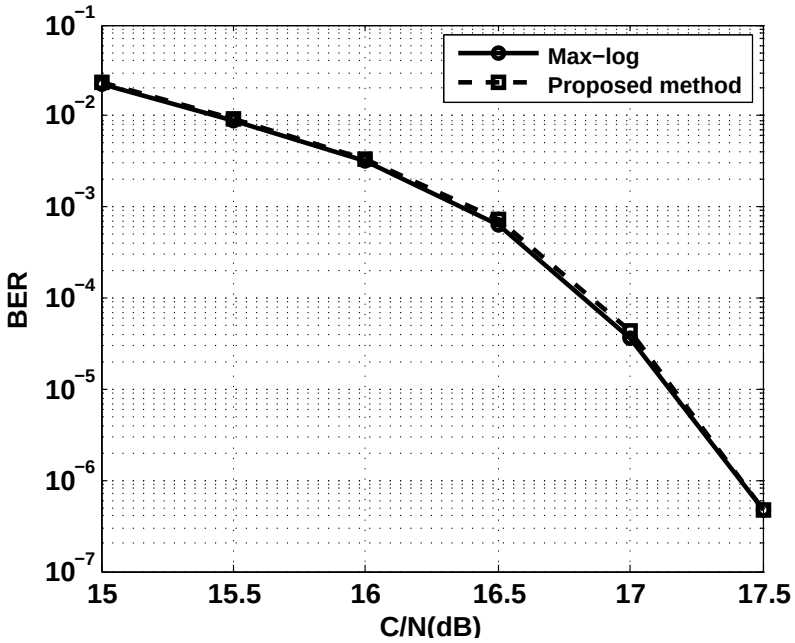

Figure 5.23: Simulation results for 8/15 code rate

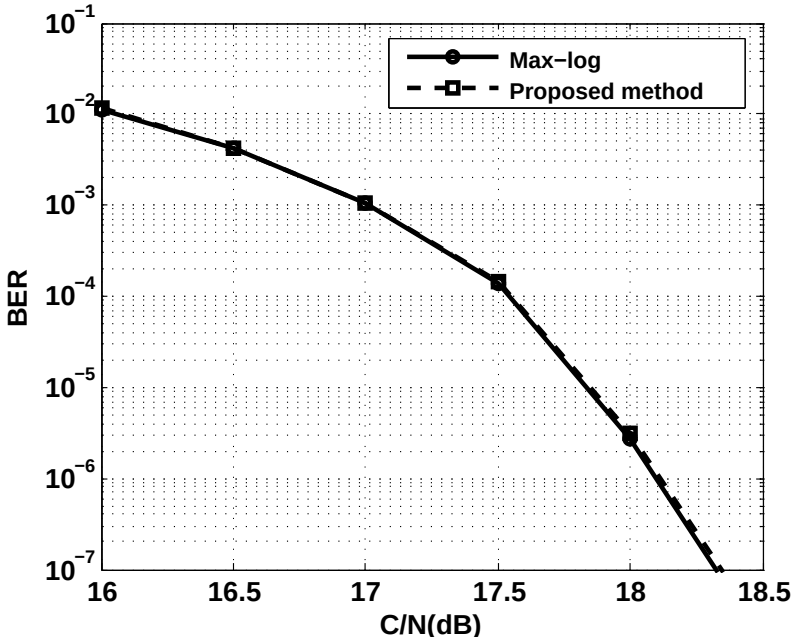

Figure 5.24: Simulation results for 9/15 code rate

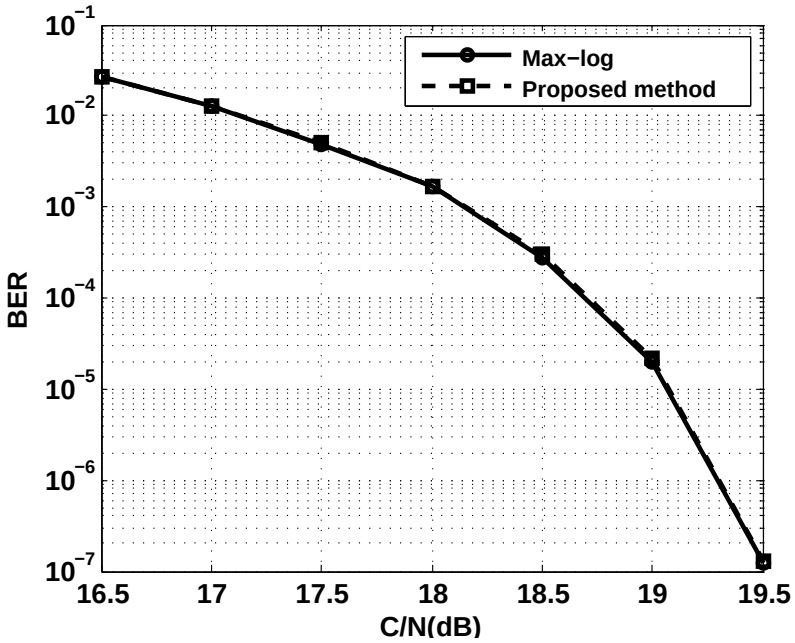

Figure 5.25: Simulation results for 10/15 code rate

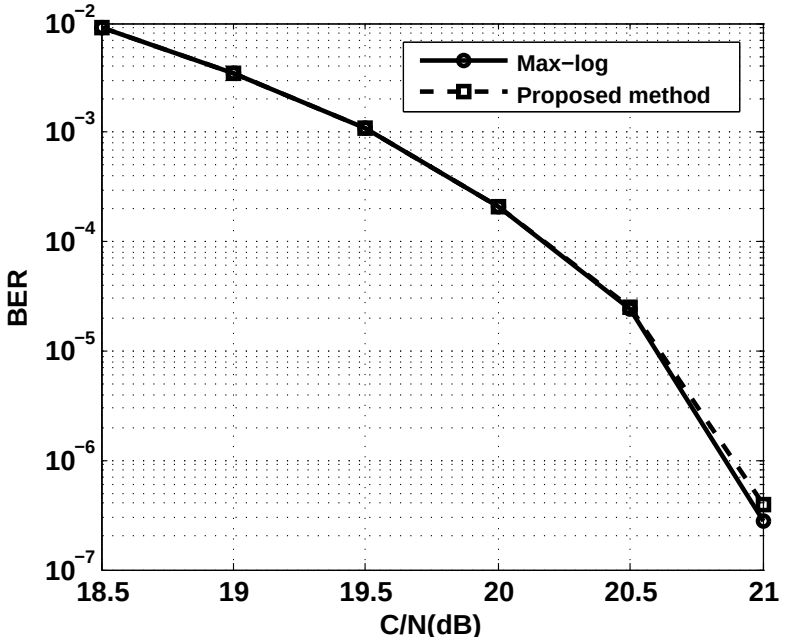

Figure 5.26: Simulation results for 11/15 code rate

5.5.2.3 Complexity reduction analysis

As shown in subsection 5.5.2 the number of multiplications to perform when using the proposed method is lower than when using the exact calculation. In order to compare the number of total operations required with both the exact and the proposed method, the additions, subtractions, and comparisons will be taken as additions and complex products will be taken as 3 real multiplications, and 5 additions following the Gauss's complex multiplication algorithm [40]. As a consequence of this assumptions follows Table 5.25. In the case of $n_{bpcu} = 10$ it can be seen a 25% reduction in the amount of multiplications at the cost of an increment of a 10% in the number of required additions.

To compute the hardware complexity reduction obtained by the use of the proposed technique, a very fair comparison method has been followed. The proposed cell (see Figure 5.17) has been modeled with Verilog-HDL and synthesized using a 180 nm technology. This process has been carried out for the exact calculation of the distance and the approximation presented in subsection 5.5.2 of this chapter. The input data of the cell is quantized using 10 bits that, as stated in [41], is a reasonable value to perform the demapping process. The resulting area for each method has been compared with the area required for a NAND gate in the used technology to obtain the equivalent gate count of each design. Table 5.26 summarizes the results obtained. From Table 5.26 it can be seen that the method presented in this paper can achieve a complexity reduction of almost an 80% and, as it was shown in subsubsection 5.5.2.2, with almost no performance loss. Note that this equivalent gate count is only for one distance calculation block. As stated earlier, for a 16-QAM+16-QAM eSM scheme, the decoder requires computing 256 distances. Depending on the receiver system clock and the decoder

Table 5.25: Overall operation reduction

	Exact calculation		Proposed method	
n_{bpcu}	Products	Additions	Products	Additions
6	1024	1984	816	2260
8	4096	7936	3136	8816
10	16384	31744	12368	34956

architecture, several distance computation blocks may be required in parallel so the area saving may be quite high.

	Exact calculation	Proposed method
Equivalent gate account	2218	460

Table 5.26: Complexity comparison

5.5.2.4 Conclusion

In this subsection a MIMO decoder simplification method has been presented. The proposed method introduces a negligible performance loss in the system (under 0.1 dB in every studied case) and reduces the demapper hardware implementation complexity greatly, reaching an 80% area reduction in the distance computation when compared to the hardware implementation of the ideal Euclidean distance.

5.5.3 Application of eSM to SISO systems

In this section a coding technique with application to SISO OFDM systems will be presented. This technique is based on the concepts acquired while working on the MIMO profile of DVB-NGH, in particular on the final codification chosen for the MIMO profile of the standard, eSM. However, SISO systems can't use the space as a diversity degree and then it is substituted by time and frequency. Because of that the name given to the developed coding technique is enhanced Time-Frequency Multiplexing (eTFM).

ETFM is based on an $L = 2$ SSD (Signal Space Diversity) technique following the nomenclature in [42], but it doesn't require a component interleaving. The technique will be tested in a DVB-T2 frame because as seen in chapter 3 it includes RQD another SSD technique with $L = 2$ [42]. RQD is substituted by eTFM in the DVB-T2 system architecture (see Figure 5.27) in order to compare the performance that can be obtained with both techniques.

The main target of these techniques is to increase the diversity level by using time and frequency domain. To this end, RQD performs a rotation in the complex plane of the original QAM constellation followed by a Q component interleaving process. This results in a virtual higher order constellation with improved spectral efficiency. The objective of the technique proposed is similar to the RQD one but consists in transmitting a linear combination of a couple of adjacent QAM symbols, improving the performance offered by RQD.

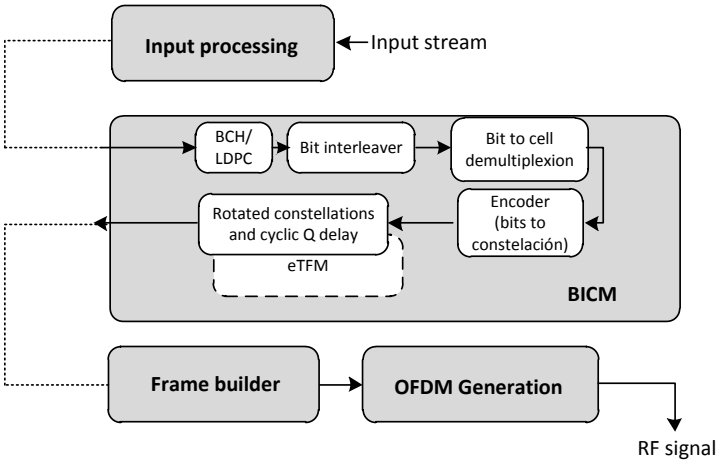

Figure 5.27: DVB-T2 block diagram

5.5.3.1 eTFM coding

The proposed technique is based on the MIMO eSM [38] and an $L = 2$ SSD code following the nomenclature in [42]. Instead of using space and frequency as diversity degrees (DVB-T2 does not contemplate MIMO architectures) as eSM, time and frequency are the exploited diversity. In this way the scheme is applicable to DVB-T2 SISO scheme.

The proposed technique is based on applying the linear combination shown in (5.19)

$$\begin{bmatrix} x_{2n} \\ x_{2n+1} \end{bmatrix} = \begin{bmatrix} \cos(\theta) & -\sin(\theta) \\ \sin(\theta) & \cos(\theta) \end{bmatrix} \begin{bmatrix} s_{2n} \\ s_{2n+1} \end{bmatrix} \quad (5.19)$$
$$n = 0, 1, 2, ..., N_{data}/2 - 1$$

where s_n represents the n-th symbol coming from the mapper (QAM constellation symbol), N_{data} the number of symbols to transmit, θ the rotation angle applied, and x_n the resulting symbol of the technique. The rotation angles applied for RQD are the ones proposed in DVB-T2, however for the proposed technique a study has been carried out to determinate the optimum value of θ. After this process, no component shuffling is needed (a Q delay is needed for RQD).

The resulting constellation after applying the proposed method is a higher order constellation (equivalent to twice the number of bits) but with an improved spectral efficiency, very similar in shape to the one obtained when RQD is applied. However, the different points obtained by both codifications contain different information. In case of RQD, the information comes from the real part of a rotated QAM symbol and the imaginary component of the following one. In case of eTFM, the symbol comes from the linear combination of two symbols.

Figure 5.28 and Figure 5.29 show the resulting symbols (even, and odd) after the proposed codification for a QPSK constellation and the evolution of the constellations points depending on the rotation angle. In these figures is shown how the constellation points are transformed, the thicker line shows how the different combinations transform a point in the first quadrant (in even symbols) and how all the points are transformed when combined with the point of the first quadrant (odd symbols).

Figure 5.30 and Figure 5.31 show the same information of the previous figure but with RQD. As can be seen, although the output constellation is the same for eTFM and RQD, the resulting output for the particular example shown with thick lines is completely different.

As happens with RQD, the original data spreads in time and frequency after the different interleaving stages applied in DVB-T2. This makes the different linear combination of the original QAM symbols to propagate though the channel

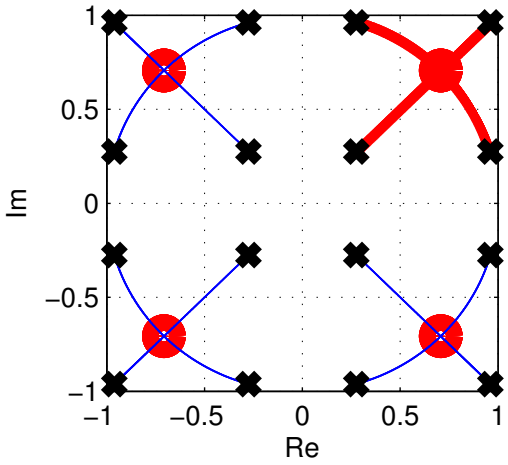

Figure 5.28: eTFM output (cross) and input (circle) constellations and angle evolution for even symbols

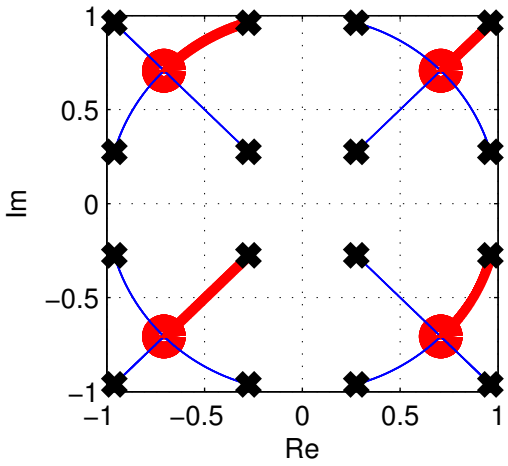

Figure 5.29: eTFM output (cross) and input (circle) constellations and angle evolution for odd symbols

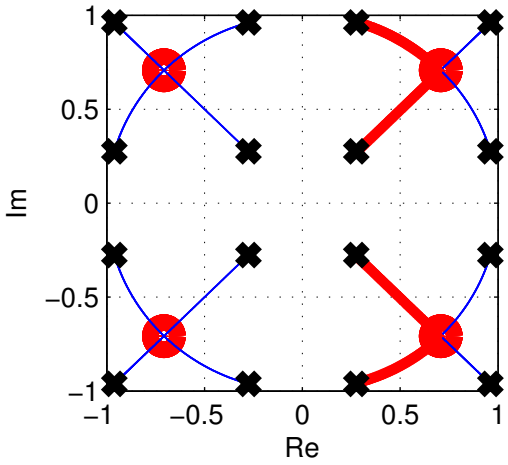

Figure 5.30: RQD output (cross) and input (circle) constellations and angle evolution for even symbols

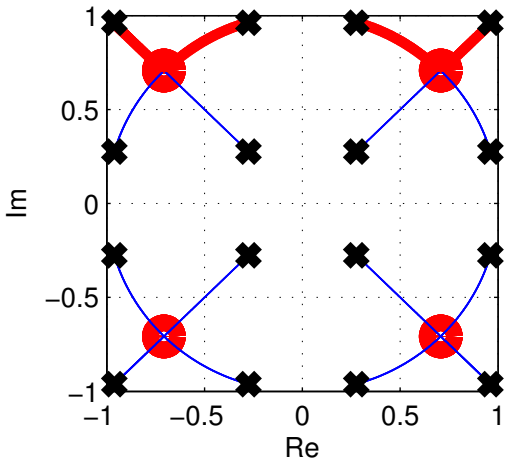

Figure 5.31: RQD output (cross) and input (circle) constellations and angle evolution for odd symbols

in different frequencies and time instants, increasing the diversity obtained. The gain, in terms of uncoded SER (Symbol Error Rate), that can theoretically be obtained with this kind of technique is derived in [42] and shown in Figure 5.32, where for comparison purpose the SER versus SNR (Symbol to Noise Ratio) curves for the diversity degree of the proposed technique, $L = 2$, the traditional QAM sybols, $L = 1$, and a higher diversity level, $L = 4$, are shown. As it can be seen for a SER of 10^{-3} the achievable gain for an $L = 2$ technique when compared to an $L = 1$ one is about 10 dB. In the subsubsection 5.5.3.3 we show the effect of the FEC code over this gain and optimize the rotation angle of eTFM to reach a good compromise solution.

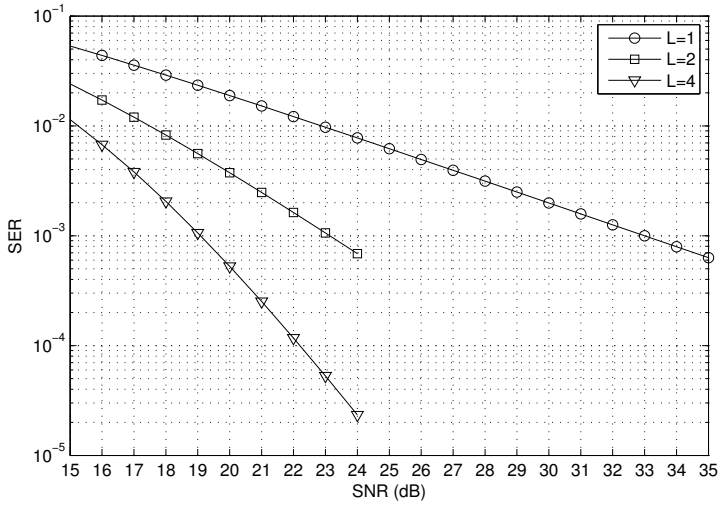

Figure 5.32: Theoretical SER for different diversity degrees (L)

5.5.3.2 Decoder Complexity

The use of eTFM increases the decoder hardware complexity in a higher way than RQD. In this section this drawback that the proposed technique presents will be studied.

For a simpler detection and calculation of the LLR metrics, needed by the demapper at the receiver side, the Max-log approximation is commonly used leading to the expression in (5.20), where b_i represents the ith bit of the received

symbol, σ^2 is the noise variance, C_i^j is the subset of symbols of the ideal constellation in which the ith bit's value is j ("0" or "1"), $\widetilde{\mathbf{H}}$ is the estimated channel, y is the received signal, and s is the ideal transmitted symbol.

$$LLR(b_i) \approx \frac{1}{2\sigma^2}\left[\min_{S\in C_i^0}\left(\left\|y-\widetilde{\mathbf{H}}s\right\|^2\right) - \min_{S\in C_i^1}\left(\left\|y-\widetilde{\mathbf{H}}s\right\|^2\right)\right] \tag{5.20}$$

In the case of eTFM, the symbols are composed by the linear combination of two QAM symbols, increasing the number of possible candidates in the C_i^j subsets when compared to the equivalent traditional QAM constellation. The number of possible candidates is $2^{n_{bps}}$, where n_{bps} represents the sum of the number of bits of the combined QAM constellations. Therefore, in order to find the minimums of Equation 5.20, we need to calculate the squared Euclidean distance shown in Equation 5.21 for every possible candidate. $\Re$ and $\Im$ represent the real and imaginary part respectively.

$$\left\|y-\widetilde{\mathbf{H}}s\right\|^2 = \left(\Re(y)-\Re(H*s)\right)^2 + \left(\Im(y)-\Im(H*s)\right)^2 \tag{5.21}$$

For example, for two 16-QAM ($n_{bps}=8$) there will be 256 possible candidates. Therefore, according to expression (5.21), the number of real multiplications required to perform the detection of one received symbol, without taking into account the product $\widetilde{\mathbf{H}}s$, is 1024.

At the decoder, the $\widetilde{\mathbf{H}}s$ product is also required in order to compute (5.21), Table 5.27 shows the total amount of operations to be performed for each received symbol when the exact squared Euclidean distance calculation is used.

For RQD, the maximum n_{bps} in the compared cases (up to 64-QAM) is 6.

This problem can be partially solved by applying spherical detection techniques that are widely studied in the literature [43, 44]. In [43, 44] it is shown how by choosing the proper initial radius of the search sphere the amount of candidates to be taken into account can be greatly reduced, and consequently the number of operations to be computed. Also several practical implementations of the sphere decoding algorithm are presented.

Table 5.27: Total amount of operations to perform in the detection process for each received symbol in eTFM

n_{bps}	Real products	Additions/Subtractions	Complex products
4	32	48	16
8	512	768	256
12	8192	12288	4096

5.5.3.3 Simulation results

In order to check the achievable performance with the proposed technique the CSP [7] is used. The RQD module is substituted by the one performing the method proposed in subsubsection 5.5.3.1 in order to compare the performance that both offer by means of BER versus SNR curves.

We use the RME channel model described in [24] as propagation scenario, being the worst propagation environment defined for DVB-T2. In the simulated cases the erasure rate is set to a 15% and 10%. More realistic scenarios are also used for performance comparison purposes, such as a P1 channel defined in [4], and a 0dB echo at 90% of the guard interval (with CP of the OFDM signal set to 1/4 of the OFDM symbol).

5.5.3.3.1 Optimum angle selection

As in DVB-T2 different angles will be selected for the different constellations available, the proposed technique will be applied to QPSK, 16-QAM, and 64-QAM. The performance enhancement achievable for 256-QAM with RQD is very poor, that is why in DVB-NGH the technique is not applied to it anymore, and also why we do not apply eTFM to it.

To select the optimum angle simulations have been run; we fix the SNR to check the BER level after the LDPC decoder at the receiver side. Tracking the evolution of the BER while changing the rotation angle used in eTFM, the one that minimizes the BER can be found. This angle of course will be optimum for the concrete propagation scenario in which the simulations were run. The BER evolution results shown in Figure 5.33, Figure 5.34, and Figure 5.35 have

Table 5.28: Chosen angles for eTFM

Modulation	Rotation angle (deg)
QPSK	26.56
16-QAM	14.03
64-QAM	7.125

been obtained for a 64800 bits code length LDPC and all code rates available in DVB-T2 using as propagation scenario an RME channel with 15% erasures probability.

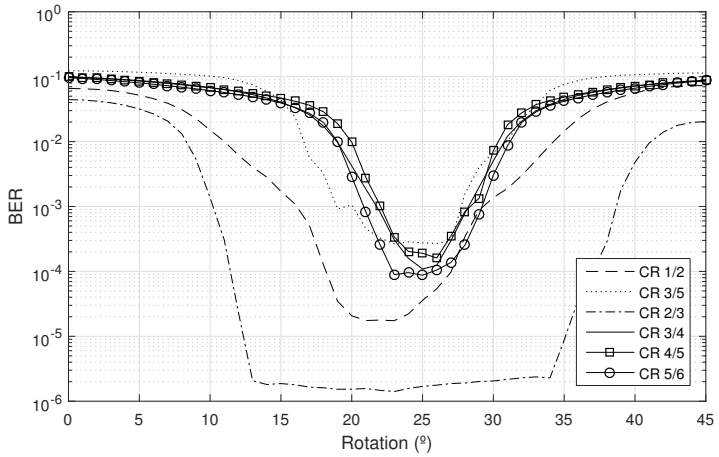

Figure 5.33: BER evolution for QPSK constellation

As it can be seen in the figures the optimum angle slightly increases with the CR fraction. Optimum angles are close to the ones selected for RQD in DVB-T2, however the performance these rotations offer is lower than the one offered by the optimum values obtained. The optimum values are in this case closer to the angles that make the projections on the I and Q axis in the complex plane be identically spaced, and thus they will be the ones chosen for eTFM. These angles can be easily found for each constellation applying basic geometry concepts, and are shown in Table 5.28.

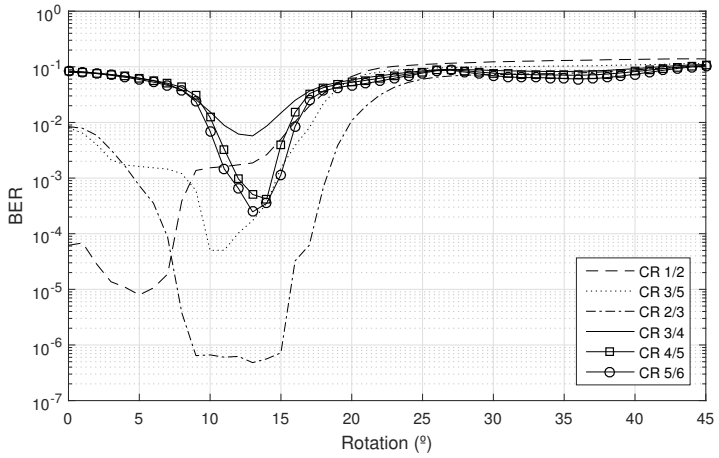

Figure 5.34: BER evolution for 16-QAM constellation

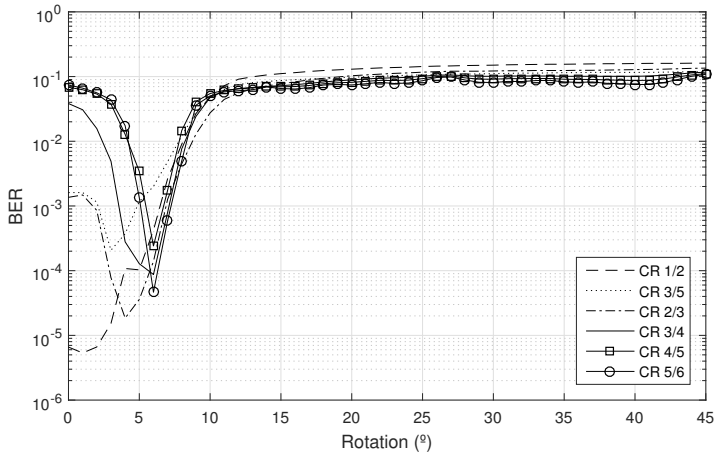

Figure 5.35: BER evolution for 64-QAM constellation

Table 5.29: eTFM performance gain in RME 15%

	Code Rate		
	1/2	3/4	5/6
QPSK	0.04	0.15	0.12
16-QAM	0.06	0.27	0.63
64-QAM	0.20	0.49	1.06

Table 5.30: eTFM performance gain in RME 15% with DVB-T2 angles

	Code Rate		
	1/2	3/4	5/6
QPSK	0.04	0.14	0.11
16-QAM	0.05	0.23	0.57
64-QAM	0.10	0.27	0.88

5.5.3.3.2 eTFM performance comparison

The performance of the proposed coding scheme will be analyzed by means of BER curves at the output of the LDPC decoder. The simulations have been obtained for 64800 bits length codewords, ideal channel estimation and all possible code rates in DVB-T2, but for the sake of brevity only the lower (1/2), higher (5/6), and an intermediate (3/4) code rate fractions results are presented. The maximum number of iterations of the LDPC decoder was set to 50, and at least 100 erroneous FEC blocks should be found. Table 5.29 shows the gain in dB achievable at a BER level of 10^{-5} in RME 15% erasure rate channel, having a maximum performance improvement over 1dB. Table 5.30 shows the gain obtained compared to RQD in the same propagation scenario when using eTFM with the same angles that are proposed in DVB-T2. As it can be seen the gain is lower than when applying the angles proposed in paragraph 5.5.3.3.1 but still appreciable.

As an illustrative example Figure 5.36 shows the BER curves for the highest gain obtained in the RME channel.

For an RME with a 10% erasures probability the results are shown in Table 5.31. As it can be denoted the gain is reduced, but still noticeable.

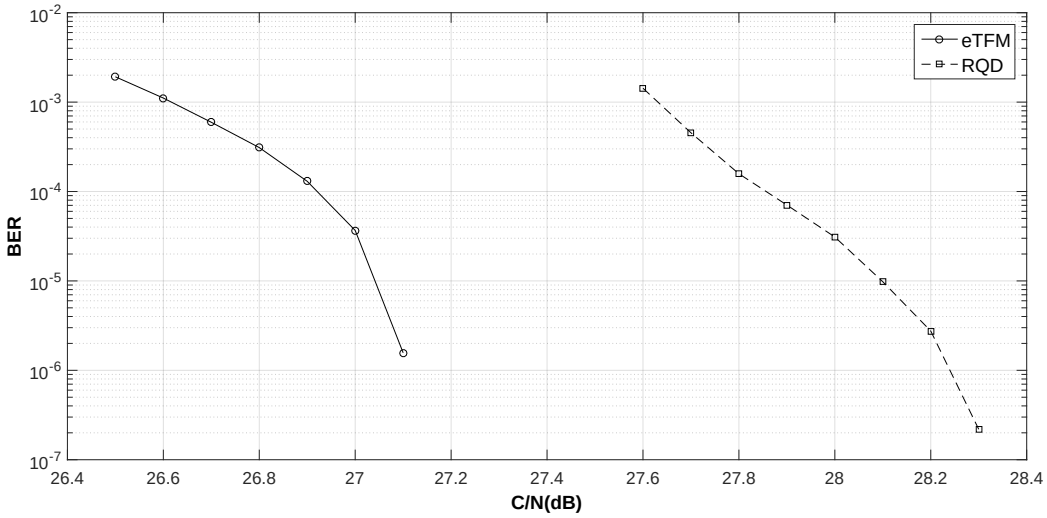

Figure 5.36: Simulation results for 64-QAM and 5/6 code rate in RME 15% channel

Table 5.31: eTFM performance gain in RME 10%

	Code Rate		
	1/2	3/4	5/6
QPSK	0.05	0.11	0.12
16-QAM	0.09	0.13	0.26
64-QAM	0.11	0.25	0.51

Table 5.32: eTFM performance gain in 0dB echo at 90% of the CP

	Code Rate		
	1/2	3/4	5/6
QPSK	0.03	0.09	0.15
16-QAM	0.06	0.09	0.09
64-QAM	0.05	0.07	0.15

Table 5.32 shows the performance gain in a 0dB echo channel set to the 90% of the CP. As it can be noticed, the gain is lower.

In Figure 5.37 for comparison purpose also the QAM constellation simulation results are presented in for the simulated 0dB echo channel. Although the gain of eTFM versus RQD seems low, the gain between RQD and standard QAM constellation is only 0.3dB, while the eTFM gain is a 33% higher.

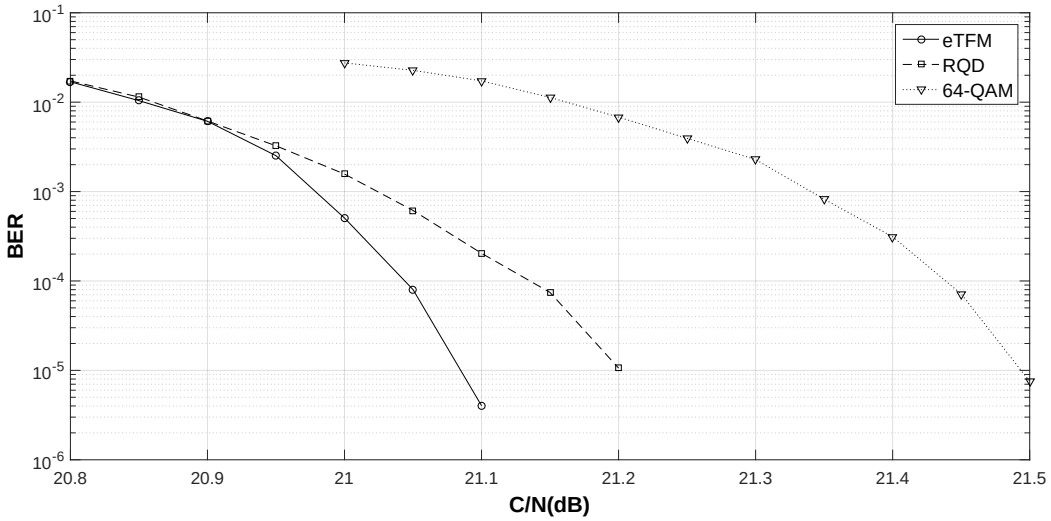

Figure 5.37: Simulation results for 64-QAM and 5/6 code rate in a 0dB echo channel

Finally, the results for P1 channel are exposed inTable 5.33, this channel is characterized for much better propagation conditions than the previously used scenarios. This fact makes that the gain obtained is very reduced, remaining

Table 5.33: eTFM performance gain in P1

	Code Rate		
	1/2	3/4	5/6
QPSK	0.05	0.05	0.05
16-QAM	0.08	0.2	0.0
64-QAM	0.05	0.01	0.0

always under 0.1 dB.

In Figure 5.38 for comparison purpose the QAM constellation simulation results are also presented for a P1 channel. As it can be seen, the gain obtained comparing RQD to the QAM constellation is very low (0.05 dB), also the gain presented by eTFM compared to the QAM constellation is low but 80% higher than the one presented by RQD.

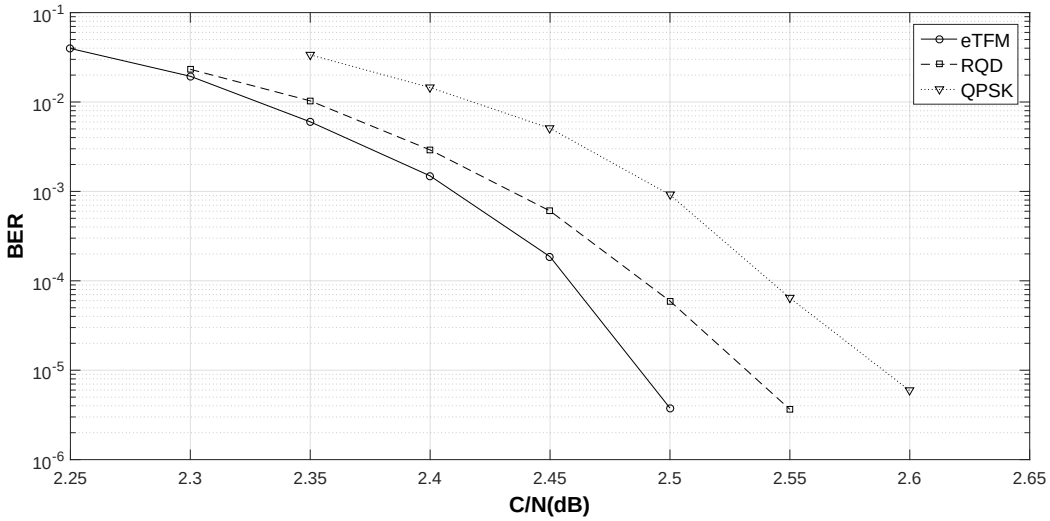

Figure 5.38: Simulation results for QPSK and 1/2 code rate in a P1 channel

5.5.3.4 Conclusion

In this subsection it was presented a technique with application to OFDM SISO systems. This technique has been tested in the frame of the DVB-T2 standard

and compared to one of the key new features in it, RQD. It has been shown that eTFM has a better performance than RQD, presenting gains as high as 1dB. This technique improves the system performance without increasing the bandwidth or reducing the data rate. However, this gain comes with a drawback; the decoding process complexity increases exponentially with the transmitted constellation order.

Chapter 6

Conclusion and future work

In this last chapter of the PhD. dissertation a summary with the most important conclusions that can be extracted from the work performed during these years of studies will be presented. Also some future work lines will be stated.

6.1 Conclusions

Along years of study I've researched about OFDM systems, more concretely about the ones belonging to the DVB standards family. I've studied its characteristics, the benefits and the drawbacks of choosing this kind of modulation schemes, making special focus on the diversity techniques applied in them.

As observed in this PhD. dissertation, diversity techniques as RQD in DVB-T2 can offer a huge performance gain in certain propagation conditions. As shown in chapter chapter 3, the gain can reach up to 9dB in terms of C/N when it can be numerically computed. There are certain configurations where the reception is not possible without using this technique. This performance gain, however, doesn't come for free. The impact in the hardware complexity of the receiver is quite noticeable and traditional simplifications (as 2x1D demapping) cannot be applied due to the correlation in the data inserted by the use of the RQD and the propagation through the communication channel.

In order to solve this complexity increase I have proposed 2 different approaches to reduce it. The first one consists in reducing the number of candidates

to compare when looking for the most probable transmitted constellation point. As shown in chapter 3, the simplification can reach up to a 78% reduction when calculating the corresponding distances at the demapper in normal propagation conditions,having a negligible performance loss. When the propagation conditions are severe this reduction decreases to a 41%, still being quite considerable. These results were published in [27] and [29].

The second approach focuses in the calculation of the LLRs needed by the LDPC decoder. It targets to reduce the complexity (in terms of hardware) of its mathematical expression, concretely when calculating the distance to the possible transmitted constellation points. The aim was to find a function that had its minimums in the same points as the traditional Euclidean distance for the working C/N. Manhattan distance was found to accomplish this having an almost null performance loss and leading to a 78% reduction in the number of multiplications to be performed. The results in this field were published in [45] and patented.

Regarding to the MIMO diversity, all the performance results presented in this PhD. were used as a tool to conceive one of the most advanced communication systems nowadays, DVB-NGH. The analysis showed that the performance gain that can be achieved with MIMO can be huge, finally an eSM-PH scheme was chosen as MIMO coding for DVB-NGH. Still being simpler to detect than other MIMO codifications, eSM presents a very high hardware complexity at the receiver. The complexity increase is critical in mobile devices (the ones DVB-NGN is conceived for) so it is crucial to focus on reducing this. The desired complexity reduction is achieved by using a generalization of the second approach used for the RQD demapper, simplifying the mathematical expression of the exact LLRs calculation. The results obtained in this topic were published in [46].

Finally, thanks to the knowledge acquired a new coding technique based on eSM and RQD is proposed for SISO OFDM systems. This codification, eTFM, uses time-fequency diversity because of the absence of space in this kind of architecture. The technique is tested in a DVB-T2 system, comparing its performance to RQD and showing that eTFM offers up to 1dB gain. The results of this last part of the PhD. were published in [47].

6.2 Future Work

The knowledge acquired in these years of investigation are going to be used in other applications of OFDM systems different from broadcasting ones. The main investigation line to follow is the application of MIMO to optic fiver communications where the different polarization modes and spatial modes make easy to use different MIMO configurations. The application of OFDM to optic fiber communications is one of the most promising research fields because of the necessity of a better usage of the optical spectrum due to the increase of the data rate needed to fulfill the requirements in bandwidth of the each time more demanding consumers.

OFDM can be also applied Visible Ligth Communications, being it a very promising technology and a wide field of research [48, 49] it can be the next step for indoor wireless communications due to its inherent advantages as increased security and unregulated spectrum. Moreover the different light sources usually placed in a room makes this the perfect scenario to further explore different MIMO configurations and scenarios.

The seveth of September 2016 ATSC 3.0 physical layer specification [50] was released. This standard describes the most advanced digital terrestrial broadcasting system nowadays. It adopts several codification techniques as MIMO eSM coding and non uniform already studied and adopted for DVB-NGH. The coding technique proposed in this PhD. dissertation, eTFM, could be tested in this new frame to check the performance improvement that could be achieved.

Bibliography

[1] C. Jégo M. Li, C. Abdel and C. Douillard. Design of rotated qam mapper/demapper for the dvb-t2 standard. *IEEE WorkShop on Signal Proc Syst. (SiPS)*, pages 18–23, October, 2009.

[2] C. E. Shannon. A mathematical theory of communication. *Bell System Technical Journal*, 27:379–423 and 623–656, July and October, 1948.

[3] European Telecommunications Standard Institute ETSI York. *Digital Video Broadcasting (DVB);Frame Structure Channel Coding and Modulation for a Second Generation Digital Terrestrial Television Broadcasting System (DVB-T2).* EN 302 755 v1.2.1., Feb 2011.

[4] European Telecommunications Standard Institute ETSI York. *Digital Video Broadcasting (DVB); Framing structure, channel coding and modulation for digital terrestrial television.* EN 300 744 v1.5.1., Nov 2004.

[5] European Telecommunications Standard Institute ETSI York. *Digital Video Broadcasting (DVB); Next Generation broadcasting system to Handheld, physical layer specification (DVB-NGH).* Draft ETSI EN 303 105 V1.1.1, Sep. 2012.

[6] European Telecommunications Standard Institute ETSI York. *Digital Video Broadcasting (DVB); Transmission System for Handheld Terminals (DVB-H).* EN 302 304 v1.1.1., Nov 2004.

[7] V. Baena. Common simulation platform tutorial. *DVB document TM-T20491*, December, 2008.

[8] DVB Fact Sheet. Introduction to the dvb project creating global standards for digital television. May, 2010.

[9] AHA products group. *Reed-Solomon Error Correction Codes.*

[10] Roger Miles Peter MacAvock. Hierarchical modulation. *DVB white paper 01*, March, 2000.

[11] Digital Video Broadcasting (DVB). *Commercial requirement for DVB-T2.* DVB Blue Book A114, April 2007.

[12] R. G. Gallagher. Low-density parity-check codes. *IRE Trans. on Inform. Theory*, vol. IT-8, pp. 21-28, 1962.

[13] European Telecommunications Standard Institute ETSI York. *Digital Video Broadcasting (DVB); Framing structure, channel coding and modulation for Satellite Services to Handheld devices (SH) below 3GHz.* EN 302 583 v1.1.1., March 2008.

[14] Siavash M. Alamouti. A simple transmit diversity technique for wireless communications. *IEEE Journal on selected areas in communications*, 16: 1451–1458, October, 1998.

[15] J. Winters. On the capacity of radio communication systems with diversity in a rayleigh fading environment. *IEEE Journal on selected areas on communications*, 5:871–878, June, 1987.

[16] M.J. Gans G. J. Foschini. On limits of wireless communications in a fading environment when using multiple antennas. *Wireless Personal Communications*, 6:311–335, March, 1998.

[17] I.E. Telatar. Capacity of multi-antenna gaussian channels. *AT & T Bell Laboratories*, 6, BL0 112 170-950 615-07TM, 1995.

[18] K. Boullé and J. C. Belfiore. Modulation scheme designed for the rayleigh fading channel. *CISS'92*, March, 1992.

[19] E. Boutillon X. Giraud and J. C. Belfiore. Algebraic tools to build modulation schemes for fading channels. *IEEE Trans. Commun.*, 43 no. 3:938–952, May, 1997.

[20] J. Boutros and E. Viterbo. Signal space diversity: A power- and bandwidth-efficient diversity technique for the rayleigh fading channel. *IEEE Trans. Inform. Theory*, 44 no. 4:1453–1467, July, 1998.

[21] C. Abedul Nour and C. Douillard. On lowering the error floor of high order turbo bicm schemes over fading channels. *IEEE Global Commun. Conf., GLOBECOM'06*, pages 1–5, November, 2006.

[22] F.M. Assis and E. S. Sousa. Rotated constellation mc-cdma system. *in IEEE Global Commun. Conf., GLOBECOM'99*, 1B:996–1001, 1999.

[23] A. Chindapol and J. Ritcey. Design, analysis, and performance evaluationfor bicm-id with square qam constellations in rayleigh fading channels. *IEEE J. Select, Areas Commun.*, 19:944–957, May, 2001.

[24] European Telecommunications Standard Institute ETSI York. *Implementation guidelines for a second generation digital terrestrial television broadcasting system (DVB-T2).* TR 102 831 V0.10.4, June 2010.

[25] Catherine Douillard Charbel Abdel Nour. Choice of the angle for rotated constellations. *DVB document TM-T20400*, March, 2008.

[26] Chang Wahn Yu Youn Ok Park Dongweon Yoon Ki Seol Kim, Kwangmin Hyun and Sang Kyu Park. General log-likelihood ratio expression and its implementation algorithm for gray-coded qam signals. *ETRI Journal*, 28: 291–300, June, 2006.

[27] A. C. Oria P. López J.G. Doblado D. Pérez-Calderón, V. Baena-Lecuyer. Rotated constellation demapper for dvb-t2. *Electronic letters*, 47:31–32, January, 2011.

[28] P. Robertson P. Hoeher, S. Kaiser. Two-dimensional pilot-symbol-aided channel estimation by wiener filtering. *Acoustics, Speech, and Signal Processing (ICASSP)*, 3:1845–1848, April, 1997.

[29] A. C. Oria P. López J.G. Doblado D. Pérez-Calderón, V. Baena-Lecuyer. Simplified rotated constellation demapper for second generation terrestrial digital video broadcasting. *IEEE Transactions on Broadcasting*, 59:160–167, 2013.

[30] H. Yang K. Bae, K. Kim. One-dimensional soft-demapping using decorrelation with interference cancellation for rotated qam constellations. *Proceedings of the 9th Annual IEEE Consumer Communications and Networking Conference (CCNC'12)*, pages 787–791, January, 2012.

[31] H. Yang K. Bae, K. Kim. Low complexity two-stage soft demapper for rotated constellation in dvb-t2. *Proceedings of 2012 IEEE International Conference on Consumer Electronics (ICCE)*, pages 618–619, January, 2012.

[32] M. Butussi S. Tomasin. Low complexity demapping of rotated and cyclic q delayed constellations for dvb-t2. *IEEE Wireless Communications Letters*, 1:81–84, April, 2012.

[33] P. Tamola E. Stare V. Pauli D. Nisar I. Gutierrez A. Mourad P. Moss M. Petrov, J. Robert. Two-dimensional pilot-symbol-aided channel estimation by wiener filtering. *DVB Document TM-H0502*, November, 2010.

[34] Nihar Jindal Andrea Goldsmith, Syed Ali Jafar and Sriram Vishwanath. *Capacity Limits of MIMO Systems*. 2003.

[35] Hamid Jafarkhani. *Space-Time Coding, Theory and Practice*. 2005.

[36] E. Viterbo J. C. Belfiore, G. Rekaya. The golden code: a 2x2 full-rate space-time code with non-vanishing determinats. *IEEE Transactions on Informantion Theory*, 51:1432–1436, April, 2005.

[37] E. Viterbo B. Biglieri, Y. Hong. On fast-decodable space-time block codes. *IEEE Transactions on Informantion Theory*, 55:524–530, February, 2009.

[38] Woo-Suk Ko. Lg response to ngh cft. *DVB Document TM-NGH076r1*, April, 2010.

[39] M.E. Frerking. *Digital Signal Processing in Communication Systems*. 1994.

[40] Donald E. Knuth. The art of computer programming volume 2: Seminumerical algorithms. *Addison-Wesley*, pp. 519-706, 1988.

[41] F. Chiaraluce G. Cancellieri Baldi, M. Finite-precision analysis of demappers and decoders for ldpc-coded m-qam systems. *IEEE Transactions on Informantion Theory*, 55:239–250, June, 2009.

[42] J. Boutros and E. Viterbo. Signal space diversity: A power- and bandwidth-efficient diversity technique for the rayleigh fading channel. *IEEE Trans. Inform. Theory*, 44:1453–1467, 1998.

[43] G. Caire M. O. Damen, H. E. Gamal. On maximum likelihood detection and the search for the closet lattice point. *IEEE Transactions on Information Theory*, 49:2389–2401, 2003.

[44] Chen Fang-chao Li Shi-ping, Wang Long. On maximum-likelihood detection and the search for the closest lattice point. *Control and Decision Conference*, pages 3322– 3325, 2012.

[45] J.G. Doblado A. C. Oria P. López D. Pérez-Calderón, V. Baena-Lecuyer. Simplified metrics calculation for soft bit detection in dvb-t2. *Radioengineering*, 23:399–404, 2014.

[46] J. Chávez Orzáez J.G. Doblado A. C. Oria D. Pérez-Calderón, V. Baena-Lecuyer. Simplified detection for dvb-ngh mimo decoders. *IEEE Transactions on Broadcasting*, 61:84–90, 2015.

[47] Dario Perez-Calderon; Vicente Baena Lecuyer; Ana Cinta Oria; Jose Garcia Doblado. Diversity technique for ofdm systems: Enhanced time-frequency multiplexing (etfm). *IEEE Transactions on Broadcasting*, 62:505–511, 2016.

[48] H. Elgala; R. Mesleh; and H. Haas. Indoor optical wireless communication: Potential and state-of-the-art. *IEEE Commun. Mag.*, 49:56–62, 2011.

[49] H. Burchardt; N. Serafimovski; D. Tsonev; S. Videv; H. Haas. Vlc: Beyond point-to-point communication. *IEEE Commun. Mag.*, 52:98–105, 2014.

[50] Advanced Television Systems Committee. *ATSC Standard: Physical Layer Protocol (A/322)*. 7 September 2016.